

# **Lignin-derived catalyst for biodiesel synthesis**

Aisha Hamilton

A thesis in the

Department of Chemistry and Biochemistry

Presented in partial fulfilment of the requirements for the

Degree of Master of Science (Chemistry) at

Concordia University

Montreal, Quebec, Canada

August 2023

© Aisha Hamilton, 2023

**CONCORDIA UNIVERSITY**  
**School of Graduate Studies**

This is to certify that the thesis prepared

By: Aisha Hamilton

Entitled: Lignin-derived catalyst for biodiesel synthesis

and submitted in partial fulfillment of the requirements for the degree of

**Master of Science (Chemistry)**

complies with the regulations of the University and meets the accepted standards with respect to originality and quality.

Signed by the final examining committee:

\_\_\_\_\_  
*Dr John Oh* Chair

\_\_\_\_\_  
*Dr Louis Cuccia* Examiner

\_\_\_\_\_  
*Dr Yves Gélinas* Examiner

\_\_\_\_\_  
*Dr Rafik Naccache* Thesis Supervisor

Approved by \_\_\_\_\_  
*Dr Louis Cuccia* Graduate Program Director 2023

\_\_\_\_\_  
*Dr Pascale Sicotte* Dean of the Faculty of Arts and Science

# **Abstract**

## Lignin-derived catalyst for biodiesel production

Aisha Hamilton

Increasing dependence and overconsumption of non-renewable, pollutant-emitting fossil fuels has been declared as a primary contributor to climate change, prompting the shift to renewable energy sources. Biodiesel has emerged as a promising, more sustainable alternative energy source, primarily formed through either the transesterification of triglycerides or the esterification of free fatty acids into fatty acid methyl esters (biodiesel). However, current biodiesel production uses refined vegetable oils as feedstock which has raised concerns due to the competition with food crops and contributes a staggering 90% to the overall cost of production. Additionally, a major hurdle in the sustainability of biodiesel production is the current basic homogeneous catalysts employed react with free fatty acids in oils to produce soap, significantly contaminating the product and requiring extensive purification steps, resulting in substantial wastewater. For this reason, heterogeneous catalysts have garnered interest as more suitable alternatives. As well as being able to perform the transesterification of triglycerides, acidic catalysts also catalyse the esterification of free fatty acids present in most non-edible and waste cooking oils into biodiesel. In this study, a lignin-derived heterogeneous catalyst converted over 97% of oleic acid - a representative of free fatty acids - into biodiesel under optimal conditions. A basic heterogeneous catalyst was also synthesised for the transesterification of canola oil - a representation of triglycerides - into biodiesel under optimal conditions. The combination of these catalysts can be integrated in a two-step conversion of waste-cooking oil into biodiesel. Lignin is currently considered a waste material, being a by-product of the paper/pulp industry, with 98% being burnt

for energy. The upcycling of lignin into a value-added product to convert waste cooking oil offers increased sustainability as well as access to environments and economies that are limited in resources and financials. Overall, the replacement of the standard basic homogeneous catalysts with solid heterogeneous ones overcomes the difficulty of separation and the employment of acidic catalysts allows utilisation of non-edible and waste cooking oils, eliminating majority of production costs and competition with the agriculture market.

## Acknowledgements

I could not have completed my master's project without the support, help and love from so many people here in Montreal, and back home.

Dr. Rafik Naccache, I cannot thank you enough for giving me the opportunity to complete my thesis and welcoming me into such a diverse research group. Thank you for your guidance, support and utmost patience with me throughout my master's project. Thank you for also giving me the space to grow as a student, a chemist and a person, allowing me to graduate your lab with confidence and optimism for my future endeavours.

To my committee members, Dr. Louis Cuccia and Dr. Yves Gélinas, thank you for your valuable insight throughout my project. I am grateful to have had such well-versed and knowledgeable professors on my committee, who helped me to strengthen my understanding of the mechanisms involved and the environmental considerations of my work.

To the administrative staff - particularly Jennifer Sachs who helped me beyond belief when I accidentally unenrolled myself from Concordia - definitely would not be here without you! To Costa, the NMR expert and the most helpful lab technician, thank you for the effort, the willingness to tackle the elucidation of my structures and guidance you offered throughout my project.

To my mentor Michelle - this project would not have happened without you. From the first day when you came up to me and told me to start running biodiesel reactions, to helping me finish the last results for my thesis - you have consistently shown me unwavering support, selflessness, kindness and reassurance in all times of doubt. Also, going through the struggles of biodiesel with me - you made it possible to be motivated in such a well-established field. I am blessed to have had such a strong, talented, innovative and thorough chemist not only as my mentor, but as a friend throughout the years. Thank you for taking me under your wing, even when you were new in the

country/lab yourself. To the girls in the lab; Adryanne, Gabi, Arezoo, Mingshan, Tayline, thank you for all the support, laughs, talks and memories together.

To my parents, thank you - for everything. To my darling Zahra and Alex, for always being my cheerleaders, even from the other side of the world. To my honorary parents - Palma and Fern, thank you for keeping me fed and helping me survive the Quebec winters. Nero, thank you for the emotional support. Michael, thank you for being my strength when I felt like I had none.

A massive thank you to my partner, Giuliano, for the constant support, patience and kindness throughout my master's degree. I could not have gotten through this without your encouragement and care, for which I will always be grateful.

Finally, to Samantha, for being by my side always.

## Table of contents

List of Figures .....	ix
List of Tables .....	xii
List of abbreviations .....	xiii
Chapter 1- Introduction .....	1
1.1 The need to shift from fossil fuel .....	1
1.2 Biodiesel .....	2
1.2.1 What is biodiesel?.....	2
1.2.2 Synthesis of biodiesel .....	3
1.3 Catalysts in biodiesel production .....	4
1.3.1 Homogeneous catalysts.....	4
1.3.1.1 Homogeneous base catalysts .....	5
1.3.1.2 Homogeneous acid catalysts .....	6
1.3.2 Heterogeneous catalysts.....	7
1.3.2.1 Heterogeneous base catalysts.....	8
1.3.2.2 Heterogeneous acid catalysts .....	8
1.3.3 Influence of catalyst on biodiesel quality .....	9
1.4 Sustainability of biodiesel production .....	11
1.4.1 Current oil feedstocks and their implications .....	11
1.4.2 Towards a circular economy .....	14
1.4.2.1 Waste-cooking oil as feedstock .....	14
1.5 Abundance of lignin biomass waste .....	15
1.5.1 Structure of lignin .....	16
1.5.2 Extraction methods.....	17
1.5.2.1 The Kraft pulping method.....	18
1.5.2.2. The sulphite pulping method .....	19
1.5.3 Applications of lignin .....	19
1.5.3.1 In biofuels .....	19
1.5.3.2 In biodiesel catalysis .....	20
1.6 Statement of problem .....	21

<b>Chapter 2- Experimental procedures .....</b>	<b>23</b>
<b>2.1 Collection of samples.....</b>	<b>23</b>
<b>2.2 Synthesis of lignin-derived catalysts .....</b>	<b>23</b>
2.2.1 Synthesis of acid catalyst .....	23
2.2.2 Synthesis of basic catalyst via molten salts .....	23
2.2.3 Synthesis of basic catalyst via base treatment .....	24
<b>2.3 Biodiesel synthesis and reusability procedure .....</b>	<b>24</b>
2.3.1 Biodiesel synthesis via conventional heating .....	24
2.3.2 Catalyst recovery and reusability procedure .....	25
<b>2.4 Characterisation techniques .....</b>	<b>25</b>
2.4.1 Scanning electron microscopy (SEM) .....	25
2.4.2 Fourier transform infrared spectroscopy (FTIR).....	26
2.4.3 Brunauer-Emmett-Teller (BET).....	26
2.4.4 X-ray photoelectron microscopy (XPS) .....	26
2.4.5 Thermogravimetric analysis (TGA).....	26
2.4.6 Zeta potential.....	27
2.4.7 Titrations.....	27
2.4.7.1 Titration for SO <sub>3</sub> H groups.....	27
2.4.7.2 Titration for total acid groups.....	27
2.4.7.3 Titration for free fatty acids in WCO .....	27
2.4.8 Proton nuclear magnetic resonance spectroscopy ( <sup>1</sup> H NMR).....	28
<b>2.5 Kinetic studies .....</b>	<b>28</b>
 <b>Chapter 3- Results and discussion of acid catalysts .....</b>	 <b>30</b>
<b>3.1 Characterisation of catalysts .....</b>	<b>30</b>
<b>3.2 Calculation of biodiesel conversion.....</b>	<b>33</b>
3.2.1 Quantitative characterisation of biodiesel .....	33
3.2.2 Qualitative characterisation .....	36
<b>3.3 Can extracted lignin catalyse biodiesel synthesis? .....</b>	<b>37</b>
3.3.1 Synthesis of a sulphonated softwood lignin catalyst .....	39
3.3.2 Characterisation of sulphonated softwood lignin catalyst (SSL) .....	42

3.4 Optimisation of reaction parameters .....	46
3.5 Kinetics and reusability .....	55
3.5.1 Reaction kinetics .....	55
3.5.2 Reusability studies.....	58
Chapter 4- Lignin-derived base catalysts .....	60
4.1 Molten salt carbonisation and activation .....	60
4.2 Base-catalysed chemical activation of lignin .....	62
4.2.1 Designing the synthesis method .....	63
4.2.2 Characterisation of 0.5-NSL catalyst .....	64
4.3 Optimisation of parameters.....	66
Chapter 5- Conclusion and future works .....	71
5.1 Conclusion .....	71
5.2 Future works .....	72

## List of figures

- Figure 1.1. (a)** Fossil fuel extraction process of coal, oil and natural gas, deposited within the layers of the earth's crust. **(b)** Chart of the gigatonnes (Gt) of CO<sub>2</sub> equivalent emissions released in 2022 by different energy sources and processes, with fossil fuel-derived coal, oil and gas making up over 80% of emissions (figure adapted from IEA, 2022). .....2
- Figure 1.2.** General reaction for the transesterification of triglycerides, forming fatty acid methyl ester, also known as biodiesel. ....3
- Figure 1.3. (a)** Base-catalysed transesterification mechanism, adapted from Meher et al. (2006) **(b)** Saponification reaction between sodium hydroxide and FFA's, adapted from Chanakaewsomboon et al. (2020). .....6
- Figure 1.4.** Acid-catalysed transesterification mechanism. ....7
- Figure 1.5.** Structure of lignin and its alcoholic monolignol monomers and their corresponding structural units: syringyl (S), guaiacyl (G) and hydroxyphenyl (H). ....16
- Figure 3.1. (a)** SEM images of corn stover, maple, poplar and softwood lignin at 9700x magnification with 10kV, legend showing 8µm. **(b)** FTIR spectra of corn stover, maple, poplar and softwood lignin samples showing characteristic vibrations of lignin, as well as sulphonic acid group vibrations .....31
- Figure 3.2. (a)** Structures of oleic acid and methyl oleate depicting the alpha-methylene and methoxy protons. **(b)** <sup>1</sup>H NMR spectra of oleic acid and biodiesel illustrating the singlet at 3.7 ppm pertaining to the methoxy protons of methyl oleate. ....34
- Figure 3.3. (a)** <sup>1</sup>H NMR spectra for all samples ranging between 0-100% methyl oleate content. The arrow showing the increase in the singlet at 3.7 ppm as methyl oleate content increases. **(b)** <sup>1</sup>H NMR spectra for 0, 50 and 100 % methyl oleate standard samples, highlighting the formation of a singlet at 3.7 ppm as the methyl oleate content increases. **(c)** Standard curve and equation used to determine the biodiesel conversion. The curve was constructed using known amounts of oleic acid and methyl oleate. ....35
- Figure 3.4.** FTIR spectra of oleic acid and biodiesel (methyl oleate), representing the characteristic vibrations associated with each material. ....37
- Figure 3.5.** Preliminary biodiesel reactions of each lignin sample with **(a)** waste-cooking oil (FFA=4.74%). **(b)** oleic acid. ....38
- Figure 3.6.** Proposed mechanism of sulphonation, adapted from Glennie, D. W. (1971) .....40
- Figure 3.7. (a)** Titration results of softwood lignin sulphonated at 180 °C for 3, 6, 9, 12, 24 hours. **(b)** Trial biodiesel reactions using the 6, 9, and 12 hour Tso-SL catalysts reacted with 1:6 oleic acid to methanol ratio, 5 wt% catalyst loading at 90 °C for 1 hour. **(c)** Varied weight ratios of p-TsOH and lignin reacted for 9 hours and applied in esterification of oleic acid in maximum conditions of 1:24 oleic acid to lignin ratio, 5 wt% catalyst loading at 90 °C for 3 hours. **(d)** 2:1 SSL catalyst in

the esterification of waste-cooking oil and oleic acid using maximum reaction conditions of 1:24 oleic acid to lignin ratio, 5 wt% catalyst loading at 90 °C for 3 hours. ....41

**Figure 3.8.** (a) FTIR spectra of softwood lignin and p-TsOH precursors as well as SSL, demonstrating the sulphonic acid vibrations of catalyst. (b) N<sub>2</sub> adsorption/desorption isotherm and BET surface area of softwood lignin precursor and (c) SSL catalyst. ....43

**Figure 3.9.** (a) XPS survey scan revealing 533eV, 285eV and 169eV binding energies corresponding to oxygen (O1s), carbon (C1s) and sulphur (Sp2) respectively. (b) Deconvoluted o1s peak. (c) Deconvoluted C1s peak. (d) Deconvoluted S2p peak. ....44

**Figure 3.10.** Proposed Fischer Esterification mechanism for the sulphonic acid-catalysed esterification. ....46

**Figure 3.11.** (a) corn stover-catalysed and (b) SSL catalysed biodiesel conversion results when varying oleic acid to methanol molar ratio .....49

**Figure 3.12.** (a) corn stover-catalysed and (b) SSL catalysed biodiesel conversion results when varying catalyst loading as a percent of the weight of oleic acid. ....50

**Figure 3.13.** Biodiesel conversions against time for 70 °C, 80 °C, 90 °C reactions for (a) corn stover (b) SSL catalyst. ....52

**Figure 3.14.** Biodiesel conversions of (a) corn stover (using 1:3, 5 wt%) and SSL catalyst (using 1:9, 3 wt%) with 5% FFA (WCO), 20% FFA, 50% FFA oil feedstocks reacted at 90 °C for 30 minutes, showing tolerance to triglycerides in oil feedstock. (b) corn stover using 1:3, 5 wt% and SSL using 1:9, 3 wt% catalysts with waste-cooking oil (FFA=5%), demonstrating transesterification capabilities. ....54

**Figure 3.15.** Kinetic studies of (a) corn stover at optimal conditions of 1:3, 5 wt%, fit into pseudo-first order kinetic model. (b) corn stover at optimal conditions of 1:3, 5 wt% fit into second order kinetic model. (c) SSL catalyst at optimal conditions of 1:9, 3 wt% fit into pseudo-first order kinetic model. (d) SSL catalyst at optimal conditions of 1:9, 3 wt% fit into second order kinetic model. ....56

**Figure 3.16.** Reusability studies for 4 reaction cycles highlighting the direct relationship between sulphonic sites ( $y_2$ ) and methyl oleate conversion ( $y_1$ ) in (a) corn stover-catalysed esterification using 1:3, 5 wt%, at 90 °C for 30 minutes. (b) SSL-catalysed esterification using 1:9, 3 wt% at 90 °C for 30 minutes. ....58

**Figure 4.1.** <sup>1</sup>H NMR spectra of MS1, MS2, MS3 catalysts synthesised at 600 °C reacted using 1:72 oil to methanol molar ratio, 5 wt% catalyst loading at 90 °C for 3 hours with canola oil, as well as MS3 reaction with WCO, showing no biodiesel conversion of any molten salt catalyst. 61

**Figure 4.2.** Proposed mechanism of NaOH-catalysed depolymerisation of lignin, adapted from Roberts et al. (2011). ....62

**Figure 4.3.** Biodiesel conversions of lignin treated with 0.01, 0.1, 0.25, 0.5 M NaOH, reacted with canola oil using 1:36 oil to methanol ratio, 5 wt% catalyst loading at 90 °C for 3 hours. ....63

**Figure 4.4.** FTIR spectra of 0.5-NSL catalyst and softwood lignin precursor, showing changes in peaks .....64

**Figure 4.5. (a)** Biodiesel conversions catalysed by 0.5-NSL when carrying the oil to methanol ratio at 1:20, 1:30, 1:36 and using 5 wt% catalyst loading reacted at 90 °C for 3 hours. **(b)** Biodiesel conversions catalysed by 0.5-NSL in loadings of 1, 2.5, 5 and 7 wt%, using a 1:30 oil to methanol ratio, reacted at 90 °C for 3 hours, demonstrating significant error bars and deviations from usual catalytic behaviour. ....67

**Figure 4.6.** Revised synthesis method of 0.5-NSL catalyst substituting rotary evaporation of solution with dialysis purification .....68

**Figure 4.6.** Biodiesel conversions of 0.5-NSL catalysts purified by dialysis, when varying catalyst loading at 1, 2.5, 5, 7 wt%, using a 1:30 oil to methanol molar ratio, reacted at 90 °C for 3 hours, showing unacceptable results due to batch-to-batch variation .....69

## List of tables

<b>Table 1.1.</b> Biodiesel standards outlined in EN 14214 and ASTM D6751.....	10
<b>Table 3.1.</b> Titration results depicting the amount of sulphonic acid and other acid sites on the surface of corn stover, maple, poplar and softwood lignin.....	32
<b>Table 3.2.</b> The oleic acid to methanol molar ratio, catalyst loading (wt%) with respect to OA mass, temperature (°C) and reaction time (hours) parameters varied in the one-factor-at-a-time (a) optimisation of corn stover catalyst and (b) optimisation of the SSL catalyst.....	47
<b>Table 3.3</b> Summary of catalytic properties and optimal esterification reaction parameters for corn stover catalyst, SSL catalyst and softwood lignin precursor, highlighting the effectiveness of the sulphonation process.....	53
<b>Table 3.4.</b> Rate constants and regression analysis ( $R^2$ ) of corn stover and SSL catalyst kinetic studies at 70 °C, 80 °C, 90 °C.....	57
<b>Table 4.1.</b> Ratio of molten salts employed and their corresponding labels.....	61
<b>Table 4.2.</b> Average pH across 10 batches of 0.5-NSL catalyst dialysis water. pH taken after 12 hour dialysis days, showing decreasing pH, indicating aqueous basic residues ( $\text{OH}^-$ ) being separated .....	68

## List of abbreviations

BET	Brunauer, Emmett and Teller
FAEE	Fatty acid ethyl esters
FAME	Fatty acid methyl esters FFAs Free fatty acids
FFA	Free fatty acids
FT-IR	Fourier-transform infrared spectroscopy
NMR	Nuclear magnetic resonance
OA	Oleic acid
TGA	Thermogravimetric analysis
TsOH	<i>p</i> -toluenesulphonic acid
SSL	sulphonated softwood lignin
WCO	Waste-cooking oil
XPS	X-ray photoelectron spectroscopy
0.5-NSL	Softwood lignin treated with 0.5 M NaOH

# Chapter 1- Introduction

## 1.1- Fossil fuels

The widespread adoption of fossil fuels as a primary energy source can be traced back to the Industrial Revolution in the late 18th century. Since then, their domination of the energy market has had catastrophic ramifications on the environment. Fossil fuels are decomposed remains of flora and fauna deposited in the Earth's crust and comprise long hydrocarbon chains along with some amounts of sulphur, nitrogen and oxygen. Upon combustion, these compounds oxidise into greenhouse gases, notably sulphur dioxide, nitrogen oxides, carbon monoxide and carbon dioxide. Since the fossil fuel deposits cannot be replenished at the same rate they are used, fossil fuels are considered to be 'non-renewable'. The overconsumption of non-renewable fossil fuels resulting from human activity in the last 100 years has drastically increased the atmospheric concentrations of the aforementioned primary pollutants. In turn, this has caused severe damage to the earth's atmosphere and ozone layer, hailing fossil fuel energy as a primary contributor to climate change. According to the World Energy Outlook 2022 report by the International Energy Agency, fossil fuel energy continues to dominate the energy market, releasing a total of 34 Gt of CO<sub>2</sub> equivalent emissions in 2022, contributing over 80% of the total emissions released that year<sup>1</sup> (**Figure 1.1**). With the global energy demand expected to increase 1.3% per year until 2040, the projected amount of anthropogenic CO<sub>2</sub> is of great international concern<sup>2</sup>. On top of the detrimental effects the burning of fossil fuels has on the environment, their finite non-renewable resource will eventually approach depletion, expected to be as early as the next 50-100 years, posing a significant threat to future generations<sup>3</sup>. This threat has been known for quite some time, nonetheless, global policies like the Paris Agreement (2015), enforcing 45% reduction in

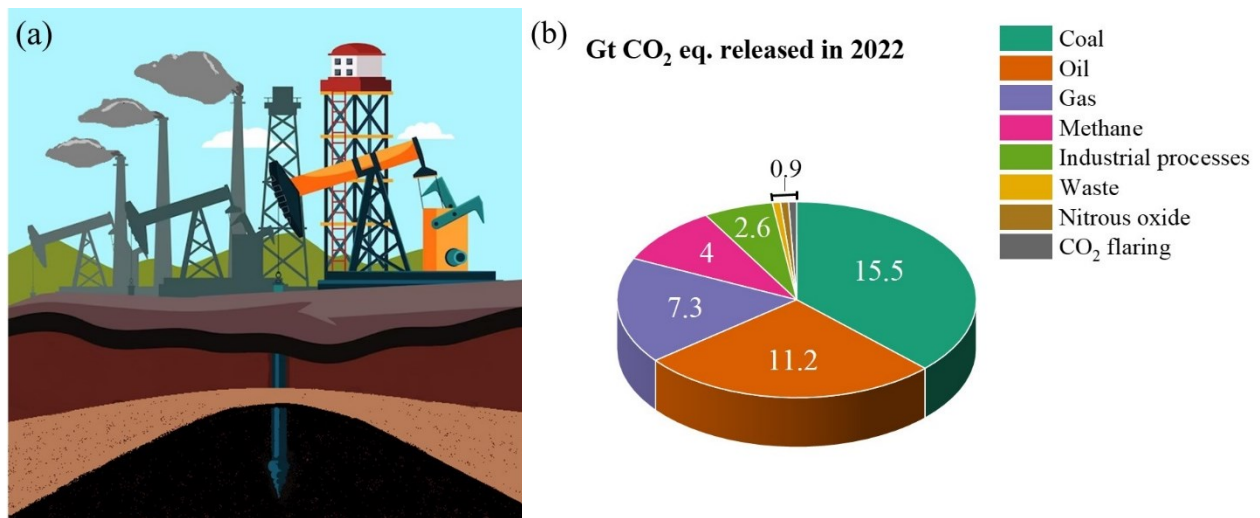


**Figure 1.1.** (a) Fossil fuel extraction process of coal, oil and natural gas, deposited within the layers of the earth's crust. (b) Chart of the gigatonnes (Gt) of CO<sub>2</sub> equivalent emissions released in 2022 by different energy sources and processes, with fossil fuel-derived coal, oil and gas making up over 80% of emissions (figure adapted from International Energy Agency (2022)).

emissions by 2030, and net zero by 2050 have been instated to address the climate crisis and prompt the transition to clean, equally-energy efficient, renewable energy sources. The current promising renewable energy sources are solar power, hydro power, wind power and biofuels. The latter, consisting of bioethanol and biodiesel, has garnered particular interest as a direct replacement for fossil fuels, and has seen significant increases in production over the last 30 years.

## 1.2 Biodiesel

### 1.2.1 What is biodiesel?

The term *biodiesel* first debuted in 1984, however, the invention of the diesel engine dates back to the 1890's<sup>4</sup>. Following its inception, it was known that the diesel engine could run on an array of fuels, including vegetable oil. However, owing to the limitations of engines at the time and the widespread availability of petroleum, the potential of vegetable oil as a fuel source remained untapped. The first use of biodiesel wasn't until 1937, when a patent for an ethyl ester derived from

palm oil was granted to fuel a passenger bus. Since then, research and production of biodiesel has seen substantial increases, with over 45000 M litres produced in 2021, and projections of over 60000 M litres expected for 2027<sup>5</sup>. Biodiesel shows promise as a direct replacement of fossil fuel-derived diesel as it shares the same physicochemical properties. In fact, biodiesel has demonstrated better combustion efficiency, lower sulphur content, higher cetane number, higher biodegradability, higher flash point and improved lubrication properties compared with the fossil fuel alternative<sup>6-10</sup>. The emissions from biodiesel also differ from those released by fossil fuels, with researchers finding decreased hydrocarbon, carbon monoxide and particulate matter amongst biodiesel and diesel blends<sup>11</sup>. Notably, emission of carbon monoxide - a volatile gas that threatens the balance of the atmospheric gases - arises from incomplete combustion and varies amongst different fuel sources<sup>12</sup>. This decreased emission of carbon monoxide by biodiesel is attributed to the increased presence of oxygen, encouraging the oxidation of CO during engine exhaust<sup>13</sup>. However, due to the lower energy by volume, as well as poor lubrication, pure biodiesel is rarely used in engines<sup>14</sup>. Instead, blends upward of 20% biodiesel are used to retain engine efficiency whilst reducing greenhouse gas emissions<sup>15</sup>.

### 1.2.2 Synthesis of biodiesel

Biodiesel synthesis methods include pyrolysis (thermal cracking), microemulsifications and transesterification<sup>16,17</sup>. The latter is the most common method used in large scale production due to its simplicity and cost-effectiveness<sup>17-19</sup>. It involves the reaction between one mole of triglycerides with three moles of alcohol, forming three moles of fatty acid methyl or ethyl ester

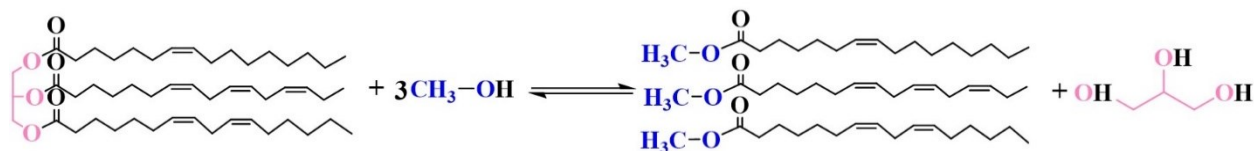


**Figure 1.2.** General reaction for the transesterification of triglycerides, forming fatty acid methyl ester, also known as biodiesel.

and one mole of glycerol as a by-product (**Figure 1.2**). Both ethanol or methanol can serve as the primary alcohol, however, methanol takes precedence in biodiesel production due to its cost-effectiveness and superior efficiency<sup>20</sup>. Whilst methanol's affordability, attributed to its fossil fuel origins, makes it an economically appealing choice, it negates the ecological benefit of biodiesel production<sup>21</sup>. In contrast, the employment of bioethanol in generating fatty acid ethyl esters (FAEE) could improve the sustainability and ecological feasibility of biodiesel production. However, the transesterification reaction between triglycerides and ethanol requires higher energy demand and increased concentrations of ethanol compared to that of methanol<sup>20</sup>. This arises from the steric hindrance encountered by ethanol during the first steps of transesterification involving ethoxide formation and nucleophilic attack on the triglyceride carbonyls resulting in elevated reaction times. Since the reaction is reversible, an excess amount of methanol is used to shift the equilibrium to the product side. Stoichiometrically, a 1:3 oil to methanol molar ratio is required, however, a minimum of 1:6 is typically employed on lab and production scales. To further improve the reaction rate, a catalyst is employed throughout the process, dividing the first step of the transesterification mechanism into acid-catalysed and base-catalysed transesterification.

## **1.3 Catalysts in biodiesel production**

### **1.3.1 Homogeneous catalysts**

Catalysts are widely applied in chemical reactions in order to increase the reaction rate by the lowering of the activation energy required, in turn decreasing the reliance on exceeding stoichiometric amounts to drive the reaction forward. By definition, homogeneous catalysts are present in the same physical phase as the reactants, undergoing ionisation upon dissolution in

solvents. Consequentially, the major drawback of homogeneous catalysts is their inability to be recovered and reused without requiring further purification methods.

### 1.3.1.1 Homogeneous base catalysts

Currently, commercial biodiesel production employs homogeneous catalysts, typically strong bases such as NaOH or KOH, as they are relatively cheap, readily available and can catalyse the transesterification reaction under mild reaction conditions at ambient pressure and temperatures as low as 60 °C within fast reaction times often around 1 hour<sup>22</sup>. This is possible due to the kinetically favourable reaction mechanism, proceeding as follows **(Figure 1.3 (a))**<sup>23</sup>: the formation of methoxide by deprotonation of methanol by NaOH/KOH, followed by nucleophilic attack by methoxide on the carbonyl of the triglyceride. This yields a tetrahedral intermediate, prompting the reformation of the carbonyl, generating a leaving group, forming a fatty acid methyl ester and remaining diglyceride. This mechanism repeats twice more, converting diglycerides to monoglycerides and then finally to biodiesel and glycerol. A major drawback of using strong basic catalysts is the sensitivity to free fatty acids (FFA's) found in most oil feedstocks. Upon dissociation of the NaOH or KOH, Na<sup>+</sup> and K<sup>+</sup> ions interact with free fatty acids to form a metal salt, also known as soap, a significant contaminant in the final product **(Figure 1.3 (b))**<sup>24</sup>. In order to isolate the biodiesel product from the crude mixture of methyl esters, glycerol and soap, substantial amounts of wastewater are often required, adding to the already extensive purification steps required for homogeneous catalysts. Not only does this hinder the biodiesel process from being sustainable with regards to water use, but it also significantly lowers the final yield of biodiesel.

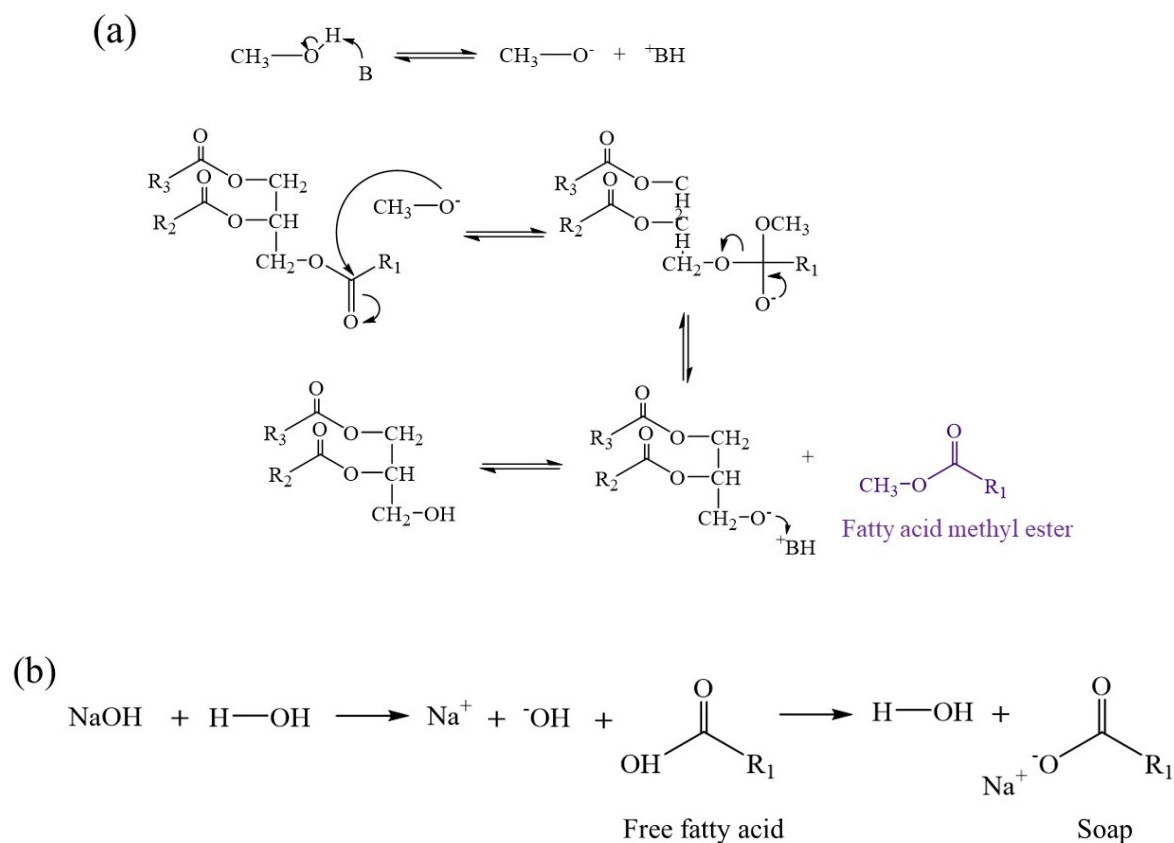


**Figure 1.3.** (a) Base-catalysed transesterification mechanism, adapted from Meher et al. (2006) (b) Saponification reaction between sodium hydroxide and FFA's, adapted from Chanakaewsomboon et al. (2020).

### 1.3.1.2 Homogeneous acid catalysts

Conversely, acid catalysts not only exhibit a tolerance to FFA content but are also able to catalyse the esterification of FFA's into their methyl esters. However, this does not take place concurrently with the transesterification, which exhibits slow kinetics, proceeding as follows (**Figure 1.4**)<sup>23</sup>: first, protonation of the carbonyl oxygen by acid catalyst takes place, forming a tertiary carbocation via resonance. This permits the subsequent nucleophilic attack on the positively charged carbon by the methanol lone electron pair, forming a tetrahedral intermediate. After proton transfers and removal of the leaving group, the carbonyl reforms to produce FAME and a diglyceride. Like the base-catalysed mechanism, this process repeats twice more until reaction completion renders a mix

of FAME and the glycerol by-product. Whilst there is no risk for the saponification reaction, acid-catalysed transesterification involves kinetically unfavourable intermediate structures, prolonging reaction times and increasing temperature and methanol amount required for the reaction to take place, rendering them less economically feasible than the basic alternative<sup>25</sup>. Despite the economic and environmental strain of multi-stage processing and purification resulting from the use of basic and homogeneous catalysts, they remain the preferred choice of catalyst in biodiesel production due to their simple and efficient conversion of oils into biodiesel. Nonetheless, the unsustainability of these catalysts prompted research to shift to heterogeneous catalysts.

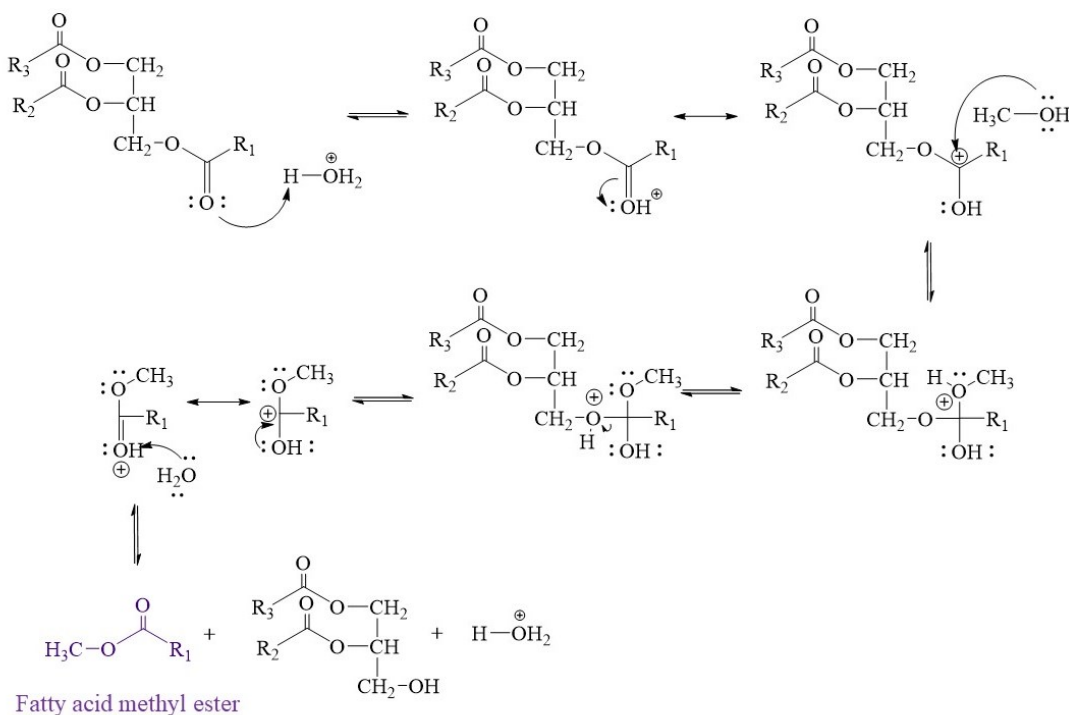


Figure 1.4. Acid-catalysed transesterification mechanism.

### 1.3.2 Heterogeneous catalysts

Heterogeneous catalysts, by definition, are in a different physical phase from the reactants in the reaction. Due to this, a mass transfer limitation is experienced between the phases of the reaction system, resulting in a low reaction rate. In turn, heterogeneously catalysed transesterification often

requires increased amounts of methanol, catalyst loadings up to 15 wt% and higher reaction temperatures and times compared to the homogeneous counterparts<sup>25</sup>. Conversely, being in a different phase allows for the catalyst to be separated post-reaction completion and reused in subsequent reactions cycles, reducing the overall cost and easing purification required for product extraction.

### **1.3.2.1 Heterogeneous base catalysts**

The prominent classes of heterogeneous basic catalysts reported for the transesterification reaction can be classified into transitional metal oxides, mixed metal oxides, alkaline earth metal oxides, basic zeolites and hydrotalcites<sup>19,26,27</sup>. Amongst these, the most studied metal-oxide base is calcium oxide (CaO) due to the negative oxygen acting as a strong Brønsted base, promoting enhanced catalytic activity whilst maintaining low solubility in methanol<sup>28</sup>. Beneficially, CaO catalysts can be derived from a multitude of biomass sources such as eggshells, oysters and animal bones, showing promise as a low-cost, sustainably sourced catalyst<sup>26,29,30</sup>. Despite the attractive efficiency and sustainability of CaO catalysts, some drawbacks associated with basic catalysts arise. The proton-accepting nature of metal oxide catalysts makes them susceptible to the undesired saponification reaction, imposing supplementary purification, which increases the overall cost of catalyst employment. Moreover, there is also the risk of metal leaching, which leads to catalyst site deactivation, hindering the reusability potential of the catalyst.

### **1.3.2.2 Heterogeneous acid catalysts**

Due to their tolerance of FFA's and ease of separation from product, heterogeneous acid catalysts have been exhaustively studied in biodiesel applications. Some of the most investigated solid acid catalysts in biodiesel are acidic mixed metal oxides, sulphated metal oxides and sulphonated solids<sup>26,31</sup>. Of particular interest, sulphonated solids derived from biomass have garnered interest

in their cost-effective sustainable sourcing and upcycling of biomass waste. The Brønsted and Lewis acid sites within these catalysts facilitate the esterification and transesterification reactions, but not simultaneously due to the slow kinetics exhibited in transesterification<sup>23</sup>. Therefore, harsher reaction conditions are required in contrast to solid basic catalysts<sup>32,33</sup>. Additionally, as seen with metal oxide basic catalysts, sulphated metal oxides as well as sulphonated carbons may also undergo leaching of active sites, diminishing the potential to separate and reuse them. Nonetheless, their catalytic capabilities in the esterification of FFA's promotes their employment in two-step conversions of low-grade oils with high FFA content into biodiesel<sup>30</sup>.

### **1.3.3 Influence of catalyst on biodiesel quality**

The physiochemical properties and overall quality of biodiesel are determined and subject to regulation by a set of government standards, ASTM D6751 and/or EN 14214<sup>34,35</sup>. The quality of biodiesel needed to attain these standards is significantly influenced by the biodiesel production process<sup>36</sup>. This encompasses various reaction parameters such as the catalyst type and loading amount, the choice of oil precursor, the methanol content and the energy input. The established standards outlined in **Table 1.1** hold the critical purpose of ensuring that the biodiesel produced can be safely and efficiently used in diesel engines. Certain biodiesel properties, notably metal content, methanol content and acid value should be carefully accounted for in the design and application of a catalyst. For example, the biodiesel product must adhere to a maximum allowable concentration of 5.0 mg/kg for alkali and alkaline earth metals. Consequently, the utilisation of heterogeneous catalysts possessing substantial amounts of these groups can exacerbate the risk of metal leaching and incorporation into the biodiesel product. This can lead to concentrations surpassing the stipulated limit, regardless of purification efforts. Furthermore, given that

Table 1.1. Biodiesel standards outlined in EN 14214 and ASTM D6751.

Property	Units	EN 14214	ASTM D6751
<b>Ester content</b>	% (m/m)	96.5	-
<b>Density at 15 °C</b>	kg/m <sup>3</sup>	860-900	880
<b>Viscosity at 40 °C</b>	mm <sup>2</sup> /s	3.5-5.0	1.9-6.0
<b>Cetane number</b>	-	Min. 51	Min. 47
<b>Acid value</b>	(mg KOH/g)	Max. 0.50	Max. 0.50
<b>Methanol content</b>	% (m/m)	Max. 0.20	Max. 0.20
<b>Free glycerol</b>	% (m/m)	Max. 0.02	Max. 0.02
<b>Total glycerol</b>	% (m/m)	Max. 0.25	Max. 0.24
<b>Monoglyceride</b>	% (m/m)	Max. 0.70	Max. 0.40
<b>Alkaline metals (Na<sup>+</sup>, K<sup>+</sup>)</b>	mg/kg	Max. 5.0	Max. 5.0
<b>Alkaline earth metals (Ca<sup>2+</sup>, Mg<sup>2+</sup>)</b>	mg/kg	Max. 5.0	Max. 5.0

heterogeneously catalysed biodiesel production typically requires higher amounts of methanol, there is an inherent chance of elevated methanol concentrations within the final purified product. Depending on the amount of methanol, this concentration may exceed the permissible maximum value of 0.20% (m/m). Another essential biodiesel property to consider is the acid value, closely related to the content of unreacted free fatty acids present in the biodiesel product. If the chosen oil precursor contains notable amounts of free fatty acids and is paired with an acid catalyst incapable of catalysing their complete esterification, the biodiesel product may retain a high acid value. Biodiesel with a high acid value has demonstrated the potential to result in significant engine deposits due to depolymerisation at elevated temperatures<sup>37</sup>. These described interplays highlight how the design of a heterogeneous catalyst extends beyond the impact of reaction efficiency to the quality of biodiesel produced, directly influencing the engine performance and overall safety of operation<sup>36</sup>.

## **1.4 Sustainability of Biodiesel production**

### **1.4.1 Current oil feedstocks and their implications**

Biodiesel, a promising alternative to fossil fuels, can be manufactured from various sources including vegetable oils, animal fats and microalgae, and must adhere to EU and ASTM standards of physicochemical properties<sup>38</sup>. The selection of feedstock for biodiesel production varies amongst countries, influenced by factors such as cost-effectiveness, local availability and impact on the environment<sup>39</sup>. Currently, the USA reigns as the largest producer of biodiesel, employing refined vegetable oils like canola, soybean and corn oil constituting 95% of biodiesel feedstock<sup>40</sup>. Other major producers such as Brasil, India and Europe also rely on these vegetable oil "first generation feedstocks"<sup>40</sup>. These refined vegetable oils, rich in triglycerides, paired with basic catalysts, demonstrate excellent kinetics in the transesterification reaction, yielding conversions exceeding 95%. Despite their efficient conversion at relatively low temperatures and pressures, these oils have been subject to global debate since the early 2000s<sup>41,42</sup>. The cultivation of crops for these edible oil feedstocks competes for agricultural land crucial for feeding a growing population, posing a threat to food security. Consequently, the prices for these oils have become inflated, contributing a staggering 88% of the total biodiesel production expenses<sup>43</sup>. Presently, the high cost associated with biodiesel production diminishes economic and financial incentive to shift from the perfected technology of fossil fuel energy, limiting its global adoption. Moreover, the expansion of crops like canola, soybean and palm for biodiesel production contributes to climate change by replacement of biodiverse regions with monoculture farming<sup>44</sup>. For example, palm oil dominates as a biodiesel feedstock in Asia, primarily exported by Indonesia and Malaysia. Whilst it is considered renewable, its sustainability is compromised by the displacement of virgin rainforests with palm plantations<sup>45</sup>. Similarly, soybean cultivation in South America has furthered the

destruction of the Amazon Rainforest<sup>46</sup>. Whilst some publications note biodiesel as having "net zero carbon emissions" due to the compensation of CO<sub>2</sub> absorption by the biomass origins of biodiesel fuels, the true sustainability must consider agricultural practices, energy and water required to harvest the oil feedstocks<sup>47,48</sup>. This was brought to light in 2009 by Europe's Renewable Energy Directive (RED) policy, which aimed to promote renewable fuels over fossil fuels but overlooked land repurposing and the ensuing emissions associated. Modelling studies released by the European Commission in 2012 and 2016 revealed that vegetable oil-based biodiesel emits more CO<sub>2</sub> than fossil fuels due to indirect land use emissions<sup>49</sup>. To address this, the European Union introduced Renewable Energy Directive II, which factors in land use emissions and the entire biodiesel supply life cycle<sup>49</sup>. All in all, the choice of edible oils as biodiesel feedstock significantly increases the costs and environmental strains of biodiesel production, hindering its adoption on a global scale.

Environmental concerns, food security risks, geopolitical uncertainties and the limited sustainability of edible oil feedstocks have spurred interest in alternative options. Non-edible plants like *Jatropha*, *Neem*, Rubber seed and *Moringa* offer cost-effective biodiesel alternatives, without competition with the food market<sup>50-53</sup>. Oil feedstocks derived from these non-edible plants are classified as "second generation" and can be cultivated in non-agricultural land under diverse conditions<sup>54</sup>. Non-edible plants can be harvested in arid zones typically unsuitable for food crops due to the low moisture, and also in rainy environments. Their cultivation requires less farmland compared to that of edible crops, offering potential for marginal land restoration<sup>55</sup>. Economically, non-edible crop cultivation can uplift rural non-farming areas and offer employment, alleviating poverty<sup>18</sup>. The potential environmental and economic benefit has been exhibited in India - a major oil importer. In recent years, non-edible *Jatropha* oil extracted from the *Jatropha* plant, which is

native to India, has demonstrated successful conversions to biodiesel, prompting dedication of land for its cultivation<sup>56</sup>. Subsequently, the National Rural Employment Guarantee Scheme in India has offered a surplus of unskilled agricultural labour employment in rural areas, contributing to improved societal and economic welfare<sup>57</sup>. Of course, the aggressive cultivation of non-edible plants would propose similar environmental concerns as those associated with edible crops today. The source of oil feedstock also influences the physicochemical properties of its biodiesel derivatives, due to the different oxygen content and composition amongst plants<sup>58</sup>. For instance, Moringa plant seeds harvested in arid regions, yield oil that produces biodiesel with higher cetane numbers and oxidative stability compared to that of other non-edible oil derived biodiesel<sup>53,59</sup>. The shift to non-edible oil feedstocks minimises the negative ramifications associated with cultivation of edible oils, paving a path to cleaner and more sustainable energy solution, while also promoting socio-economic wellbeing. Another way to do this is to employ waste-cooking oil as the oil feedstock. Whilst technically considered vegetable oil, its status as 'waste' negates almost all environmental and economic costs faced by first generation feedstocks. The composition of waste-cooking oil (WCO) relies heavily on the duration of use as upon heat, triglycerides undergo hydrolysis into their FFA chains. Given this, many studies have explored the transesterification as well as the two-step conversion of waste-cooking oil into biodiesel and proven successful<sup>60,61</sup>. The upcycling of what is considered a waste material maximises its utility and is a core principle within the concept of a circular economy<sup>45</sup>.

#### **1.4.2 Towards a circular economy**

A circular economy is a conceptual economic system that aims to minimise resource exploitation and prevent waste generation<sup>45</sup>. However, within this concept, there are concerns over practices

promoted as 'sustainable' having negative impacts on the environment. The production of biodiesel from edible oils has fallen subject to this debate, as the environmental strain of harvesting certain types of feedstocks supersede the environmental benefits of renewable biodiesel, as described in Section 1.4. The strengthening of the relationship between sustainability and circular economy is needed in order to streamline and adopt environment-preserving practices. A way to do this is through the implementation of Life Cycle Assessment, a standardised method for quantifying the environmental impacts associated with a material<sup>62</sup>. Analysis conducted on the life cycle of a product encompasses acquisition of raw materials, the production and/or use of a product and the final disposal, investigating the impact on a number of environmental factors and ecosystems throughout.

#### **1.4.2.1 Waste-cooking oil as feedstock**

A strategy that addresses both principles within the circular economy concept is to utilise waste materials. Hence, the employment of waste-cooking oil as a biodiesel feedstock has attracted attention due to the reduced water and energy required in contrast to harvesting edible and non-edible oils. Researchers have also conducted life cycle assessments on biodiesel production from waste-cooking oil, considering raw material transportation, catalyst preparation, pre-treatment of WCO and the transesterification of WCO. Out of these parameters, an assessment by Chung et al. (2019) showed that the transesterification process contributed the highest environmental impact due to the demand for electricity supply<sup>63</sup>. The overall impact of WCO employment was compared to that of Jatropha, a leading non-edible oil feedstock in biodiesel production in Asia, and demonstrated the latter had higher impact on the environment due to the plantation and fertilising of the non-edible crop. Furthermore, the sourcing, disposal and effects of the catalyst were

assessed, comparing the environmental impact of a waste chicken eggshell-derived CaO catalyst with homogeneous KOH. Whilst the eggshell-derived catalyst required high energy for calcination, the biodiesel catalysed by KOH required large amounts of water for purification. In combination with its non-reusable properties, KOH was deemed more harmful to the environment, particularly to aquatic ecotoxicity due to the pH change from wastewater. A crucial element to be considered when comparing life-cycle assessments is the renewability of the electricity used to meet the energy demands of the transesterification reactions, with coal-powered electricity significantly worsening the environmental impact through the release of heavy metals during electricity production<sup>64</sup>. Alternatively, using renewable energy like that of hydro power can lessen the environmental impact score for processes conducted via the same method. Overall, the utilisation of waste-cooking oil as an oil feedstock for biodiesel has been confirmed to minimise waste and environmental pollution and promotes a circular bioeconomy.

### **1.5 Abundance of lignin biomass waste**

In a similar vein, utilising a biomass waste precursor in biodiesel production can alleviate environmental impact and enhance the contribution to circular economy, whilst also aligning with green chemistry principles throughout the process<sup>65</sup>. Whilst the concept of a circular economy prefers the closed-loop regeneration of biomass, the waste of lignocellulosic biomass from the forestry and agricultural industries is produced in excess and seems unavoidable in the foreseeable future due to the capital-intensive nature of these industries<sup>66</sup>.

### 1.5.1 Structure of lignin sources

Lignin, alongside cellulose and hemicellulose, is one of the three major components of the lignocellulosic biomass, providing cell walls of plants with their rigid structure (**Figure 1.5**). Lignin comprises a cross-linked amorphous copolymer primarily composed of three primary phenylpropane monomers: *p*-coumaryl, coniferyl and synapyl alcohol, most commonly linked together by ether and carbon-carbon linkages<sup>67,68</sup>. These monolignols polymerise through oxidative coupling reactions to form lignin, with the resulting polymer described by three main

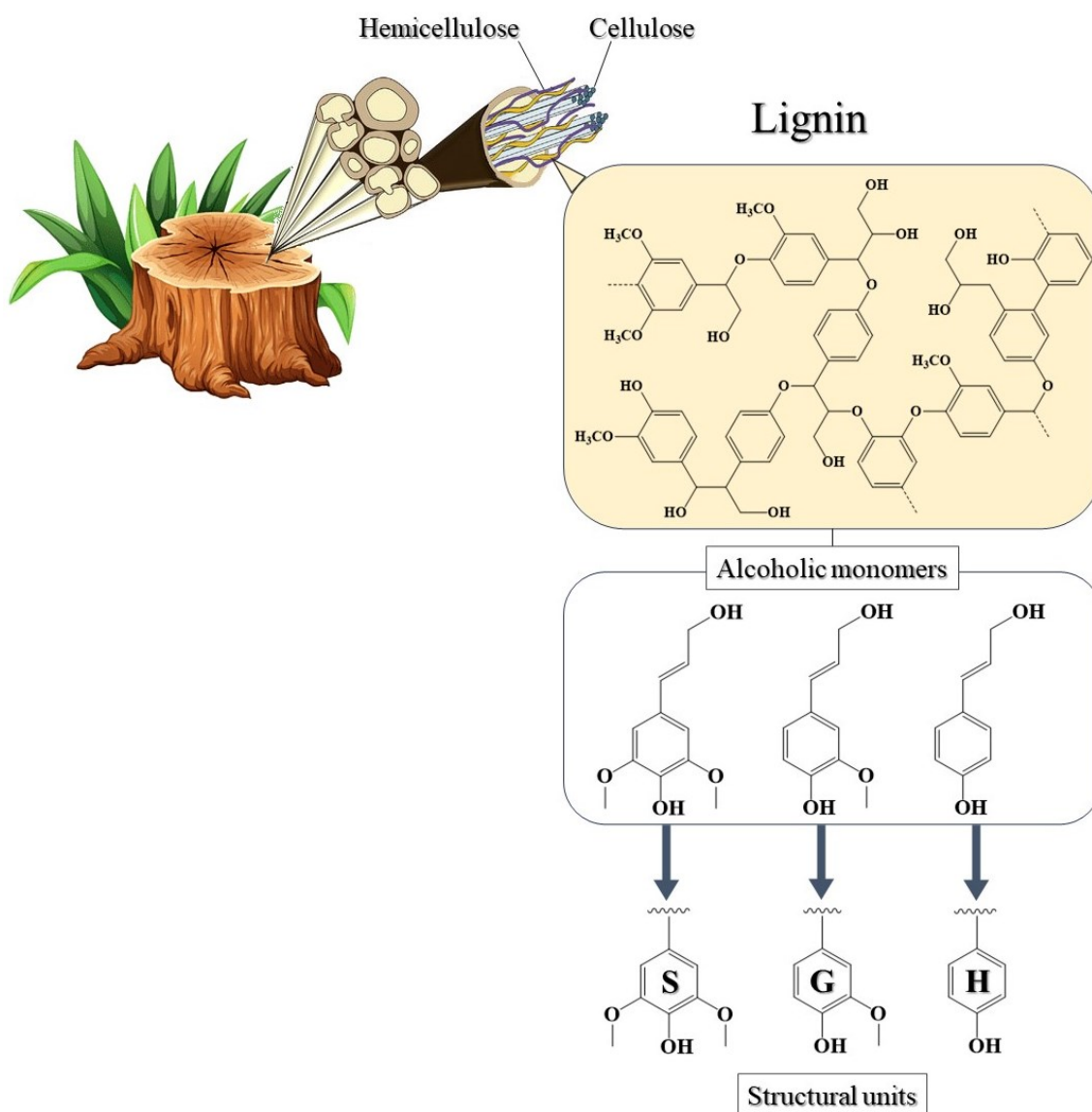


**Figure 1.5.** Structure of lignin and its alcoholic monolignol monomers and their corresponding structural units: syringyl (S), guaiacyl (G) and hydroxyphenyl (H).

structural units: guaiacyl (G), syringyl (S) and *p*-hydroxyphenyl (H) units. The ratio and arrangements of the alcoholic monomer units vary depending on the source of lignin and location of extraction. Softwoods such as pine and spruce, are mainly comprised of the guaiacyl unit, whereas hardwoods like oak and maple, contain a near equal mixture of guaiacyl and syringyl units<sup>67</sup>. The combination of G and S units necessitates increased branching and diverse linkages in hardwoods compared to that seen in the simpler softwood structures. The composition of lignin extracted from grass sources, such as corn and wheat, varies depending on the location (stem, leaf) and type of plant (woody, leafy), however, they typically possess all three alcoholic monomers with dominance of the S unit<sup>69</sup>. The variation of alcohol monomers can dictate the products derived from lignin and the catalytic potential. Lignin contains abundant functional groups including methoxyl, phenolic hydroxyl, aliphatic hydroxyl, benzyl alcohol, noncyclic benzyl ether and carbonyl groups<sup>67</sup>. Additionally, lignin is the most abundant source of natural aromatics, making up 30% of total biosphere carbon. The rich composition of lignin facilitates its application in a multitude of fields including but not limited to adsorption of heavy metals in water, photocatalysis, nanoparticle synthesis, food packaging, in antimicrobial and agricultural sectors<sup>70-72</sup>. However, the complex structure, poor surface-to-volume ratio and impurities leftover from extraction present hurdles in the widescale adoption of lignin derived materials<sup>73</sup>.

### **1.5.2 Extraction methods**

Lignin's intricate and strong hydrogen-bonded structure requires harsh extraction conditions to isolate it from the former lignocellulosic biomass. Consequently, the characteristics and resulting chemical behaviour of extracted lignin can diverge significantly from those inherent to the native lignin found in the wood and plant origins. Various techniques have been developed for extracting

lignin from biomass and can be generally categorised into two primary groups: (1) approaches that involve the degradation of lignin into soluble fragments, which are then separated by extracting the solid residue from solution and (2) methods that selectively degrade polysaccharides, leaving lignin and condensed carbohydrates byproducts as solid residues. The former includes pulping techniques like Kraft, sulphite, soda and organosolv processes, whereas the latter involves dilute acid hydrolysis of lignocellulose. The two common methods employed in industry are the Kraft and sulphite pulping methods.

#### **1.5.2.1 The Kraft pulping method**

The Kraft (sulphate) pulping method stands as the predominant global technique, accounting for 90% of pulp production. Employed by the paper and pulp industry, it involves using strong alkaline solutions, typically sodium hydroxide (NaOH) and sodium sulphide (Na<sub>2</sub>S), for the dissolution of lignin and hemicellulose from wood chips, obtaining the desired strong cellulose fibres, suitable for producing various paper grades. Throughout this pulping process, lignin undergoes two primary reactions: 1. degradation yielding smaller fragments that enhance solubility in water and alkali solutions, and 2. condensation reactions forming alkali-stable linkages that dampen digestion efficiency. The dissolved organic and inorganic components used in pulping exit the reactor as an aqueous stream, containing 15% solid content, referred to as black liquor. The harsh degradation and condensation reactions employed in this process induce significant chemical and structural changes in native lignin, which make the subsequent depolymerisation of Kraft lignin challenging. Despite the potential recovery of Kraft lignin through acidification of black liquor, only 2% of Kraft mills produce commercial lignin for sale. The remaining 98% incinerate the organic content

of black liquor to generate electricity<sup>74</sup>. The intensive energy consumption, the strong chemicals used and the generation of waste have made the Kraft process a subject of concern.

### **1.5.2.2 The sulphite pulping method**

Alternatively, the sulphite pulping process relies on sulphur-driven sulphonation reactions that lead to distinctive hydrolytic pathways, distinguishing the resulting products from those alkali-induced by the Kraft method. The central transformation in sulphite pulping is the sulphonation of lignin, with sulphonic acid introduced to alpha-carbon atoms, enabling lignin hydrolysis. The degree of sulphonation per phenylpropane monomer unit varies, with the liginosulphonates produced in this method having notable elevated sulphur content, ranging from 4-8%<sup>75</sup>. This improves the water-solubility of the lignin produced, resulting in employment of liginosulphonates in various industries such as agriculture and construction. The global production of lignocellulosic waste from agricultural sources like corn stover and wheat straw amount to hundreds of millions of tonnes per annum, exceeding the annual production of the top petrochemicals (ethylene, propylene *p*-xylene)<sup>66</sup>. A core concept of a bio-based circular economy lies in the transformation of waste into valuable products. As the versatility of lignin applications has come to light, the valorisation of the unavoidable lignocellulosic waste into value-added products has been a subject of interest for biorefineries worldwide<sup>76,77</sup>.

## **1.5.3 Applications of lignin**

### **1.5.3.1 In biofuels**

Due to the enriched carbonaceous nature and abundant functional groups, the conversion of lignin to high value-added chemicals has garnered significant interest over the past few decades. Lignin's

aromatic structure enables its depolymerisation through hydrothermal carbonisation, pyrolysis, biomass liquefaction and gasification, yielding high-value phenolic products. However, these processes are often energy intensive, have high investments costs and complex procedures that limit their industrial use<sup>78</sup>. Amongst these conversion techniques, pyrolysis has proven as a notably efficient approach, particularly in the absence of oxygen. The pyrolysis method demonstrates operational simplicity and cost-effectiveness in the conversion of lignin to gases (e.g., H<sub>2</sub>O, CO<sub>2</sub>, H<sub>2</sub>, CH<sub>4</sub>) as well as liquid biofuels comprised of mono and polyphenols. However, the high oxygen content, acidity and corrosiveness resulting from this technique necessitates the further upgrading of oils produced<sup>79</sup>. The pyrolysis method also yields solid activated carbon biochar, which has been investigated as a precursor for functionalised acid and base catalysts<sup>80</sup>.

### **1.5.3.2 In biodiesel catalysis**

Lignin can be functionalised, copolymerised and recombined with a range of chemicals to produce efficient acid, base and supported catalysts. Several lignin-derived heterogeneous acid catalysts have been exhaustively studied for the both the esterification of FFA's and transesterification of triglyceride reactions in biodiesel production. For example, an acid catalyst from sugarcane bagasse was synthesised via sulphonation and applied in the microwave-assisted transesterification of waste cooking oil, yielding 89% of biodiesel within an impressive 15-minute reaction time<sup>81</sup>. Another work carbonised, pyrolysed and sulphonated refined lignin, yielding a highly acidic catalyst that was able to convert >95% of oleic acid and >90% Jatropha oil into biodiesel<sup>82</sup>. However, the conditions required for pyrolysis and carbonisation usually have high energy demands, reaching temperatures over 400 °C for extended periods of time. Additionally, the acid-catalysed transesterification of Jatropha oil in the previously mentioned work required a

temperature of 220 °C and a reaction time of 5 hours, yielding biodiesel with an acid value substantially higher than that outlined in the ASTM and EU biodiesel standards. Remarkably, the integration of sulphonated lignin catalysts has shown cost-effective, more eco-friendly biodiesel synthesis via esterification, owing to the abundant OH, COOH, and SO<sub>3</sub>H functional groups endowed in sulphur pulping extractions<sup>83</sup>. Although, in the absence of high temperatures and reaction times, strong concentrated acids, namely sulphuric acid, are used for further sulphonation processes of lignin, dampening the sustainability of their application. Furthermore, recalling that heterogeneous acids face mass transfer limitations, higher reaction times and methanol amounts are required for sufficient biodiesel conversion.

## **1.6 Statement of problem**

Recognising the critical significance of depleting fossil fuel reserves and the impending imperative for the paradigm shift to renewable alternatives, biodiesel has emerged as a promising candidate. Whilst biodiesel is regarded as sustainable, its production process involves environmentally damaging practices through the employment of edible oil feedstocks and homogeneous basic catalysts, rendering the process environmentally and economically unfeasible. In order to introduce green chemistry principles and alleviate the strain on water and other crucial resources, the oil feedstock selection has expanded to non-edible and waste-cooking oils. Consequently, rapid development of acid catalysts capable of tolerating FFA's has grown, with particular interest in heterogeneous, biomass-derived catalysts. One of the largest produced biomass wastes is lignin-generated in quantities of a 100 million of tonnes by the agriculture and forestry industries. The applications of lignin so far have required concentrated acids, or high energy demands associated

with increased temperatures and reaction times owing to the mass transfer limitation of their heterogeneous nature.

In this work, the synthesis of lignin-derived heterogeneous catalysts were conducted using facile and greener methods for the application in a cost-effective and more sustainable biodiesel synthesis process. Conventional heating was used in both the synthesis of catalyst and the biodiesel process, keeping all temperatures below 180 °C, mindful of the typically high energy needed for lignin processes. Characterisation techniques such as titration, Fourier-transform infrared spectroscopy (FTIR) and X-ray photoelectron spectroscopy (XPS) were crucial in understanding the surface properties and subsequent catalytic mechanism of the lignin catalysts. This work also investigates the optimal reaction parameters, as well as catalyst recovery and reusability potential of the catalyst. This work highlights how the utilisation of sustainable materials like lignin biomass waste can provide improved sustainability to the biodiesel process, whilst reducing energy demands, overall encouraging the widespread adoption of biodiesel.

## **Chapter 2- Experimental procedures**

### **2.1 Collection of samples**

Lignin samples were obtained from the Lavoie Research group at University of Sherbrooke, Sherbrooke, Quebec. The 4 samples used within this work were lignin extractions from corn stover, poplar, maple and softwood sources. Waste-cooking oil was collected from a local restaurant in Montreal.

### **2.2 Synthesis of lignin-derived catalysts**

#### **2.2.1 Synthesis of acid catalyst**

The lignin-derived acid catalyst was synthesised via one-step carbonisation. Briefly, lignin and p-toluene sulphonic acid were added in varying ratios to a Teflon reaction vessel which was sealed in an autoclave and placed in a muffle furnace at the desired temperature and time. Following synthesis, the crude product was manually ground with a mortar and pestle to expose maximum amount of surface area and then transferred to a Buchner funnel where it was washed under vacuum multiple times with deionised water until the pH increased 3 units. The water washed catalyst was then transferred to a 30-mL centrifuge tube for organic washes to be performed in order to remove any remaining impurities. The organic washes were performed for three cycles where mixtures of ethanol and acetone (2:1, 1:1, 1:2 v/v) were added to the centrifuge tube and then vortexed for 30 seconds before centrifugation at 10,000 x g for 10 minutes and the resulting supernatant was discarded. The purified catalyst was then put in an 85 °C oven until it was dry.

### **2.2.2 Synthesis of basic catalyst via molten salts**

One g of lignin was added to a porcelain evaporating bowl, alongside 1:1 molar NaCl:KCl (**MS1**), 1:1:15 molar NaCl:KCl:CaCO<sub>3</sub> (**MS2**) and 3:1:1 molar ZnCl:NaCl:KCl (**MS3**). A lid was placed, loosely covering the bowl and the solid reaction mixture was heated at the desired temperature in a muffle furnace for 2 hours. Following, the solid product was transferred to a 30-mL centrifuge tube and organic washes using the same purification protocol as the acid catalyst (**2.1.1**) were performed. The purified product was then put in an 85 °C oven until it was dry.

### **2.2.3 Synthesis of basic catalyst via base treatment**

In order to depolymerise lignin, 0.5 g of lignin was weighed and transferred to a 20-mL scintillation vial and 20 mL of varied concentrations of sodium hydroxide was added. The vial was sonicated for 10 minutes to obtain a homogeneous dispersion and then transferred to a Teflon vessel sealed inside a hydrothermal autoclave. The reaction mixture was placed in a muffle furnace and heated at 180 °C for 3 hours. Upon completion, the mixture was left to cool to room temperature and then transferred to a 30-mL centrifuge tube and put on dialysis using membrane with a MWCO of 3.5 kD for 3 days. Once the dialysis water achieved a maximum pH of 7.5, the reaction mixture underwent rotor evaporation to remove the solution, leaving the solid crude product. The dried product then underwent organic washes using the same purification protocol as the acid catalyst (**2.1.1**). The purified product was then put in an 85 °C oven until it was dry.

## **2.3 Biodiesel synthesis and reusability procedure**

### **2.3.1 Biodiesel synthesis via conventional heating**

The biodiesel reactions were performed in a 10-mL crimped reaction vial in an oil bath with magnetic stirring and temperature control. To achieve this, varying amounts of lignin-derived catalyst, dependent upon catalyst loading (wt%), was added to methanol and sonicated for 5 min to obtain homogeneous dispersion. The catalyst/methanol solution was then transferred to the 10-mL reaction vial to which 2 mL of oil feedstock (oleic acid or canola oil) was then added and crimp sealed. Following reaction completion, the reaction mixture was transferred to a 15-mL centrifuge tube and centrifuged at 10,000 x g for 5 minutes to separate the biodiesel and aqueous layers. The crude product mixture was put in a 70 °C oven for 12 hours to evaporate the residual methanol and aqueous layer. The remaining lower biodiesel layer was used for <sup>1</sup>H NMR analysis.

### **2.3.2 Catalyst recovery and reusability procedure**

Following layer separation, the biodiesel layer was removed and the catalyst was subject to three washes with n-hexane to remove any residual glycerol and/or biodiesel. The sample was then vortexed for 30 seconds and centrifuged at 10,000 x g for 5 minutes and the hexane layer was discarded. Following, an organic wash with ethanol and acetone (1:1) was performed with the same parameters as the hexane washes, then the catalyst was dried in an 70 °C oven. When dry, the catalyst was transferred to a 10-mL vial for the aforementioned biodiesel reaction (2.2.1 Biodiesel Synthesis).

## **2.4 Characterisation techniques**

### **2.4.1 Scanning electron microscopy (SEM)**

Scanning electron microscopy (SEM) images were obtained on a Phenom ProX desktop SEM using magnification ranging from 760 x – 18000 x at 10kV.

### **2.4.2 Fourier transform infrared spectroscopy (FTIR)**

FT-IR spectra were collected using a Thermo Scientific Nicolet iS5 equipped with an iD5 ATR accessory. Spectra were collected using 32 scans with a resolution of  $0.4\text{ cm}^{-1}$ , a gain of 1, an optical velocity 0.4747 and an aperture setting of 100. Data was processed using the Omnic 9 software.

### **2.4.3 Brunauer-Emmett-Teller (BET)**

The surface area of the catalyst was calculated using the Brunauer-Emmett-Teller (BET) method on data obtained from the sorption/desorption isotherms of  $\text{N}_2$  at 77 K using a Micrometrics Tristar II Plus. The samples were activated prior to analysis at  $100\text{ }^\circ\text{C}$  for 24 h, under vacuum.

### **2.4.4 X-ray photoelectron microscopy (XPS)**

X-ray photoelectron microscopy (XPS) analysis of the lignin-derived catalysts was performed using a Thermo Scientific K-Alpha X-ray photoelectron spectrometer, where each analysis was carried out on three different points, in triplicate, with 10 runs for each scan. The averages were plotted for the survey and high-resolution scans.

### **2.4.5 Thermogravimetric analysis (TGA)**

Thermogravimetric analysis was carried out using a TGA Q500 analyzer from TA instruments. Samples were heated from 25 to  $1000\text{ }^\circ\text{C}$  at a heating rate of  $5\text{ }^\circ\text{C}\cdot\text{min}^{-1}$  under an argon atmosphere with a flow rate of  $50\text{ mL}\cdot\text{min}^{-1}$ .

## **2.4.6 Zeta potential**

Zeta potential measurements were carried out using a Zeta Sizer from the Malvern Instruments – Nano Series. The samples were dispersed in methanol at the concentration of  $0.5 \text{ mg.mL}^{-1}$

## **2.4.7 Titrations**

### **2.4.7.1 Titration for SO<sub>3</sub>H groups**

The sulphonic acid surface concentration was determined via base titration, where 40 mg of acid catalyst was mixed with 20 mL of 1 M sodium chloride (NaCl) for 24 h to promote ion interaction of the strong acid (i.e. SO<sub>3</sub>H). Post mixing, the supernatant was collected from the mixture and titrated against 0.01 M sodium hydroxide (NaOH), using phenolphthalein as an indicator.

### **2.4.7.2 Titration for total acid groups**

Total acidic sites on the surface of acid catalysts were determined via base titration, where 40 mg of acid catalyst was mixed with 0.01 M NaOH for 4 hours. After which, the supernatant was collected from the mixture and back titrated against 0.01 M HCl.

### **2.4.7.3 Titration for free fatty acids in WCO**

Given that waste cooking oils present a higher FFA content, the acid value of the oil was determined via titration. Briefly, 2.0 g of the oil was mixed with 25.0 mL of an ether: alcohol (2:1) solution and titrated with sodium hydroxide 0.1 M, using phenolphthalein as an indicator.

#### 2.4.8 Proton nuclear magnetic resonance spectroscopy (<sup>1</sup>H NMR)

Quantitation and composition of the biodiesel product was determined using a Bruker Fourier Ultrashield™ operating at 300 MHz. All samples were prepared in CDCl<sub>3</sub> for analysis. Sample analysis was carried out using the Mestrelab Mnova software. The quantification was calculated using Equation 1, where the area under the singlet chemical shift at 3.66 ppm (A<sub>CH<sub>3</sub></sub>), assigned to the methoxy protons in methyl esters was input along with the area under the triplet chemical shift at 2.3 ppm (A<sub>CH<sub>2</sub></sub>), representative of the α-methylene protons present in oil feedstock reagents (oleic acid, canola oil) as well as methyl ester product.

$$\text{Conversion(\%)} = \frac{2A_{\text{CH}_3}}{3A_{\text{CH}_2}} * 100 \quad (\text{equation 2.1})$$

The conversions derived from **equation 2.1** were additionally verified through alternative calculations from a calibration curve. Briefly, a calibration curve was obtained by preparing 10 known sample mixtures of methyl oleate and oleic acid (for acid catalysts) or canola oil (for basic catalyst) from 0% to 100% methyl oleate. The ratio between the integrated peaks at 3.66 ppm and 2.30 ppm were calculated and plotted against the known percentage of methyl oleate present in the sample. For the quantification of the biodiesel conversion, the ratio of the integrated peaks (3.66 ppm/2.30 ppm) was calculated, and the percent conversion value was obtained from the linear regression equation of a calibration curve.

#### 2.5 Kinetic studies

Kinetic studies were carried out at the established optimal conditions of the acid catalyst at 70 °C, 80 °C and 90 °C to determine which model suited the esterification of oleic acid and the

transesterification of canola oil. The resulting data was fitted to the pseudo-first order (equation 2.2) and second order (equation 2.3).

$$-\ln (1-X_O) = k_1 t \quad (\text{equation 2.2})$$

$$1/1-X_O = k_2 C_{O0} t \quad (\text{equation 2.3})$$

Where  $X_O$  is the fractional methyl oleate conversion at a specific time ( $t$ ),  $C_{O0}$  is the initial concentration of oil feedstock (oleic acid or canola oil) and  $k_1$  and  $k_2$  are the kinetic rate constants.

## 2.6 Acetylation of lignin

To a small amount of lignin, a mixture of pyridine and acetic anhydride (1:1, v/v) was added under stirring for 48 hours. Post-stirring, the mixture was put on ice and 1% HCl was added. The final precipitate was collected, washed with water until a pH of  $\sim 7$  was obtained. Subsequently, the sample was dried at room temperature before preparation for  $^1\text{H}$  NMR analysis

## Chapter 3: Lignin-derived acid catalysts

### 3.1. Characterisation of lignin samples

Lignin, being a highly branched, three-dimensional polymer, has a wide variety of functional groups including but not limited to hydroxyl, methoxyl, carbonyl and carboxylic groups<sup>84</sup>. However, raw lignin shows almost no catalytic reactivity due to poor surface to volume ratio and impurities leftover from extraction methods<sup>85</sup>. Industrial lignins can generally be divided into two major categories - those containing sulphur as a result of their pulping/extraction method and the second comprising lignin's without sulphur in their extraction or composition<sup>84</sup>.

Given the final structure of lignin largely depends on the extraction method and solvents chosen, characterisation of the surface was performed in order to garner information on the catalytic groups and capabilities of the lignin samples. Furthermore, since the extraction process is confidential, limited to the Dr. Lavoie research group, characterisation of the structure and therefore catalytic properties of lignin is most necessary in verifying it as candidate for a heterogenous biodiesel catalyst.

As preliminary examination of the surface, the morphology of the four lignin samples from corn stover, maple, poplar and softwood were analysed from SEM images. Applicable to all samples, SEM images show irregular and heterogeneous morphology, covered by irregularly shaped particles from 2-5  $\mu\text{m}$  in size (**Figure 3.1(a)**). In order to identify the functional groups present after the extraction process, FTIR-ATR was performed on all four raw lignin samples: corn stover, maple, poplar and softwood (**Figure 3.1(b)**). All samples expectedly possessed the O-H stretch (3000-3700  $\text{cm}^{-1}$ ), C-H stretch (2930  $\text{cm}^{-1}$ ), the methoxy C-H stretch at ( $\sim 2840 \text{ cm}^{-1}$ ) and C-O stretches ( $\sim 1230, 1270 \text{ cm}^{-1}$ ) associated with the many phenolic and methoxy functional groups on the alcoholic monomers of lignin<sup>67,86</sup>. The two different C-O stretches observed are

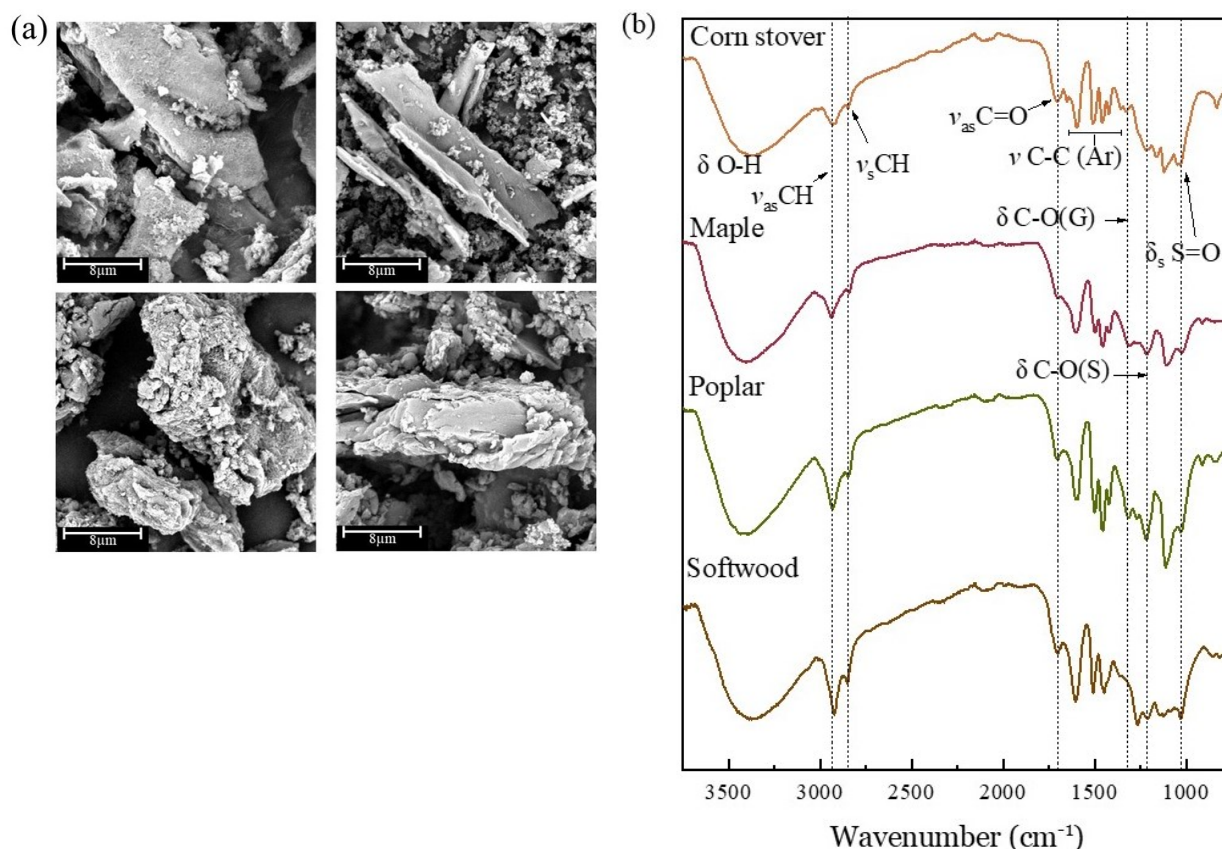


**Figure 3.1(a)** SEM images of corn stover, maple, poplar and softwood lignin at 9700x magnification with 10kV, legend showing 8μm. **(b)** FTIR spectra of corn stover, maple, poplar and softwood lignin samples showing characteristic vibrations of lignin, as well as sulphonic acid group vibrations

representative of the guaiacyl ( $1270\text{ cm}^{-1}$ ) and syringyl ( $1230\text{ cm}^{-1}$ ) alcohol monomers units of lignin<sup>87</sup>. The sole presence of the guaiacyl C-O stretch in the softwood lignin compared with the presence of both the guaiacyl and syringyl in the hardwood lignins (maple, poplar) align with the reported ratios, reinforcing the fact that softwood lignin has the least functional groups available<sup>88</sup>. Corn stover, a grass lignin possessing all three alcoholic monomers, also presents the C-O stretch of guaiacyl and syringyl units in a shouldering peak from  $1230\text{-}1270\text{ cm}^{-1}$ . All lignins also displayed a strong intensity peak at  $\sim 1100\text{ cm}^{-1}$ , indicative of the copious aliphatic  $\beta\text{-O-}4$  ether linkages between the alcoholic monomers<sup>89</sup>. The aromaticity of the lignin structure is seen in the aromatic skeletal vibration from  $1500\text{-}1600\text{ cm}^{-1}$ , linked to the conjugation of the C=O stretching at  $\sim 1700\text{ cm}^{-1}$  in all samples, peaking at a slightly lower wavenumber ( $50\text{-}60\text{ cm}^{-1}$ ) due to

**Table 3.1.** Titration results depicting the amount of sulphonic acid and other acid sites on the surface of corn stover, maple, poplar and softwood lignin.

<b>Lignin</b>	<b>SO<sub>3</sub>H sites (mmol g<sup>-1</sup>)</b>	<b>Total acid sites (mmol g<sup>-1</sup>)</b>	<b>Other acid sites (OH, COOH) (mmol g<sup>-1</sup>)</b>
<b>Corn stover</b>	0.85 ± 0.04	1.39 ± 0.41	0.54 ± 0.22
<b>Maple</b>	0.11 ± 0.01	1.42 ± 0.02	1.31 ± 0.02
<b>Poplar</b>	0.12 ± 0.00	1.25 ± 0.01	1.13 ± 0.01
<b>Softwood</b>	0.10 ± 0.03	1.03 ± 0.01	0.93 ± 0.02

conjugation with the aromatic, phenyl rings<sup>87</sup>. Apart from the characteristic lignin peaks exhibited in FTIR, all samples interestingly displayed peaks at 1030 cm<sup>-1</sup> attributed to the symmetric S=O stretching. This assignment was proposed based on the fact that majority of lignin extraction processes involve the use of sulphuric compounds (i.e. sulphite, sulphuric acid) as acid treatment, resulting in the production of lignosulphonates- the most abundant type of commercial lignin<sup>83,90</sup>. Acknowledging the peaks assigned to SO<sub>3</sub>H stretches and that the vibrations also overlap with those assigned to groups prevalent in the raw lignin structure (i.e. phenolic OH and aliphatic C–H in methyl groups (~1350-1380 cm<sup>-1</sup>), further analysis was performed to validate the presence of SO<sub>3</sub>H groups. To do this, Boehm titration was performed (2.4.7.1) to calculate the surface SO<sub>3</sub>H groups on each lignin<sup>91,92</sup>(**Table 3.1**). After 24 h mixing with 1.0 M NaCl, the supernatant was back titrated with 0.01 M NaOH, revealing corn stover to have the highest amount of sulphonic acid sites (0.845 mmol g<sup>-1</sup>), whilst all the hard and softwood lignins possessed less than 0.17 mmol g<sup>-1</sup> sulphonic acid sites. Given that the extraction method was replicated for all lignin sources, the difference in sulphonic acid sites can be linked to the varying ratios of alcoholic monomers and therefore available functional sites in lignin types<sup>67</sup>. Grass lignins, such as corn stover, typically have a combination of all three alcoholic monomers with higher concentration of synapyl alcohol. However, due to the lack of a standard lignin sample and the fluctuation of alcohol monomer ratio between areas of plant sources (stems, leaves of leafy and woody plants), it is inaccurate to report

an average percentage of synapyl and coniferyl groups in grass lignins<sup>69</sup>. Nonetheless, the corn stover lignin in this project had more functional or ether linkage groups available for sulphonation to take place. Back titration for total acidic sites (2.4.7.2) was also performed and revealed a relatively similar amount (1-1.4 mmol g<sup>-1</sup>) of weaker/medium strength acid sites such as phenols and carboxylic acids<sup>93</sup>. Extensive investigation of the catalytic capabilities of sulphonic acid on esterification and transesterification have been conducted<sup>94-96</sup>. Hence, preliminary biodiesel reactions using each lignin in the catalysis of canola oil as a source of triglycerides, oleic acid as a representative of free fatty acids and waste-cooking oil as a combination of both components. Knowing that upon heating, a varying proportion of the triglycerides break down into their FFA's, the amount of FFA's in the waste-cooking oil was calculated (2.4.7.3) to be 9.47 KOH g<sub>oil</sub><sup>-1</sup> value translating to 4.74%, a sufficient imitation of acidic non-edible oils<sup>97-100</sup>.

## **3.2 Calculation of biodiesel conversion**

### **3.2.1 Quantitative characterisation of biodiesel**

In order to compare biodiesel conversions between the lignin samples, an appropriate quantitative analysis was established and carried out by a <sup>1</sup>H NMR protocol (2.3.8). In industry, biodiesel is typically characterised by gas chromatography (GC), however, the inertness of the column which is required to sufficiently generate peak shapes and satisfactory recovery, cannot be easily maintained in routine analysis<sup>101</sup>. Furthermore, GC analysis often requires sample derivatisation, external standards and tedious calibrations amongst other time-consuming practices<sup>102</sup>. Given this, <sup>1</sup>H NMR was considered due its straightforward, quick, robust nature not requiring sample treatment or derivatisation<sup>102</sup>. The basis of <sup>1</sup>H NMR is dependent upon how protons respond to an applied magnetic field as a result of their electronic environments, producing corresponding resonant frequencies. Upon the esterification of oleic acid to its methyl ester, the hydroxyl group

is esterified into a methoxy group, giving rise to three equivalent protons in a new chemical environment. These methoxy protons ( $H_a$ ) in the methyl ester display a chemical shift at 3.66 ppm, whereas the methylene protons ( $H_b$ ) remain at 2.3 ppm (**Figure 3.2**). The conversion of biodiesel can be determined by taking the ratios of the integrated areas under these two specific chemical shifts, illustrated in the NMR spectrum of biodiesel (**Figure 3.2(b)**). Upon the formation of biodiesel, the appearance of the singlet at 3.66 ppm, ascribed to the methoxy protons, is coupled with the change in area under the triplet at 2.3 ppm associated with the  $\alpha$ -methylene protons present in both oleic acid and its methyl ester. To obtain a percentage conversion of biodiesel, a calibration

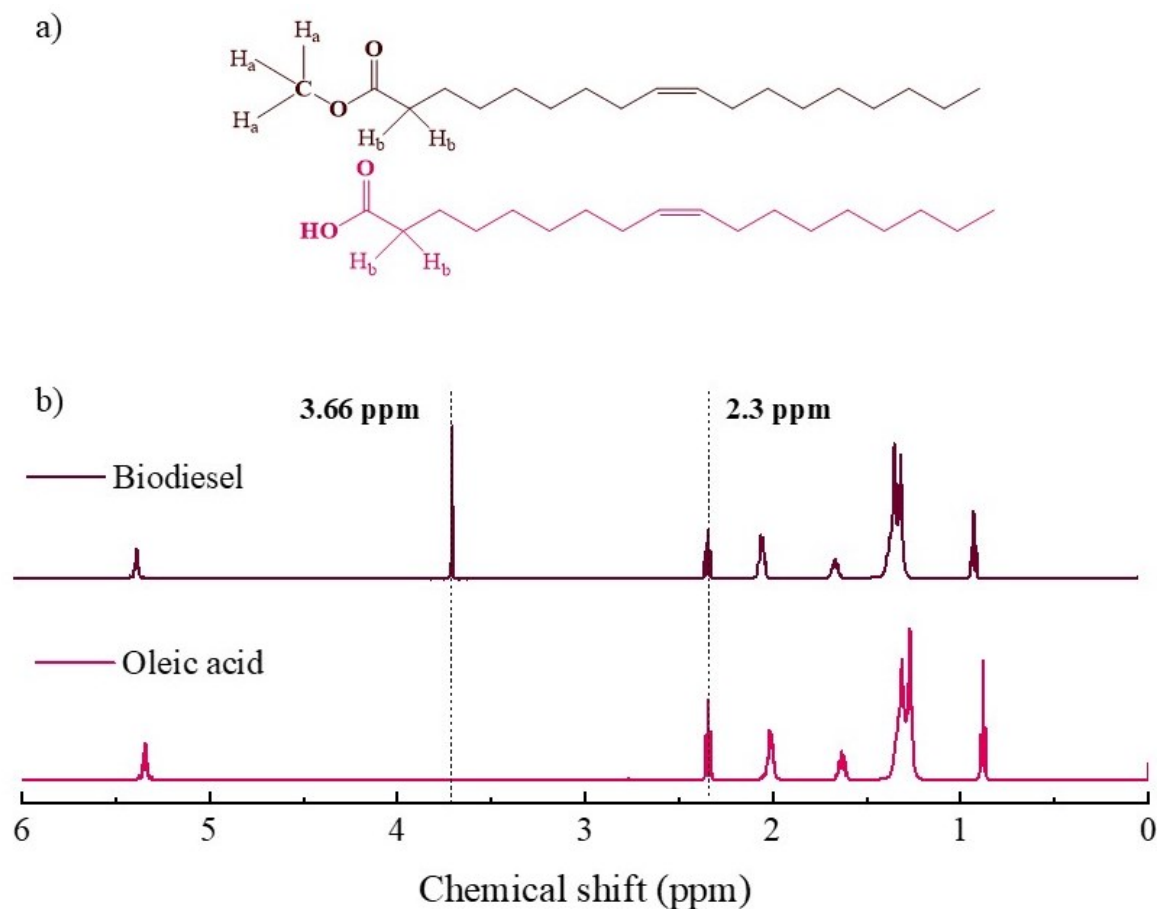


**Figure 3.2.** (a) Structures of oleic acid and methyl oleate depicting the alpha-methylene and methoxy protons. (b)  $^1H$  NMR spectra of oleic acid and biodiesel illustrating the singlet at 3.66 ppm pertaining to the methoxy protons of methyl oleate.

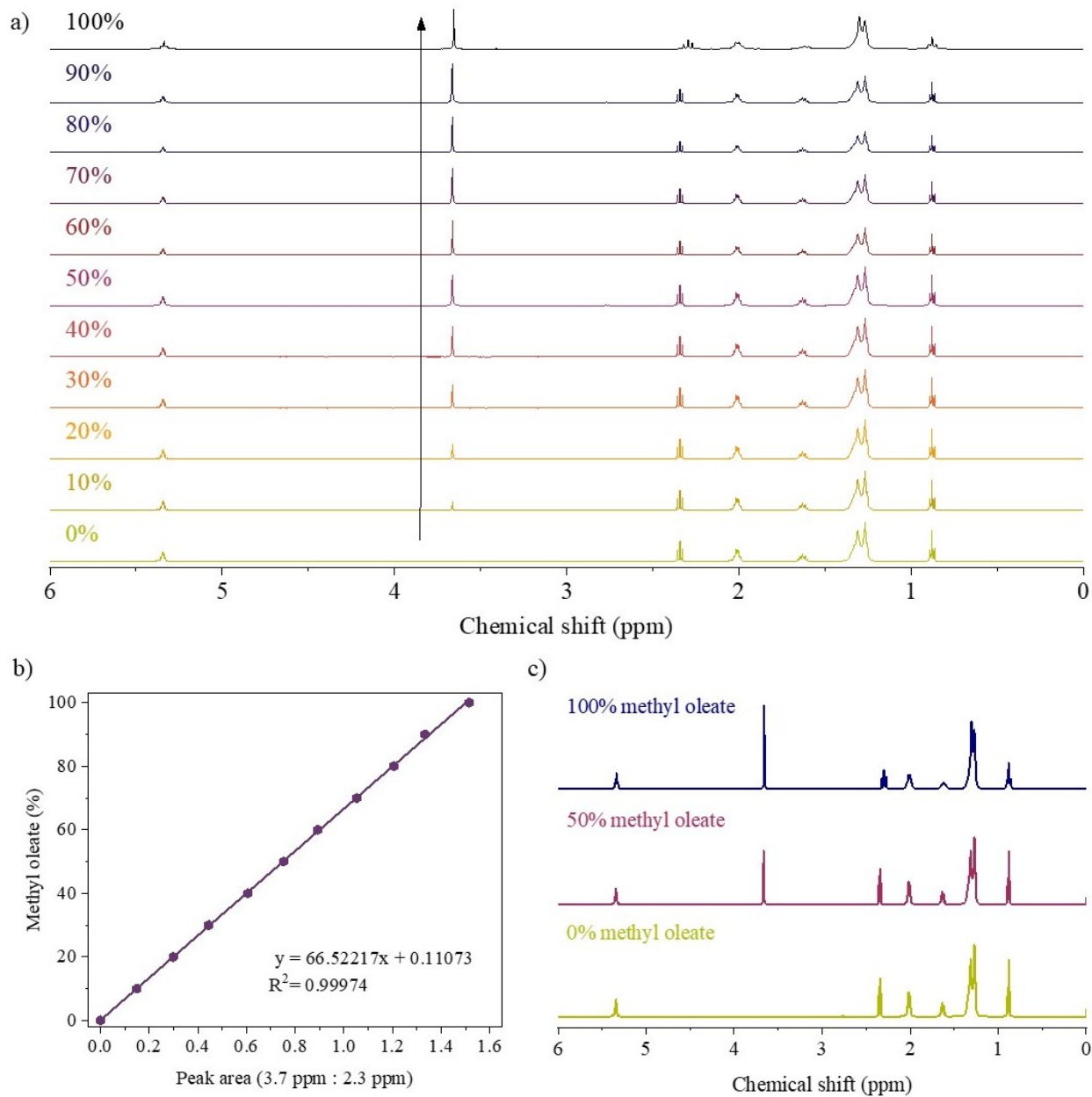


**Figure 3.3.** (a)  $^1\text{H}$  NMR spectra for all samples ranging between 0-100% methyl oleate content. The arrow showing the increase in the singlet at 3.66 ppm as methyl oleate content increases. (b)  $^1\text{H}$  NMR spectra for 0, 50 and 100 % methyl oleate standard samples, highlighting the formation of a singlet at 3.66 ppm as the methyl oleate content increases. (c) Standard curve and equation used to determine the biodiesel conversion. The curve was constructed using known amounts of oleic acid and methyl oleate.

curve was constructed using known weights of oleic acid and varying amounts of methyl oleate (0-100%). Methyl oleate was elected as it is the ester of oleic acid and one of the major components in biodiesel from non-edible oils<sup>103</sup>. The oil feedstock samples were analysed by  $^1\text{H}$  NMR and the

peak ratios (3.7 ppm:2.3 ppm) were measured. By plotting the peak ratios against the amount of methyl oleate (%) in each sample, a standard curve was constructed, and the associated equation of the curve was used in the quantification of biodiesel samples (**Figure 3.3**). Alternatively, the integrated areas of the methoxy and methylene protons can be input in **equation 3.1**<sup>104</sup> to calculate biodiesel conversion.

$$\text{Conversion(\%)} = \frac{2A_{\text{CH}_3}}{3A_{\text{CH}_2}} * 100 \quad (\text{Equation 3.1})$$

Where  $A_{\text{CH}_3}$  represents the integrated area of the methyl protons in methyl ester and the coefficient (2) pertaining to the number of methylene protons, while  $A_{\text{CH}_2}$  is the integrated area for the methylene protons with the coefficient (3) pertaining to the number of methoxy protons.

### 3.2.2 Qualitative characterisation

Qualitative analysis of the esterification reaction and resulting biodiesel production can be performed via Fourier-Transform infrared spectroscopy, with monitoring of two specific vibrations (**Figure 3.4**). Examination of the FTIR spectra for oleic acid and biodiesel reveals the characteristic asymmetric and symmetric stretching vibrations of C-H bonds in the methylene at  $2920 \text{ cm}^{-1}$  and  $2852 \text{ cm}^{-1}$ , respectively, present in both compounds. Alongside, the asymmetric stretching vibration of the carbonyl group in both compounds is shown by the intense band at  $1740 \text{ cm}^{-1}$  and  $1708 \text{ cm}^{-1}$  in biodiesel and oleic acid, respectively<sup>105</sup>. The distinguishing vibration of biodiesel is the asymmetric bending vibration at  $1440 \text{ cm}^{-1}$  of the  $\text{CH}_3$  moiety of the methoxy group and the complementary symmetric stretch of the O-C bond of the methoxy group at  $1196 \text{ cm}^{-1}$ <sup>106,107</sup>. In contrast, oleic acid displays characteristic bands at  $1463 \text{ cm}^{-1}$  and  $935 \text{ cm}^{-1}$ , indicative of the OH stretch in and out of plane, respectively<sup>108</sup>.

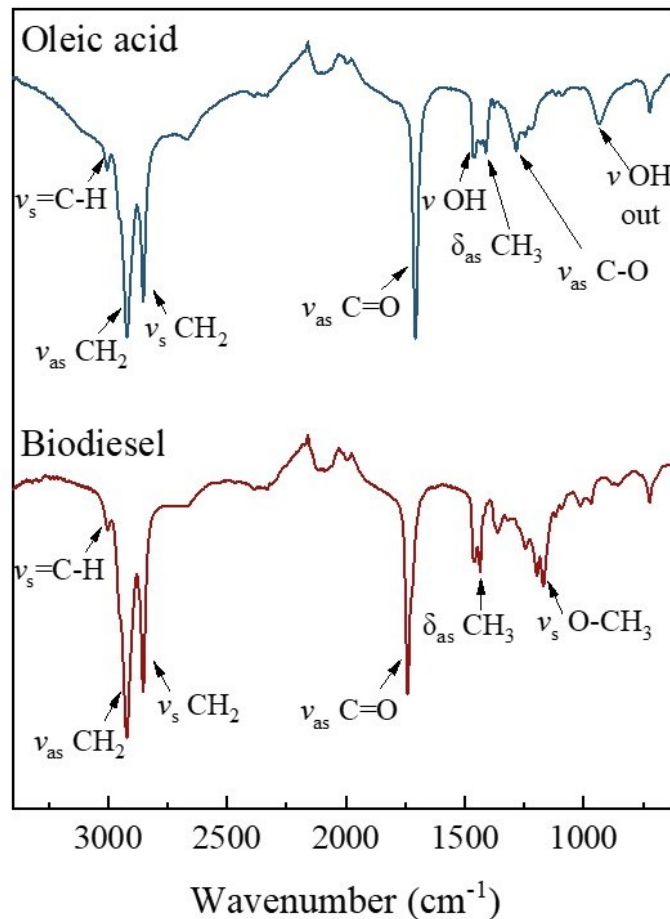


**Figure 3.4.** FTIR spectra of oleic acid and biodiesel (methyl oleate), representing the characteristic vibrations associated with each material.

### 3.3 Can extracted lignin catalyse biodiesel synthesis?

The starting conditions for each reaction parameter (O:MeOH, catalyst loading, time, temperature, mixing speed) were previously established by a colleague, Dr. Tayline de Medeiros, using relatively high values to assess the possibility of conversion. The molar ratio between methanol and canola and waste-cooking oil is three times the amount of methanol to oleic acid molar ratio, reflective of the stoichiometric requirement of 3 moles alcohol in the transesterification reaction. Hence, 1:72 was used in the canola and waste-cooking oil transesterification and 1:24 was used in oleic acid esterification. Otherwise, the remaining reaction parameters were set at 5 wt% (of oil)

catalyst loading heated to a temperature of 90 °C for 3 hours with magnetic stirring at 600 rpm. Post reaction completion, biodiesel products were purified and prepared for <sup>1</sup>H NMR analysis (2.4.8) to quantitate and compare their conversions. All lignins showed no conversion for canola oil transesterification, likely because acid catalysts exhibit slow kinetics for this reaction<sup>109,110</sup>. Similarly, the tree lignins showed no conversion of the waste-cooking oil, which primarily comprise triglycerides since it is originally refined vegetable oils (Figure 3.5(a)). However, corn stover lignin catalysed 13% conversion of the waste-cooking oil, hinting that the SO<sub>3</sub>H groups could catalyse the esterification of the minor amount of FFA's (~5%) present. This was confirmed with the impressive 99.5% conversion of oleic acid catalysed by corn stover, whilst the other lignins were unable to convert above 20% (Figure 3.5(b)). When comparing the values of sulphonic acid sites with oleic acid esterification, there is a clear correlation between the amount of acid sites and conversion, confirming the catalytic capabilities of sulphonic acid groups left over from the extraction methods.

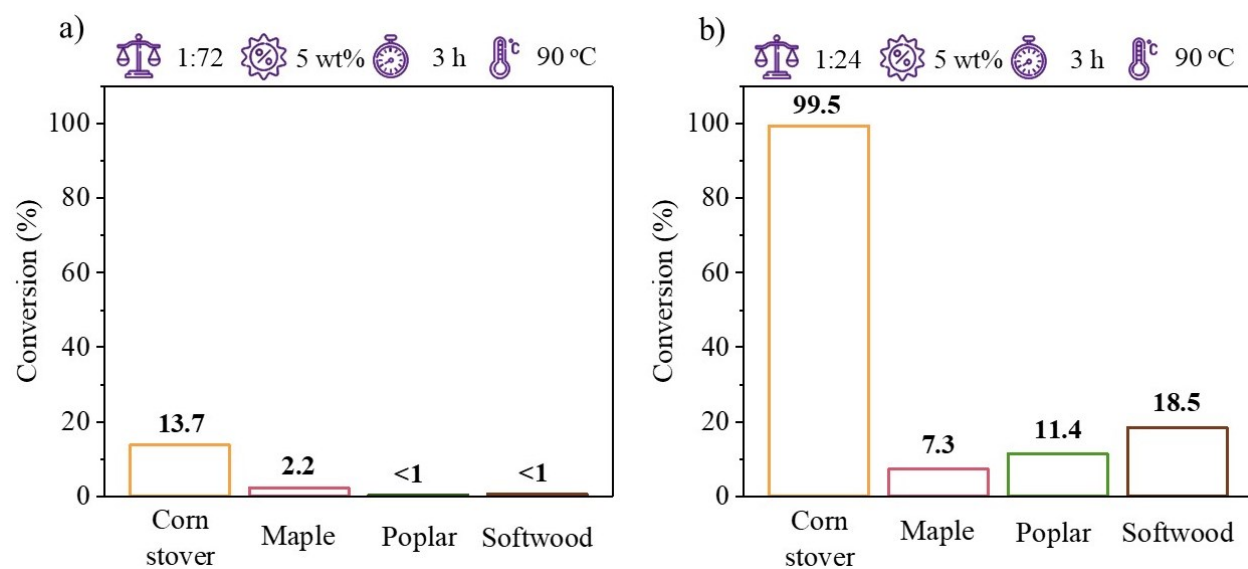


**Figure 3.5.** Preliminary biodiesel reactions of each lignin sample with (a) waste-cooking oil (FFA=4.74%). (b) oleic acid.

### 3.3.1 Synthesis of a sulphonated softwood lignin catalyst

Based on these preliminary biodiesel reactions, it is evident that the catalytic efficiency of extracted lignin is dependent upon the degree of sulphonation in the extraction process. Given that a large proportion of lignin waste is generated from the paper/pulp industry, which utilises significantly more softwood than hardwood, the sulphonation of softwood lignin was performed to generate an efficient, solid acid catalyst from biomass waste. Briefly, a specific ratio of *p*-toluene sulphonic acid (*p*-TsOH) was added to softwood lignin and heated in an autoclave-sealed Teflon reaction vessel in a one-step, solvent-free carbonisation-sulphonation. Commercially, liginosulphonates are synthesised via initial base treatment to deprotonate the phenolic hydroxyl, followed by reaction with sulphite to endow sulphonic acid groups on the  $\beta$ -benzylic position, which in turn favours the addition of the SO<sub>3</sub>H on the adjacent ether<sup>111</sup>. The formation of liginosulphonates can proceed through multiple pathways, dependent upon the pH of the reaction medium<sup>83</sup>. However, the sulphonation in this work was performed in the solid-state carbonisation method, so the pathway of sulphonation could not be directly linked to those previously established. Lignin is comprised of randomly linked phenylpropane units, with softwood consisting of primarily coniferyl alcohol and coniferyl aldehydes, which readily react with sulphite under mild sulphonation conditions<sup>111</sup>. In near neutral conditions (pH 5-9), it has been observed that sulphonation of phenylpropane units in lignin are favoured according to the reaction in **Figure 3.6**.

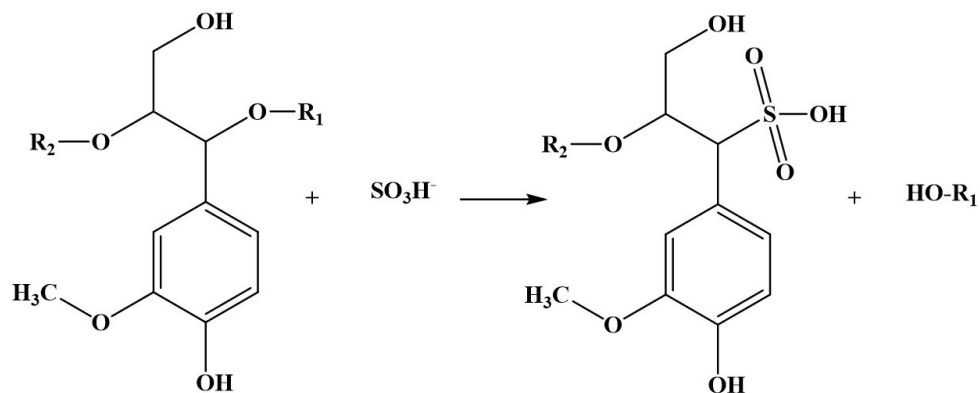
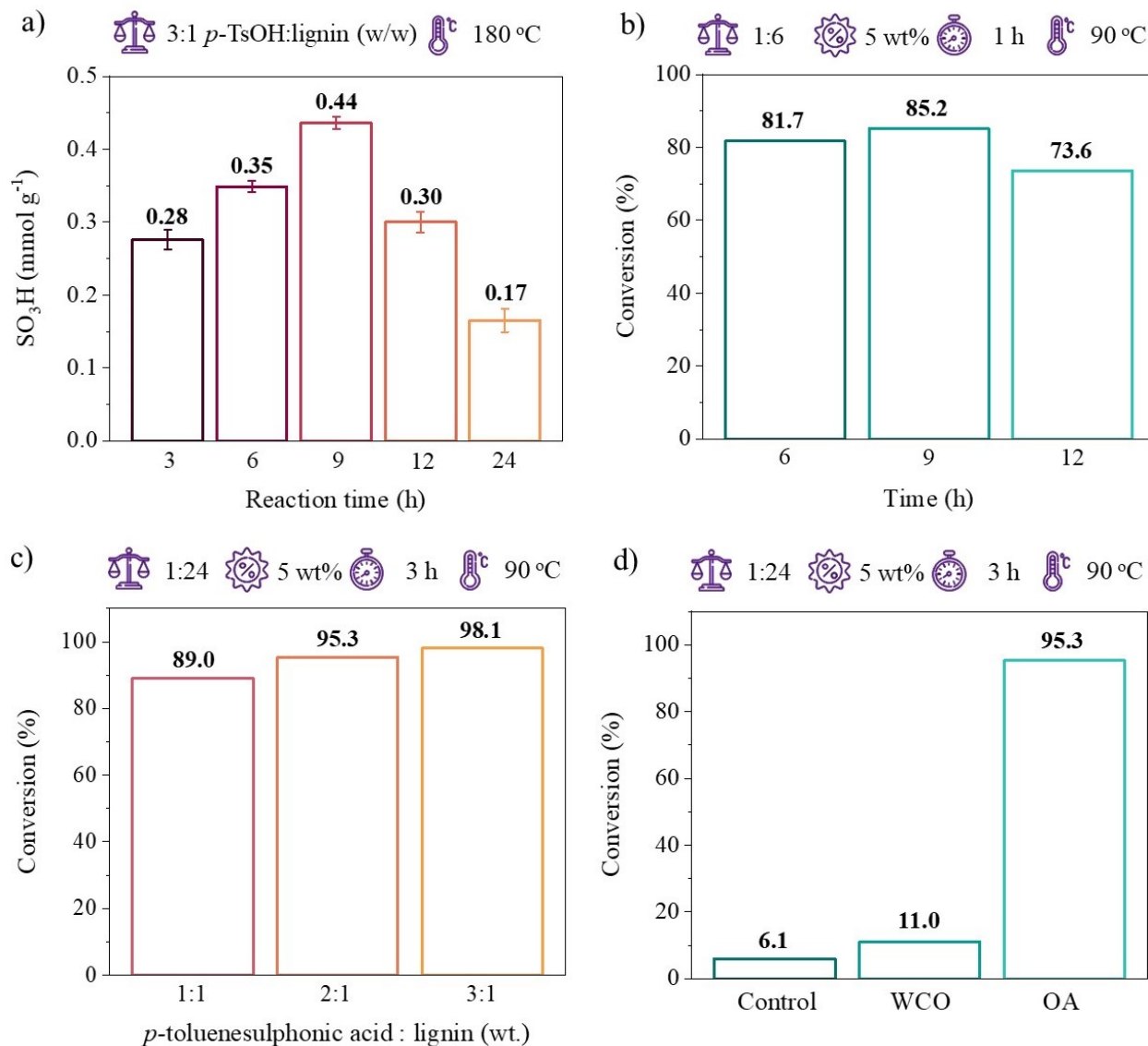


Figure 3.6. Proposed mechanism of sulphonation, adapted from Glennie, D. W. (1971)

To optimise the degree of sulphonation of softwood lignin, the effect of *p*-TsOH to lignin ratio and reaction time were assessed. The reaction time was varied at 3, 6, 9, 12 and 24 hours using 3:1 (w/w) *p*-TsOH to lignin ratio. After reaction completion and purification, titration (2.4.7.1) was performed to investigate the effect of time on surface sulphonic acid sites of the lignin-derived catalyst. As seen in **Figure 3.7 (a)**, the sulphonic acid sites number increased with time up to a period of 9 hours, then, a drop in the number of sulphonic acid sites is observed at longer times. The time-dependent decrease in sulphonic sites raises questions about the mechanism of addition of sulphonic acid groups to lignin. Based off the work in Matsushita et al. (2015), it was hypothesised that the decrease in surface sulphonic acid groups exhibited in the 12 and 24-hour reaction times can be reasoned to the incorporation of sulphonic groups into the structure of lignin as opposed to the surface, where catalytic ability is superior. To confirm the relationship between surface sulphonic sites and catalytic capability, the 6 h, 9 h and 12 h samples were reacted under the same conditions (1:6, 3 wt%, 1 h, 90 °C) in the esterification of oleic acid. It can be seen that the 6 and 9-hour reaction time samples converted similarly (<4% difference), whereas the 12-hour sample, which was suspected to undergo depolymerisation, converted nearly 10% less (**Figure 3.7 (b)**). In comparison with the initial biodiesel trial of raw softwood, the findings in these biodiesel

reactions demonstrate successful sulphonation and the ensuing improved catalytic performance. Considering the highest sulphonic acid density, 9 hours was chosen as the reaction time in the synthesis of the solid lignin-derived acid catalyst. The *p*-TsOH to lignin weight ratio (*p*-TsOH:lignin (w/w)) was also investigated, where ratios of 1:1 and 2:1 were reacted for 9 hours in the muffle furnace. To compare catalytic capabilities, the purified catalysts were then employed in



**Figure 3.7.** (a) Titration results of softwood lignin sulphonated at 180 °C for 3, 6, 9, 12, 24 hours. (b) Trial biodiesel reactions using the 6, 9, and 12 hour Tso-SL catalysts reacted with 1:6 oleic acid to methanol ratio, 5 wt% catalyst loading at 90 °C for 1 hour. (c) Varied weight ratios of *p*-TsOH and lignin reacted for 9 hours and applied in esterification of oleic acid in maximum conditions of 1:24 oleic acid to lignin ratio, 5 wt% catalyst loading at 90 °C for 3 hours. (d) 2:1 SSL catalyst in the esterification of waste-cooking oil and oleic acid using maximum reaction conditions of 1:24 oleic acid to lignin ratio, 5 wt% catalyst loading at 90 °C for 3 hours.

the esterification of oleic acid using the conditions of 1:24, 5 wt%, 90 °C, 3 h. The amount of methanol used was kept relatively high at our maximum acceptable amount for the esterification methyl oleate conversions. Whilst a conversion of 95% achieved by the 2:1 *p*-TSOH: lignin ratio is impressive, the chosen optimal ratio was 3:1 as it gave opportunity for biodiesel reaction parameters to be lowered, namely the ratio of methanol required, while maintaining conversion above 95% (**Figure 3.7 (c)**). To briefly analyse the conversion of FFA's and triglycerides, the 2:1 *p*-TsOH:lignin sample was reacted with waste-cooking oil (FFA=4.74%) and compared to the conversion with pure oleic acid as well as a control reaction in the absence of a catalyst. The conversion of waste-cooking oil is ~5% lower than that of the control, suggesting only the 4.7% of FFA's were esterified by the sulphonated catalyst. To summarise, the chosen reaction conditions for the sulphonation of softwood lignin was 3:1 *p*-TsOH:lignin (w/w), heated at 180 °C for 9 hours, generating an improved catalyst by endowing 0.332 mmol g<sup>-1</sup> of sulphonic acid sites on softwood lignin, hereon referred to as SSL.

### 3.3.2 Characterisation of sulphonated softwood lignin catalyst (SSL)

To qualitatively characterise the addition of sulphonic acid groups, FTIR analysis was performed on the SSL catalyst and compared with the FTIR spectra of the softwood lignin precursor and TsOH reactant (**Figure 3.8 (a)**). Whilst the SSL catalyst retained the OH stretch associated with the many hydroxyl groups of lignin, the disappearance of the CH stretches previously ascribed to the methoxy groups was observed. Additionally, the symmetric bend of S=O bond at 1030 cm<sup>-1</sup> and the asymmetric vibration of S-OH of sulphonic acid at 1000 cm<sup>-1</sup> were intensified and presented sharper peaks<sup>112</sup>. Since this technique is purely qualitative, confirmation of sulphonation relied heavily on titration results indicating the presence of sulphonic acid surface groups **Figure 3.7 (a)**. In order to investigate the accessibility of the sulphonic acid surface groups, BET analysis

was performed on the softwood precursor and SSL catalyst. BET theory utilises the gas adsorption data to generate a specific surface area expressed in  $\text{m}^2/\text{g}$ . Catalyst surface area and pore structure can affect its performance, with it being generally accepted that increased surface area scales in the same linear trend as number of active sites<sup>113</sup>. It can be observed that sulphonation treatment resulted in  $\sim 9 \text{ m}^2\cdot\text{g}^{-1}$  increase in surface area of the softwood lignin. In combination with the titration data, it can be concluded that the sulphonation reaction was able to endow the softwood lignin with sulphonic and carboxylic acid groups whilst also increasing the surface area and therefore access to these active catalytic sites.

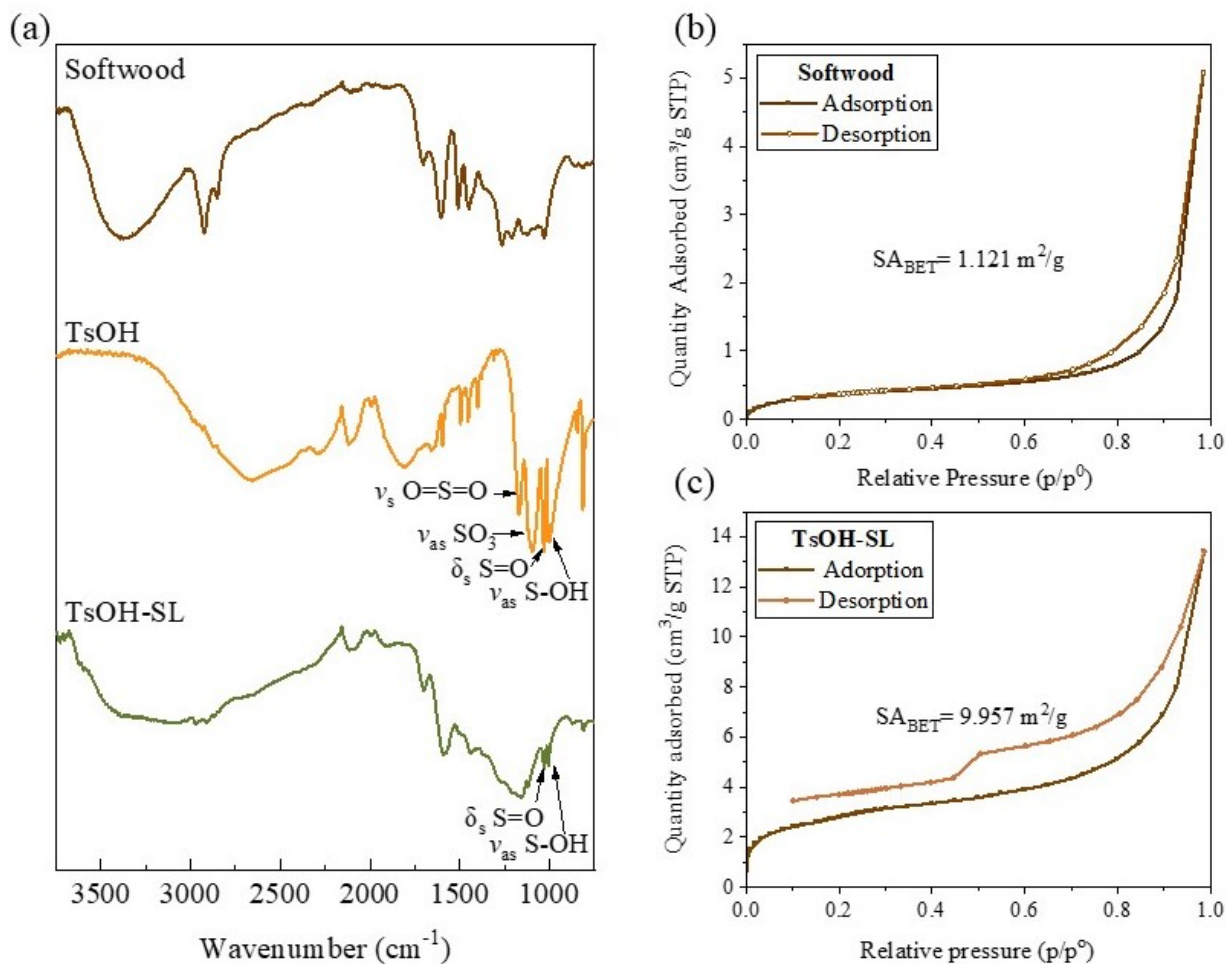


**Figure 3.8.** (a) FTIR spectra of softwood lignin and p-TsOH precursors as well as SSL, demonstrating the sulphonic acid vibrations of catalyst. (b)  $\text{N}_2$  adsorption/desorption isotherm and BET surface area of softwood lignin precursor and (c) SSL catalyst.

The catalytic sites were also assessed using XPS analysis, which is based on the photoelectric effect and utilises the core level shift to quantitate the chemical and electronic state of the elemental components of a sample. Reaching a penetrative depth of  $\sim 5\text{nm}$ , it is primarily a surface-sensitive technique, particularly useful in this project to identify surface functional groups of the lignin-derived catalysts. The XPS survey scan of corn stover lignin revealed 533 eV, 285 eV and 169 eV binding energies corresponding to oxygen (O1s), carbon (C1s) and sulphur (Sp2) respectively (**Figure 3.9**). The chemical states at the surface of the lignin catalysts were determined by high resolution XPS analysis of the binding energies found in the survey spectrum and subsequent deconvolution of the observed peaks. Deconvolution of the O1s peak revealed two binding

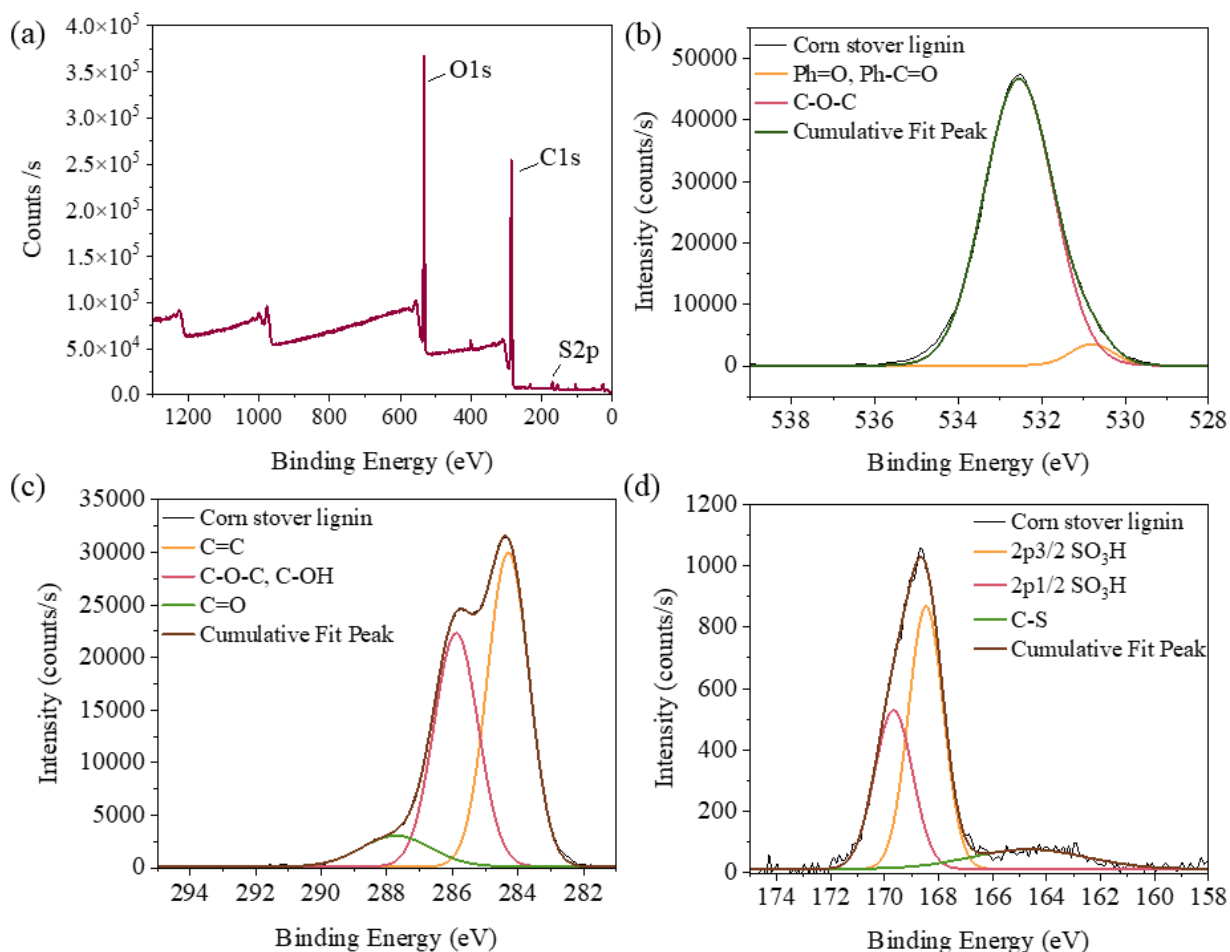


**Figure 3.9.** (a) XPS survey scan revealing 533eV, 285eV and 169eV binding energies corresponding to oxygen (O1s), carbon (C1s) and sulphur (S2p) respectively. (b) Deconvoluted O1s peak. (c) Deconvoluted C1s peak. (d) Deconvoluted S2p peak.

energies at 532.5 and 530.8eV, representative of C-O-C ether bonds and Ph=O, Ph-C=O of carboxylic acids respectively. Deconvolution of the C1s peak showed three binding energies at 284.3, 285.9, 287.7eV attributed to the C=C, C-O-C/C-OH and C=O present in the aromatic structure, ether linkages and the carboxylic acid groups generated from sulphonation. The deconvolution of the  $sp^2$  peak confirmed the presence of surface sulphonic acid sites with the binding energies at 169.7 and 168.4 eV ascribed to  $2p_{3/2}$  and  $2p_{1/2}$  of  $SO_3H$ , respectively. The C-S bond is represented by the binding energy at 164.6 eV, further confirming the endowing of  $SO_3H$  on the lignin carbon backbone.

Sulphonic acid is a well-established, highly efficient catalytic group for the esterification of oleic acid<sup>93,95-97,114,115</sup>. Through qualitative and quantitative characterisations, the presence of sulphonic acid groups on the lignin surface was confirmed and the promotion of the catalytic activity of softwood lignin was observed (**Figure 3.7 (c)**). Considering previously published works on acid-catalysed oleic acid esterification and the understanding of surface properties ascertained from the data of the aforementioned characterisations of SSL catalyst, the following mechanism for sulphonic acid-catalysed esterification is proposed (**Figure 3.10**): First, the carbonyl is protonated by the acid catalyst, making it susceptible to a nucleophilic attack from the methanol reagent which forms a bond with the carbonyl carbon, resulting in an oxonium ion. After the succeeding proton transfers, an unstable tetrahedral intermediate is formed, resulting in the 1,2 elimination of water, giving the protonated ester. The positive oxygen is then deprotonated by the  $SO_3^-$  resonance structure of the catalyst, giving the final methyl oleate product - biodiesel. The proposed mechanism follows the conventional acid-catalysed Fischer esterification reaction, generating one mole of methyl ester and water as a by-product.

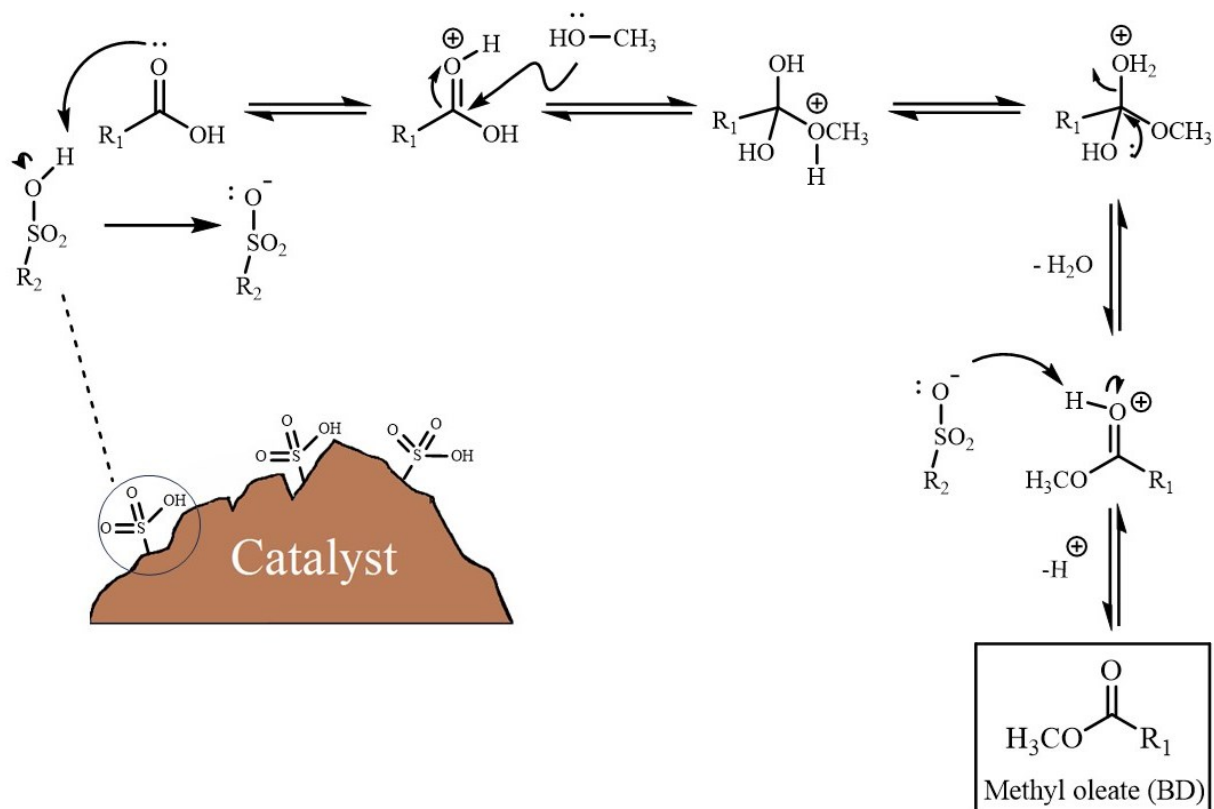


**Figure 3.10.** Proposed Fischer esterification mechanism for the sulphonic acid-catalysed esterification.

### 3.4 Optimisation of reaction parameters

In order to optimise the reaction conditions, single-factor experiments were carried out to assess the effect of oleic acid to methanol ratio, catalyst loading, time and temperature reaction parameters had on conversion of oleic acid into methyl oleate. The esterification reactions of each catalyst were carried out at various reaction conditions as summarised in **Table 3.2**, showing the conversion achieved in each trial. When performing the optimisation steps, the desired minimum conversion was 96.5%, in accordance with the requirements of the ASTM biodiesel standards(**ref**). However, since this work is on a lab scale, conversions above 80% were still recognised as successful. Furthermore, the decision of which parameter to be kept at the lowest value was based off the environmental impact of sourcing and synthesis of each material (i.e. methanol, lignin), as

**Table 3.2.** The oleic acid to methanol molar ratio, catalyst loading (wt%) with respect to OA mass, temperature (°C) and reaction time (hours) parameters varied in the one-factor-at-a-time **(a)** optimisation of corn stover catalyst and **(b)** optimisation of the SSL catalyst.

(a)

Oil : MeOH	Catalyst (wt%)	Temperature (°C)	Time (h)
1:24	5	90	3
1:12	5	90	3
1:6	5	90	3
1:3	5	90	3
1:2	5	90	3
1:3	1	90	3
1:3	2.5	90	3
1:3	5	90	2
1:3	5	90	1
1:3	5	90	0.5
1:3	5	80	3
1:3	5	80	2
1:3	5	80	1
1:3	5	80	0.5
1:3	5	70	3
1:3	5	70	2
1:3	5	70	1
1:3	5	70	0.5

(b)

Oil : MeOH	Catalyst (wt%)	Temperature (°C)	Time (h)
1:9	3	90	3
1:6	3	90	3
1:3	3	90	3
1:9	1	90	3
1:9	2	90	3
1:9	7	90	3
1:9	3	80	3
1:9	3	80	2
1:9	3	80	1
1:9	3	80	0.5
1:9	3	70	3
1:9	3	70	2
1:9	3	70	1
1:9	3	70	0.5

well as the sustainability of the energy source maintaining reaction temperatures. In the esterification reaction, the stoichiometric molar ratio of oleic acid to methanol is 1, however, an excess of methanol is used to promote the equilibrium shift in the forward reaction, enhancing the production of methyl oleate. Considering the production of methanol from fossil fuels and the impact it has on the environment, the minimum amount required to achieve the desired conversion was investigated first<sup>21,116,117</sup>. First, the corn stover catalyst performance was investigated using five molar ratios of oleic acid to methanol (1:2, 1:3, 1:6, 1:12, 1:24) to analyse their effect on conversion, whilst other parameters were held constant at 5 wt% catalyst loading with a 3-hour reaction time at 90 °C. The results revealed excellent conversions using low amounts of methanol, with 1:2 and 1:3 ratios converting 67.9% and 96.4% of oleic acid into biodiesel (**Figure 3.11 (a)**). These high conversions can be attributed to the plentiful amount of sulphonic acid sites on the catalyst surface, in accordance with reports of other carbonaceous biomass-derived catalysts for esterification<sup>94,96,114</sup>. Given the successful conversion, 1:3 was elected as the optimal oleic acid to methanol molar ratio for the corn stover lignin catalyst. Using the results from the corn stover optimisation as a guide, the sulphonated softwood lignin catalyst was assessed using molar ratios of 1:3, 1:6 and 1:9. A successful conversion of  $97.3 \pm 0.7\%$  was achieved with an oleic acid to methanol ratio of 1:9, three times that higher than required by the corn stover catalyst, most likely due to difference in sulphonic acid sites (**Figure 3.11 (b)**). In contrast to the corn stover catalyst, a molar ratio of 1:3 only prompted 70.9% conversion using the sulphonated softwood lignin, confirming the direct dependence on sulphonic acid sites for catalytic capabilities. Therefore, 1:9 was chosen as the optimal oleic acid to methanol molar ratio for the sulphonated softwood lignin catalyst. When compared with recently published solid acid catalysts with similar or higher

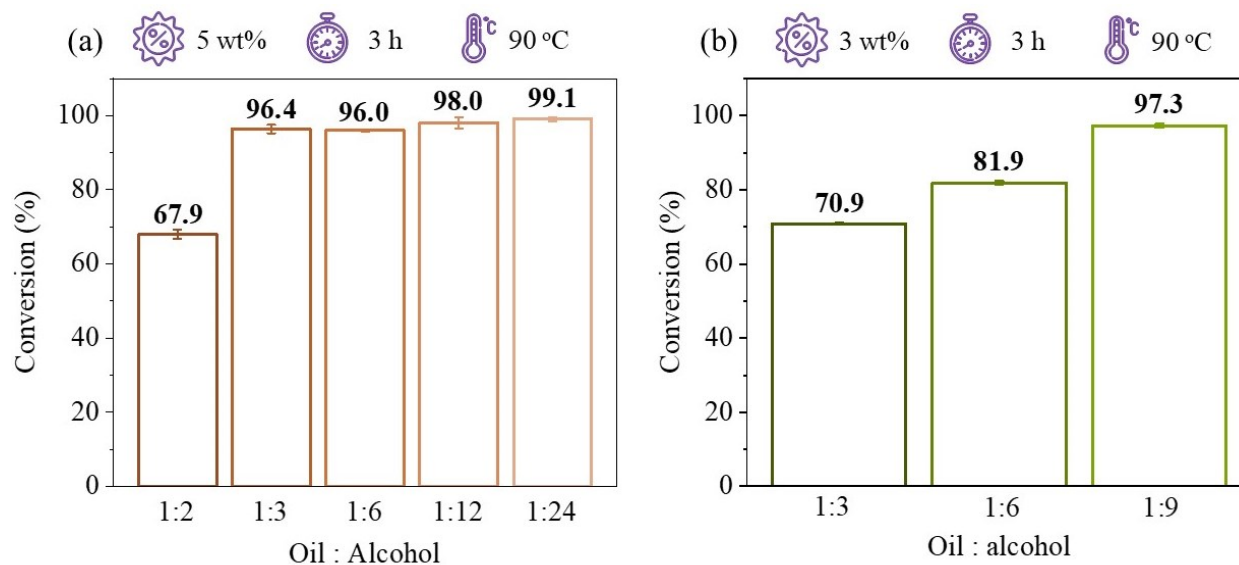


**Figure 3.11.** (a) corn stover-catalysed and (b) SSL catalysed biodiesel conversion results when varying oleic acid to methanol molar ratio

sulphonic acid sites, the conversions displayed in this optimisation step are impressively low<sup>94-96,118,119</sup>.

The amount of catalyst is a significant reaction parameter as it directly increases the amount of catalytic active sites, in turn increasing the biodiesel conversion. On the other hand, too high of catalyst loading can amplify unfavourable mass transfer limitations experienced by heterogeneous catalysts. This limitation results in heterogeneous catalysts usually requiring catalyst loading from 3-15 wt% of the oil precursor, whereas homogeneous ones are able to catalyse reactions using as little as 1% catalyst loading. In order to isolate the effect of catalyst loading on conversion, 1, 2.5, 5 wt% amounts were chosen for the corn stover catalyst loading optimisation, whilst other parameters were held constant using the previously established 1:3 oleic acid to methanol molar ratio at 90 °C for 3 hours. Whilst notable conversions near 85% and 90% were achieved using 1 and 2 wt% catalyst loading, respectively, 5 wt% remained as the optimal amount of corn stover catalyst in the further optimisations (**Figure 3.12 (a)**). Similarly, the SSL catalyst also achieved

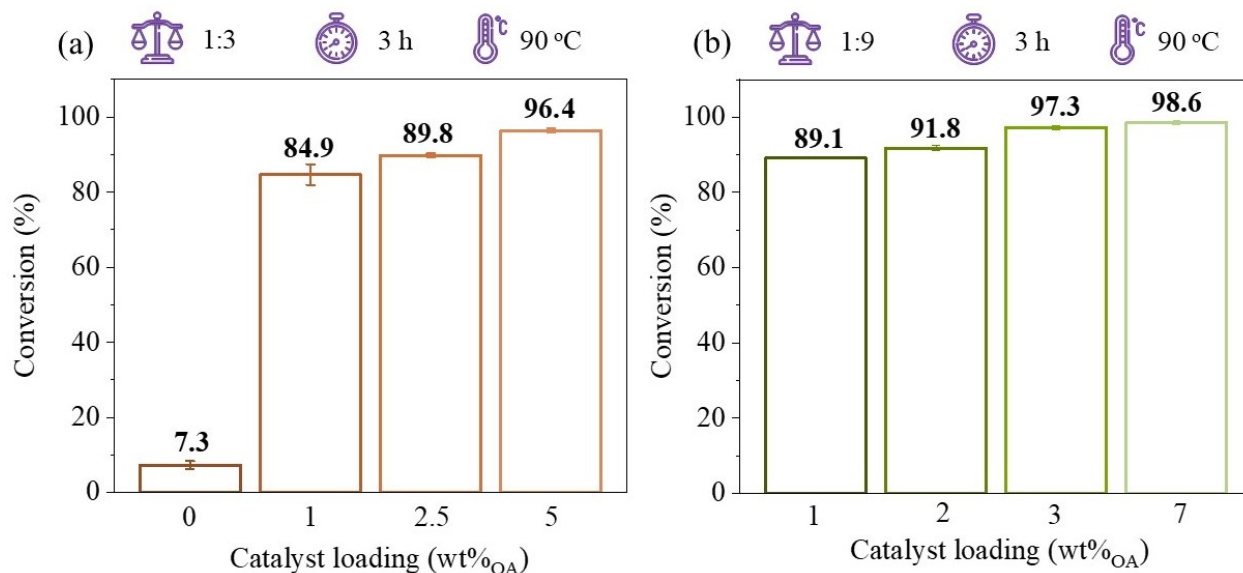


**Figure 3.12.** (a) corn stover-catalysed and (b) SSL catalysed biodiesel conversion results when varying catalyst loading as a percent of the weight of oleic acid.

notable conversions around 90% for 1 wt% and 2 wt% catalyst loading. However, 3 wt% sufficiently catalysed  $97.3 \pm 0.7\%$  of oleic acid conversion and was elected as the optimal catalyst loading for the softwood lignin catalyst (**Figure 3.12 (b)**). Whilst the corn stover catalyst has nearly double the amount of sulphonic acid sites, the slightly higher mass of catalyst required to maintain conversion is due to the lower amount of methanol reagent required. To confirm this, corn stover lignin was run using a 1:9 reagent molar ratio with 3 wt% at the same temperature and time conditions, expectedly achieving  $>99.5\%$  methyl oleate conversion. Recalling that corn stover and softwood lignin are generated as by-product waste in the agricultural and paper/pulp industries, respectively, the expense of amount of catalyst was of lower priority than that of methanol used, with respect to sustainability. Alternatively, the attention to biofuels has consequentially prompted the research of low-environmental impact biomethanol synthesis<sup>21</sup>. If methanol is sourced with environmental considerations demonstrating a sufficient life cycle assessment, then the prioritising of its reduction as a biodiesel reaction parameter could be

reconsidered. Overall, due to the difference in methanol amounts required for the corn and SSL catalysts, 5 wt% and 3 wt% catalyst loadings, respectively, were selected as the optimal amount. As seen in any catalysed reaction, temperature plays a significant role in driving the reaction rate. Given that the esterification of oleic acid is an endothermic reaction, increasing the temperature should shift the equilibrium to the product side. In conventionally heated reactions, heterogeneous-catalysed reactions often require higher temperatures to overcome the mass transfer limitation experienced due to being in a different phase as the reaction system<sup>120,121</sup>. To assess the effect of temperature on the reaction time required to reach optimal conversion, the previously established optimal amounts of methanol and catalyst were used in reactions run at 70 °C, 80 °C and 90 °C and monitored from 5 minutes to 3 hours (**Figure 3.13**). In the case of corn stover catalysed esterification at 80 °C and 90 °C, similar trends in conversion are observed. There is an initial conversion of 40 % and 67 % for 80 °C and 90 °C, respectively, within the first 5 minutes, followed by an almost linear increase until rapid conversion to the maximum amount of biodiesel obtained. At 90 °C, this rapid conversion takes place between 20 and 30 minutes - at which an impressive conversion of 97.1% is obtained. Considering the 80 °C reaction displays a conversion of 54% at 30 minutes, followed by rapid conversion to the maximum 97% at 60 minutes, 90 °C was elected as the optimal reaction temperature. The molar amount of methanol used in the temperature optimisation is relatively low (1:3 OA:MeOH), and as such, the effect of reagent molar ratio on the reaction time was further investigated in order to assess the potential of using 80 °C as a lower reaction temperature. Using the same catalyst loading as previous optimisations, molar ratios of 1:6 and 1:9 of oleic acid to methanol presented conversions of 89.8% and 92.6%, respectively, at 30 minutes of reaction time. The choice of optimal temperature was based on the quickest conversion to >96.5 %, hence, 90 °C remained as the elected optimal reaction temperature and the

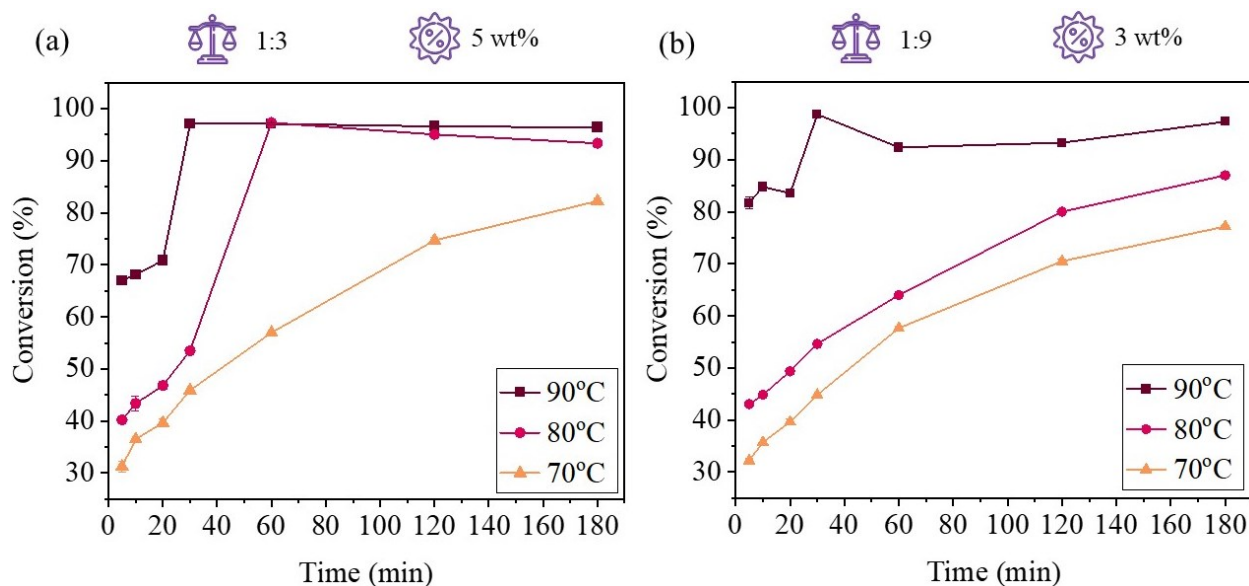


**Figure 3.13.** Biodiesel conversions against time for 70 °C, 80 °C, 90 °C reactions for (a) corn stover (b) SSL catalyst.

subsequent optimal reaction time was 30 minutes. Interestingly, when comparing the trend of conversion at 80 °C and 90 °C with that of the reaction carried out at 70 °C, it's apparent the rate of the catalytic steps is irregular at higher temperatures, whereas a steady nearly linear trend is displayed at lower temperature of 70 °C. In the case of the SSL, a similar trend is observed, however, only 90 °C displays an irregular trend in conversion, reaching the maximum 98.1% at 30 minutes, followed by a slight decrease to 92% at 1 hour and eventual approach to 97% at 3 hours. This decrease in conversion is attributed to the reverse shift in equilibrium immediately following the maximum conversion at 30 minutes. On the other hand, 80 °C and 70 °C follow similar regular trends in conversion, reaching maximum conversions of 85% and 75%, respectively, at 3 hours. Given these results, 90 °C was chosen as the optimal reaction temperature for the esterification reaction using the SSL catalyst, producing a 98% conversion within 30 minutes.

The sulphonation process with lignin also introduces oxygenated acid groups, namely carboxylic acids, which have been shown to contribute to a synergistic effect on catalytic activity<sup>122,123</sup>. Throughout the esterification reaction, the strong nature of sulphonic groups ( $pK_a \sim$

-7) can lead to the protonation of methoxide groups). When a weaker acid such as carboxylic acids is present, the deprotonated form can form a hydrogen bond with the hydroxyl group of methanol, providing the oxygen with a negative charge and promoting the overall nucleophilicity of methanol, increasing reaction rate and therefore conversion of oleic acid<sup>124</sup>. As seen in **Table 3.3**, the sulphonation process added 4 mmol g<sup>-1</sup> of total acid sites to the softwood lignin, likely predominantly carboxylic acids, which aid in the catalytic process. Since there is <1% difference between conversion achieved by the corn stover and SSL catalyst, the roles of methanol and surface acid sites are emphasised, as displayed in **Table 3.3**. Whilst corn stover required only a third of the amount of methanol reactant, the nearly double amount of sulphonic acid groups on the surface as well as 2 wt% more catalyst loading was able to achieve maximum conversion within the same time as the SSL catalyst. As previously mentioned, the selection of optimal parameters with regards to sustainability will be dependent upon multiple factors such as sustainability of sourcing of catalyst, methanol and oil feedstock as well as option for renewable electricity to meet the energy demands of the reaction.

For the solid catalysts produced in this work to be incorporated into a two-step conversion of non-edible or waste cooking oils, tolerance of triglycerides is imperative, as it is another major component of most oils<sup>125</sup>. To assess this tolerance, each catalyst was reacted with waste- cooking oil with a FFA content of 4.74 %, as well as mixtures of oleic acid and canola oil corresponding

**Table 3.3** Summary of catalytic properties and optimal esterification reaction parameters for corn stover catalyst, SSL catalyst and softwood lignin precursor, highlighting the effectiveness of the sulphonation process.

Catalyst	Acid groups (mmol/g)		Oil:MeOH	Catalyst loading	Reaction temperature	Reaction duration	Methyl ester conversion	TOF
	SO <sub>3</sub> H	Other (COOH, OH)						
<b>Corn stover</b>	0.854	0.543	1:3	5 wt%	90 °C	30 min	97.1%	2.45 min <sup>-1</sup>
<b>SSL</b>	0.432	4.942	1:9	3wt%	90 °C	30 min	97.5%	7.86 min <sup>-1</sup>
<b>Softwood lignin</b>	0.104	0.932	1:24	5 wt%	90 °C	3 hours	18.5%	0.24 min <sup>-1</sup>

to 20 and 50 % FFA's to imitate non-edible oils with high FFA content<sup>126</sup>. These reactions were conducted using the optimal reaction parameters for each catalyst, as outlined in **Table 3.3**.

The results revealed sufficient conversions slightly higher than the percentage of FFA's in the corresponding oil mixtures, indicating the catalysts can maintain their efficiency in the presence of triglycerides in the oil feedstock. The catalytic capabilities of the corn stover and SSL in the complementary transesterification reaction were also investigated through the reaction of each catalyst with waste-cooking oil (FFA = 4.74 %) using 1:36 oleic acid to methanol molar ratio, 5 wt% catalyst loading at 90 °C. As depicted in **Figure 3.14**, both catalysts required nearly 48 hours to achieve >90 % conversion, neither being economically feasible, despite simultaneous catalysis of esterification and transesterification. Conversely, recent biodiesel production via the microwave irradiation method has demonstrated substantially faster reaction speed due to irradiation providing rapid homogeneous heating, unlike conventional heating methods. Through a microwave reaction system, solid acid catalysts have been proficient in catalysing the transesterification of triglycerides within outstanding reaction times as low as 1 hour<sup>81,96,115</sup>.

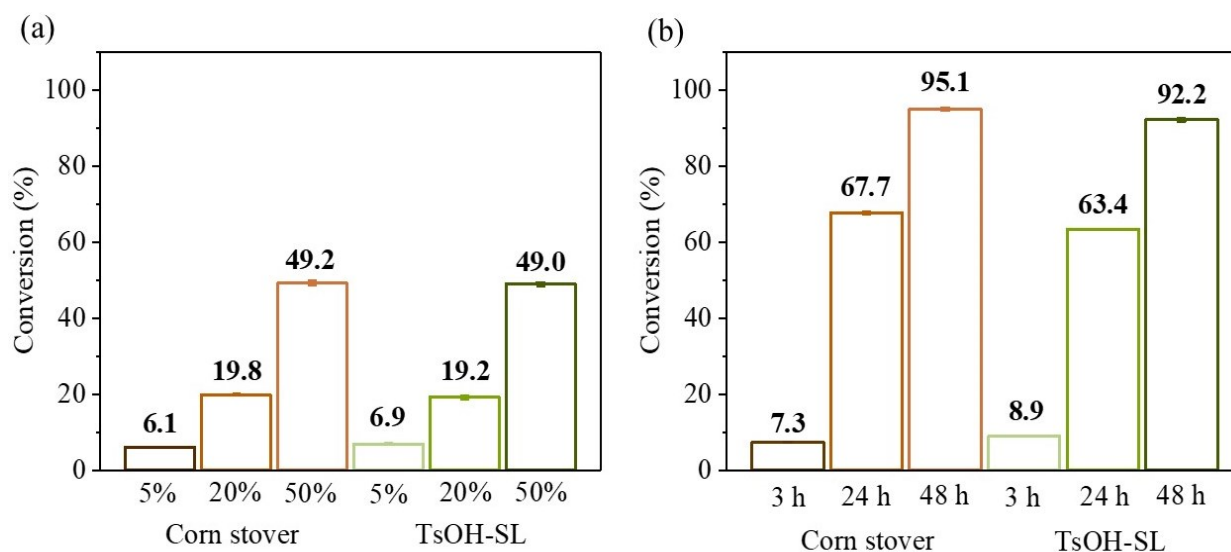


**Figure 3.14.** Biodiesel conversions of (a) corn stover (using 1:3, 5 wt%) and SSL catalyst (using 1:9, 3 wt%) with 5% FFA (WCO), 20% FFA, 50% FFA oil feedstocks reacted at 90 °C for 30 minutes, showing tolerance to triglycerides in oil feedstock. (b) corn stover using 1:3, 5 wt% and SSL using 1:9, 3 wt% catalysts with waste-cooking oil (FFA=5%), demonstrating transesterification capabilities.

## 3.5 Kinetics and reusability

### 3.5.1 Reaction kinetics

In order to optimise the synthesis design of conversion of non-edible and waste-cooking oils containing both triglycerides and FFA's, a kinetic equation for the esterification reaction is needed. To estimate the kinetics of the esterification reaction with corn stover lignin and SSL catalysts, pseudo-first and second order mathematical models were fit to provide understanding of the reaction rate (**Figure 3.15**). Furthermore, to better understand the rapid conversions experienced at 90 °C for both catalysts, the kinetic studies were performed at 70, 80 and 90 °C under the established optimal conditions for each catalyst (**Table 3.3**). The rapid conversions seen in the corn stover catalysed reactions at 80 and 90 °C did not provide an acceptable R-squared value for the pseudo-first and second order kinetic models. Whilst temperatures this high overcome the mass transfer limitations, temperatures above 80 °C are typically avoided in kinetic studies due to the build-up of excess pressure in the reaction vial and the consequential error in monitoring the progress of the reaction<sup>127</sup>. However, the kinetics exhibited at 70 °C fit into pseudo-first order ( $R^2 = 0.997$ ), aligning with what has been reported for the acid-catalysed esterification of oleic acid<sup>127,128</sup>. The kinetic study of the SSL catalyst displayed similar findings, with the 90 °C reaction unable to fit either model, and the 80 and 70 °C fitting best into the pseudo-first order kinetic model validated by R-squared value of 0.996. Instead of the reaction rate depending linearly on the molar concentration of one reactant as seen in first order kinetics, pseudo-first order reactions are considered to be second order that behave like first-order reactions due to the excess of one reactant. In this work, the excess of methanol used to drive the reaction forward is considered to be at a constant concentration compared with oleic acid. Hence, the sulphonic acid-catalysed esterification reaction presented is of pseudo-first order with respect to oleic acid.

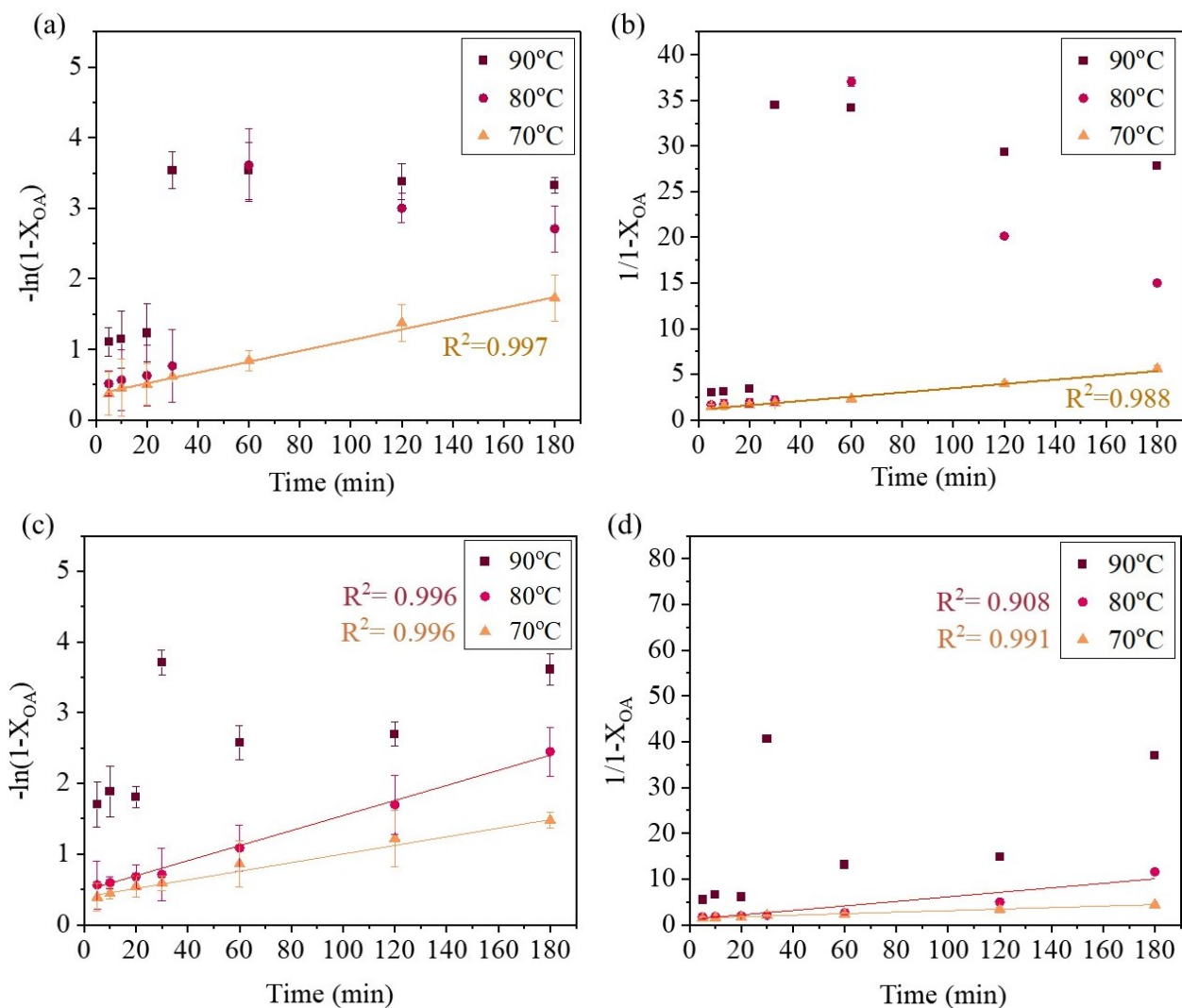


**Figure 3.15.** Kinetic studies of (a) corn stover at optimal conditions of 1:3, 5 wt%, fit into pseudo-first order kinetic model. (b) corn stover at optimal conditions of 1:3, 5 wt% fit into second order kinetic model. (c) SSL catalyst at optimal conditions of 1:9, 3 wt% fit into pseudo-first order kinetic model. (d) SSL catalyst at optimal conditions of 1:9, 3 wt% fit into second order kinetic model.

The rate constants for each pseudo-first order fitted reaction as well as the turnover numbers were calculated (Table 3.4) and confirm the increasing temperature provides kinetic energy, consequently increasing the rate constant and turn over frequency<sup>129</sup>. In regard to the reactions at higher temperatures that followed an irregular reaction progression, heterogeneous-catalysed reactions generally proceed in three stages: i) the adsorption of reactants on the catalyst surface,

**Table 3.4.** Rate constants and regression analysis ( $R^2$ ) of corn stover and SSL catalyst kinetic studies at 70 °C, 80 °C, 90 °C.

Catalyst	Temperature	Pseudo-first order		Second order	
		$k_1, \text{min}^{-1}$	$R^2$	$k_2 \text{ L/mol.min}$	$R^2$
Corn stover	70 °C	0.010	0.997	0.014	0.988
	80 °C	0.060	-	0.270	-
	90 °C	0.118	-	0.502	-
TsOH-SL	70 °C	0.008	0.996	0.0106	0.991
	80 °C	0.014	0.996	0.028	0.908
	90 °C	0.124	-	0.593	-

ii) the reaction on the catalyst surface and iii) the desorption of products. The rapid conversion seen at these higher temperatures may be linked to the second step of heterogenous catalysis, where the reaction on the catalyst surface is kinetically amplified at approximately 30 minutes of reaction. Other catalysts in the esterification of oleic acid have also reported neither fitting into the pseudo-first and second order model, with different reaction systems influencing the reaction pressure and overall reaction rate<sup>129,130</sup>. Furthermore, the difference in kinetics at 80 °C between the corn stover and SSL catalysts highlights the impact of catalytic active sites and their diffusion on the reaction rate. The reaction temperature and subsequent reaction time required were the last parameters optimised in this work due to the supply of renewable energy, which seemed a reasonable trade-off for using low amounts of methanol. In the case of economies that do not use renewable electricity to meet the energy demands of reactions, the impact on the environment may be higher, and this optimisation step should be considered before that of biomass catalyst loading. However, these statements require further investigation into the total life cycle assessment of the sourcing of energy, equipment required, sourcing of biomass and the processing involved for all material synthesis.

### 3.5.2 Reusability studies

In contrast to homogeneous catalysts, heterogeneous catalysts have the advantage of being able to be separated with minimal water washing and neutralisation and reused in multiple cycles, improving the environmental and economic feasibility of the biodiesel reaction<sup>120</sup>. Hence, the reusability of the corn stover and SSL catalysts were assessed by washing 3 times with hexane to remove residual methyl esters, followed by further organic washes before applying the catalyst in a biodiesel reaction cycle, using the previously established reaction parameters of each catalyst. This process was repeated for 4 cycles with corresponding  $\text{SO}_3\text{H}$  titrations (2.4.7.1) to monitor the commonly reported deactivation and leaching of sulphonic acid in the esterification reaction<sup>95,131,132</sup>. As expected, both catalysts exhibited a  $\sim 25\%$  decrease in conversion in the second biodiesel reaction, followed by  $\sim 30\%$  in the third cycle and almost no catalytic activity by the following  $\sim 32\%$  decrease in the fourth cycle, where conversion was similar to the control reaction pertaining to auto-catalysis by oleic acid (Figure 3.16). The complementary sulphonic acid titrations corroborated with the conversion results, with the superior amount of sulphonic acid sites on corn stover lignin being drastically reduced from  $0.854 \text{ mmol g}^{-1}$  to  $0.369 \text{ mmol g}^{-1}$  after

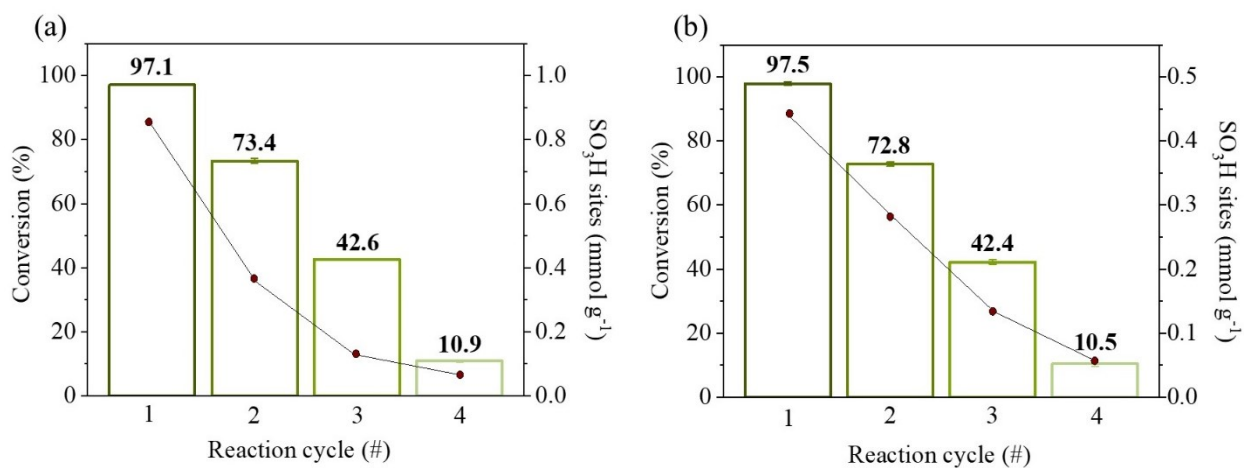


**Figure 3.16.** Reusability studies for 4 reaction cycles highlighting the direct relationship between sulphonic sites ( $y_2$ ) and methyl oleate conversion ( $y_1$ ) in (a) corn stover-catalysed esterification using 1:3, 5 wt%, at  $90^\circ\text{C}$  for 30 minutes. (b) SSL-catalysed esterification using 1:9, 3 wt% at  $90^\circ\text{C}$  for 30 minutes.

the first esterification reaction, leading to conversion of ~73% in the second cycle similar to that of the SSL catalyst possessing 0.289 mmol g<sup>-1</sup> of sulphonic acid sites. This loss of catalytic sites is commonly reported in not only sulphonic acid catalysts, but also metal oxide catalysts employed in the esterification reaction<sup>133</sup>. A previously reported lignosulfonate solid acid catalyst reported a 29 % leaching of sulphonic acid sites when the catalyst was exposed to hot water (~95 °C), quite close to the optimal temperature and leaching in this work<sup>134</sup>. This leaching has been attributed to the by-production of water throughout the esterification reaction consequentially creating a hydrophilic layer separate from layer where the biodiesel reaction is taking place<sup>132,135</sup>. In turn, the sulphonic acid groups are leached into this layer, as their benzylic position makes them susceptible to a hydrolysis reaction, resulting in a replacement phenol group and sulfuric acid as a product<sup>111,132</sup>. To further confirm the leaching of sulphonic sites into the aqueous layer, the upper aqueous layer was collected after a first reaction cycle using corn stover and used as the methanol reactant in a second reaction cycle, resulting in 35.4 % conversion of methyl oleate. This is well above the autocatalysis seen in the control reaction at this temperature and upholds the reporting of sulphonic acid leaching into the methanol layer. In light of this, recent works have focused on evading this leaching of catalytic sites by adding an alkyl chain to the sulphonic acid group, promoting the hydrophobicity of the material and catalytic activity in reuse cycles<sup>127</sup>. Whilst there are synthesis modifications, namely alkylation, that could avoid the reduction in catalytic activity resulting from sulphonic acid leaching, the status of corn stover and softwood as agricultural and industrial waste, respectively, with biodegradable properties offers alleviation on the strain on sustainability by single-use catalysts<sup>136</sup>. Additionally, the facile and relatively moderate reaction conditions are environmentally favourable over the usual high pyrolytic temperatures and sulphuric acid typically used to catalytically activate lignin.

## Chapter 4: Lignin-derived base catalysts

After characterising and optimising the solid acid lignin-derived catalyst, attempts at synthesising a heterogeneous base catalyst were made. The amount of reported basic lignin-derived catalysts pale in comparison to the publications of acidic catalysts, likely due to the ease of endowing acidic sites within the lignin structure. In order to catalytically activate lignin from its recalcitrant structure, processes such as pyrolysis and hydrothermal carbonisation are required, some of which are assisted by the use of a catalyst. Within these activation methods, the molten salt catalytic approach has garnered attention due to its energy saving abilities, encouraging the widespread application in lignin activation.

### 4.1 Molten salt carbonisation and activation

Molten salt catalytic activation results from thermal instability at high temperatures initiating an ionic environment from the molten salts, leading to in situ activation and introduction of desired ions into the carbonaceous structure<sup>137</sup>. The resulting biocarbon typically possesses a large surface area and specific surface oxygen-containing groups, which may aid in base-catalysed transesterification. The molten salts used for this process typically include alkali and alkaline earth metal cations in combination with halide, nitrate, carbonate and hydroxide anions. In attempt to carbonise and activate lignin, molten salt mixtures comprising sodium chloride (NaCl), potassium chloride (KCl), calcium carbonate (CaCO<sub>3</sub>) and zinc chloride (ZnCl<sub>2</sub>), in the ratios outlined in **Table 4.1**, were added to 1 g of lignin. A solid state carbonisation was performed at 180 °C, 250 °C, 400 °C and 650 °C for 2 hours, as described in section **2.2.2**. Each purified catalyst: MS1, MS2 and MS3 was employed in the transesterification reaction of canola oil. Additionally, since zinc oxide is amphoteric, MS3 was also reacted in the conversion of waste-cooking oil into biodiesel

to assess the potential catalytic capabilities in the esterification of the 4.74% of free fatty acids present. However, none of the molten salt combinations reacted at any of the temperatures were able to catalyse the biodiesel reactions. As seen in the example NMR spectra (**Figure 4.1**) of each molten salt at the highest reaction temperature, the absence of the 3.7 ppm chemical shift indicative

**Table 4.1** Ratio of molten salts employed and their corresponding labels

Label	Molten salts used	Ratio of molten salts
MS1	NaCl : KCl	1:1
MS2	NaCl : KCl : CaCO <sub>3</sub>	1:1:15
MS3	NaCl : KCl : ZnCl	1:1:3

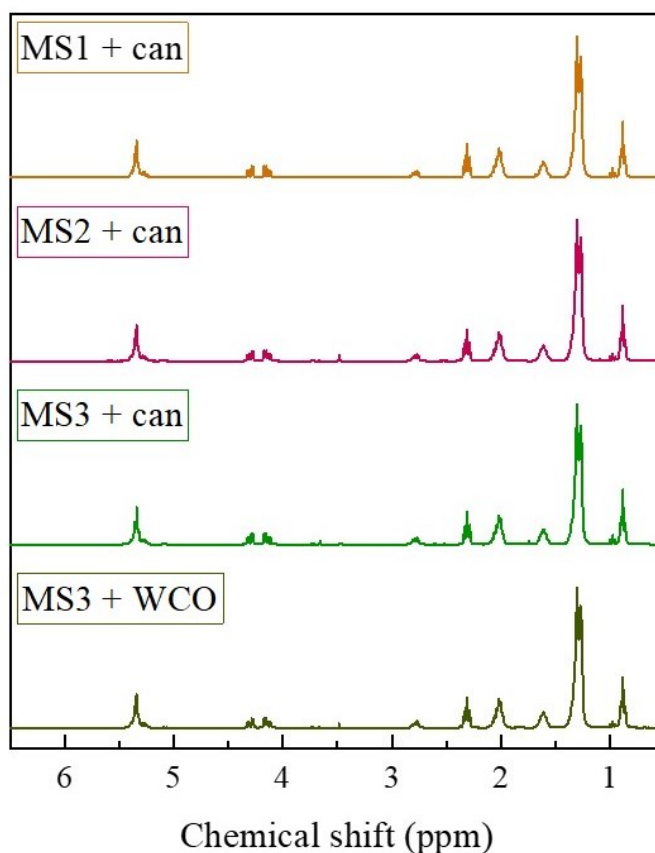


**Figure 4.1.** <sup>1</sup>H NMR spectra of MS1, MS2, MS3 catalysts synthesised at 600 °C reacted using 1:72 oil to methanol molar ratio, 5 wt% catalyst loading at 90 °C for 3 hours with canola oil, as well as MS3 reaction with WCO, showing no biodiesel conversion of any molten salt catalyst.

of biodiesel formation confirmed the carbonisation and activation method was not successful. This is most likely due to temperatures not reaching those of the melting points of NaCl, KCl and CaCO<sub>3</sub> at 801 °C, 770 °C and 825 °C, respectively. In order to convert from inorganic crystals at room temperature to molten salts, the melting point of the metal salt needs to be surpassed. However, since one of the aims in this project was to minimise the use of high temperatures, the carbonisation and activation of lignin via molten salts was not pursued further.

#### 4.2 Base-catalysed chemical activation of lignin

Instead, the complex and rigid lignin structure was subjected to depolymerisation in aims of degrading the biopolymer into lower molecular weight compounds with accessible functional groups. To achieve this, catalysts are employed and can be metallic, acidic or basic, amongst other categories. Recently, sodium hydroxide (NaOH) base has been applied to the depolymerisation of lignin-containing biomass sources including wheat straw, wood pulp, milled birch wood and others<sup>138–140</sup>. Roberts et al. (2011) investigated the effect of parameters on NaOH base-catalysed depolymerisation of lignin, proposing the generally accepted mechanism<sup>141</sup>:

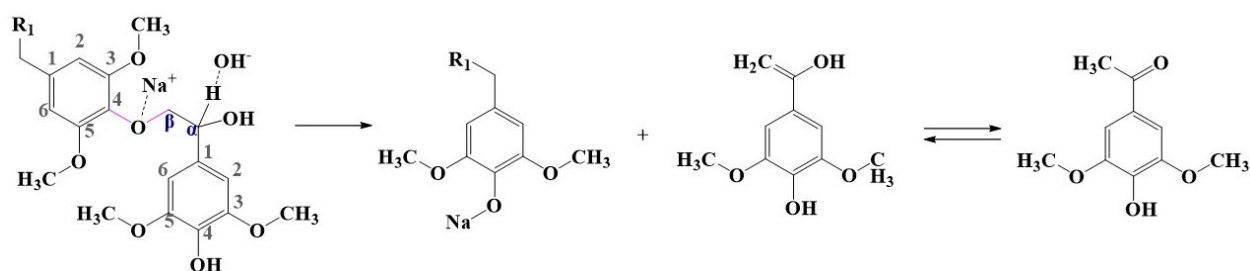
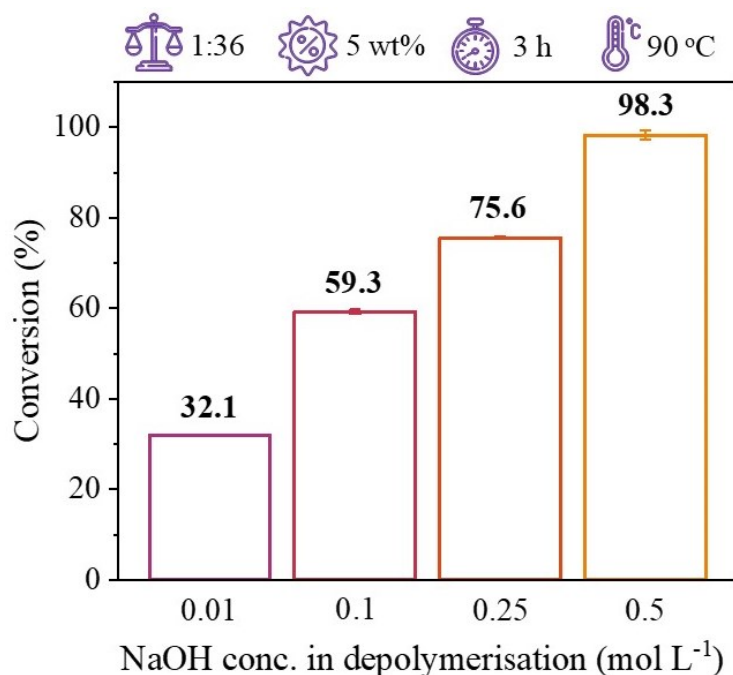


Figure 4.2. Proposed mechanism of NaOH-catalysed depolymerisation of lignin, adapted from Roberts et al. (2011).

Whereby sodium ions form cation adducts with lignin whilst the hydroxide ions act as nucleophiles for the cleavage of the β-O-4 ether band - the most common linkage within lignin. In combination, this polarises the ether bond, in turn increasing the negative partial charge on the oxygen and reducing the energy required for the heterolytic bond cleavage.

#### 4.2.1 Designing the synthesis method

In order to investigate the degree of depolymerisation, softwood lignin and 20 mL of NaOH solutions with varied concentrations of 0.01 M, 0.1 M, 0.25 M and 0.5M NaOH were added to their reaction vessel and heated at 180 °C for 3 hours. The temperature was elected based off previous publications demonstrating NaOH depolymerisation at temperatures as low as 16 °C<sup>142</sup>. After reaction completion, the crude mixture of the catalyst and aqueous solution were transferred to a centrifuge tube and the water was removed by rotary evaporation. The remaining solution was dried in an oven for a minimum of 12 hours. After organic washes, the final catalysts were used in the transesterification of canola oil, a rich source of triglycerides with minimal FFA's (<2%). The biodiesel reaction parameters used were an oil to methanol ratio of 1:36, using 5 wt% catalyst loading at 90 °C for 3 hours. As seen in **Figure 4.3**, only lignin catalysts treated with concentrations of 0.25 M and 0.5 M NaOH were able to convert over 70% of triglycerides into FAME's. Given that the 0.5 M NaOH treated catalyst successfully converted 98% of canola oil, this concentration



**Figure 4.3.** Biodiesel conversions of lignin treated with 0.01, 0.1, 0.25, 0.5 M NaOH, reacted with canola oil using 1:36 oil to methanol ratio, 5 wt% catalyst loading at 90 °C for 3 hours.

was used in the following synthesis of the softwood lignin-derived basic catalyst, hereon referred to as 0.5-NSL.

#### 4.2.2 Characterisation of 0.5-NSL catalyst

To assess the change in structure and generation of functional groups as a result of depolymerisation with NaOH, FTIR was performed on the catalyst (**Figure 4.4**). Upon comparison, one of the differences in the FTIR spectrum of the 0.5-NSL catalyst was the disappearance of the asymmetric stretch at  $1700\text{ cm}^{-1}$  previously ascribed to the C=O bond of carboxylic acids in the softwood precursor. Furthermore, there was a difference in intensity of the C=C vibrations of the aromatic skeleton of lignin, with the 0.5-NSL presenting a stronger intensity of peaks between  $1500\text{-}1600\text{ cm}^{-1}$ . Whilst the FTIR spectra highlighted changes within the aromatic and carboxyl groups after NaOH treatment, it served as a preliminary qualitative characterisation, necessitating further evaluation.

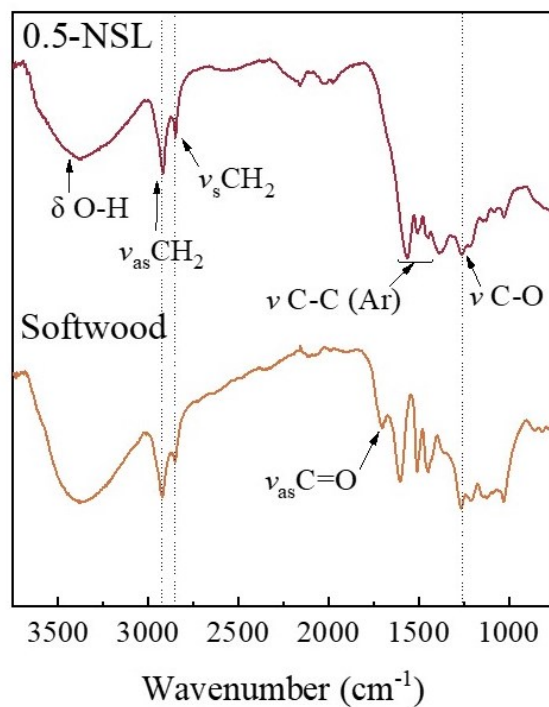


**Figure 4.4.** FTIR spectra of 0.5-NSL catalyst and softwood lignin precursor, showing changes in peaks

To investigate whether the depolymerisation process affected the surface area of the 0.5-NSL catalyst, the N<sub>2</sub> adsorption/desorption isotherm was analysed in order to calculate the BET surface area. However, the isotherm did not meet the criteria for BET calculation, presenting a surface area as little as <1 m<sup>2</sup>/g. The possibility of incomplete removal of solvent was eliminated, as the same final organic washes were employed prior to the BET preparation of the acid catalyst, and their removal was sufficient. The relatively small BET surface area may contribute to the accessibility and consequential performance of catalytic active sites.

In order to assess the surface charge of the catalyst, zeta potential was measured in methanol. This solvent was elected in attempt to mimic the chemical environment of the transesterification reaction. The zeta potential of the catalyst was relatively negative, giving a value of -28.6 mV, suggesting basic sites were present.

To garner understanding of the depolymerised products resulting from reaction with NaOH, <sup>1</sup>H NMR analysis were carried out. Due to the hydrophobic nature of lignin, solubilisation in different solvents for <sup>1</sup>H NMR analysis was a struggle. As this is a notorious issue encountered when elucidating the structure of lignin and its derivatives, researchers typically perform acetylation of lignin to add sufficient hydrophilicity, encouraging solubility in <sup>1</sup>H NMR sample preparation<sup>142</sup>. An acetylation process was employed (**2.6**), however, in the sample preparation for <sup>1</sup>H NMR analysis, the acetylated lignin catalyst was still not completely soluble into solvents over a range of different hydrophilicities as well as more non-polar solvents. Whilst structural elucidation was lacking, the negative charge presented in zeta potential measurements indicated the treatment with NaOH generated negatively charged groups, necessary for the initial deprotonation of the methanol step in the base-catalysed transesterification.

### 4.3 Optimisation of parameters

As described in the optimisation of parameters of the acid catalysts (3.4), the effect of the oil to methanol molar ratio on the reaction equilibrium and subsequent conversion was investigated first, owing to the environmental impact of methanol synthesis. Given the stoichiometric requirement of reactants in the transesterification process is 3 moles of methanol for every mole of triglyceride source (i.e. canola oil), excess amounts of methanol were used to drive the reaction forward, varied at ratios of 1:20, 1:30, 1:36 of canola oil to methanol (**Figure 4.5 (a)**). Upon calculation of conversion, large error bars were noted for the 1:20 ratio, spanning conversions of 87-97%. However, 1:30 and 1:36 displayed conversions of 98.3% and 99.5%, respectively, with minimal deviations, hence, 1:30 was elected as the optimal ratio of canola oil to methanol. The variance in conversions using the 1:20 oil to alcohol ratio could possibly be attributed to the reverse shift of equilibrium taking place in these reaction conditions for some of the replicates, however, it is unlikely since the reactions with more methanol (1:30, 1:36) did not experience the reverse shift. Nonetheless, the optimisation of catalyst loading was performed to further investigate the magnitude of the effect of catalytic sites and conversion, whilst also being cautious of the accuracy of the triplicates.

When optimising the catalyst loading parameter, a range of loadings using 1, 2.5, 5 and 7 wt% with respect to the mass of canola oil were employed for the transesterification reaction, using the previously established 1:30 oil to alcohol molar ratio, reacted at 90 °C for 3 hours. As seen in **Figure 4.5 (b)**, more discrepancies were observed, raising great concern as they contradict the direct relationship between catalyst loading and active sites, and the consequential conversion of product. This is illuminated by the substantial difference in conversion between the 1 and 2.5 wt% catalyst loadings where 2.5 wt% of NSL catalyst converted 30% less than 1 wt%. If this was due

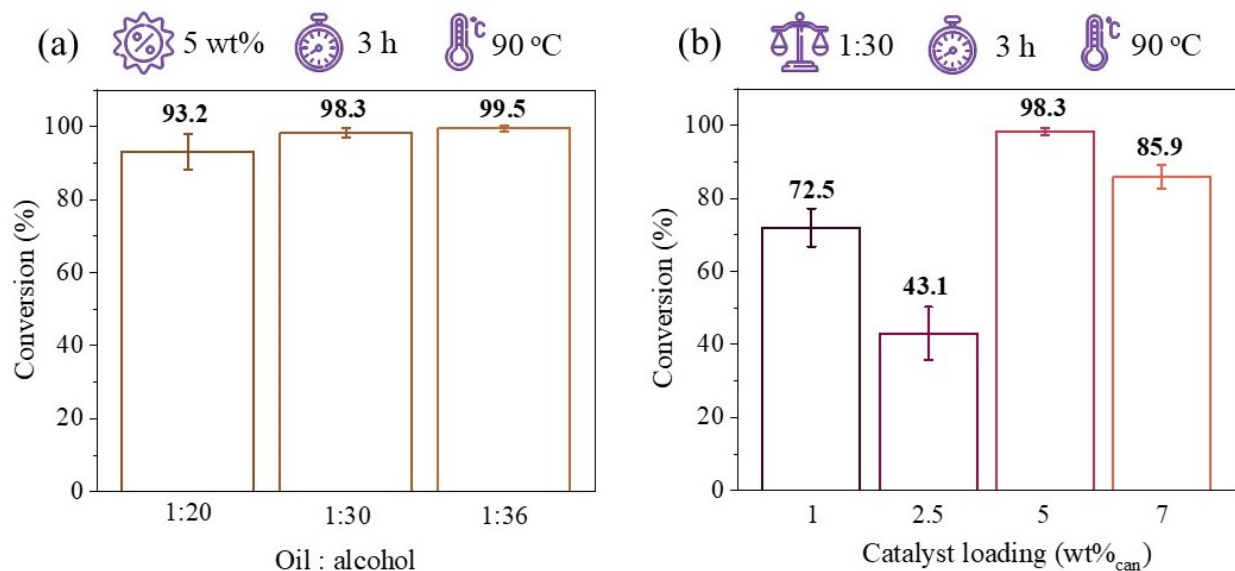


**Figure 4.5 (a)** Biodiesel conversions catalysed by 0.5-NSL when carrying the oil to methanol ratio at 1:20, 1:30, 1:36 and using 5 wt% catalyst loading reacted at 90 °C for 3 hours. **(b)** Biodiesel conversions catalysed by 0.5-NSL in loadings of 1, 2.5, 5 and 7 wt%, using a 1:30 oil to methanol ratio, reacted at 90 °C for 3 hours, demonstrating significant error bars and deviations from usual catalytic behaviour.

to the mass transfer limitation being emphasised by the amount of heterogeneous catalyst, the 5 wt% loading would have also suffered loss in conversion. Instead, the 98.3% conversion of the 5 wt% was marginally larger than the conversion of 85.9% by 7 wt% catalyst loading, raising further concerns regarding the inaccuracy of the results.

The depolymerised lignin from the hydrothermal reaction with NaOH was suspected to possess significant batch-to-batch variation, and so the purification method was revised with focus on the efficient removal of solution post-reaction. The water washing technique employed in the acidic catalyst synthesis (2.2.1) was attempted in order to remove any by-product residues. However, the core of the product was extremely insoluble, likely due to the hydrophobicity of lignin. Notably, the hydrophobic product was encased by a semi-soluble layer with a glutinous consistency, making the washing under vacuum quite difficult. Given the partial hydrophilicity of the product, it was suspected that there were aqueous residues of sodium or hydroxide ions that were not being

removed by the acetone and ethanol organic washes. Hence, a dialysis purification step with a MCWO of 3.5 kD was integrated in the synthesis plan of the basic lignin-derived catalyst, as demonstrated in **Figure 4.6**. By monitoring the pH of the dialysis water, it was confirmed that basic ions (i.e. OH<sup>-</sup>) were progressively being removed over the course of 3 days (**Table 4.2**). Once the pH of the dialysis water was 7.5 or lower, the dialysis tube was removed and placed in an oven to dry the remaining neutralised solution. Subsequently, organic washes with acetone and ethanol were performed for further removal of impurities before application to the transesterification reaction.

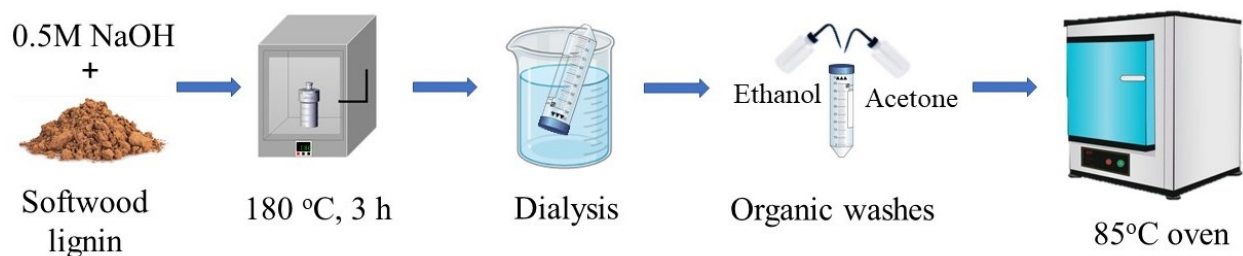


**Figure 4.6.** Revised synthesis method of 0.5-NSL catalyst substituting rotary evaporation of solution with dialysis purification.

**Table 4.2.** Average pH across 10 batches of 0.5-NSL catalyst dialysis water, taken after 12 hour dialysis days, showing decreasing pH, indicating aqueous basic residues (OH<sup>-</sup>) being separated

Day	Avg. pH
1	11.56
2	9.37
3	7.36

In order to reassess the reproducibility of the depolymerisation, the reaction employing an oil to methanol molar ratio of 1:20 was repeated in triplicates. Upon analysis of the conversions, the error bars were minimised substantially, demonstrating a 3% range of biodiesel conversion, averaging 83.8%. Using the updated purification method, batches of the 0.5-NSL catalyst were synthesised and investigated by repeating the catalyst loading optimisation step using a 1:30 oil to methanol ratio at 90 °C for 3 hours. Again, catalyst loadings of 1, 2.5, 5 and 7 wt% were reacted, comparison of their conversions revealed batch-to-batch variation remained an issue. Although the discrepancies between catalyst loadings were somewhat smaller, the decreased conversions for 1 wt% and the previously successful 5 wt% emphasised the irreproducibility of the synthesis method. On account of the inaccurate conversions demonstrated, the optimal reaction temperature and time required by the 0.5-NSL catalyst were not investigated.

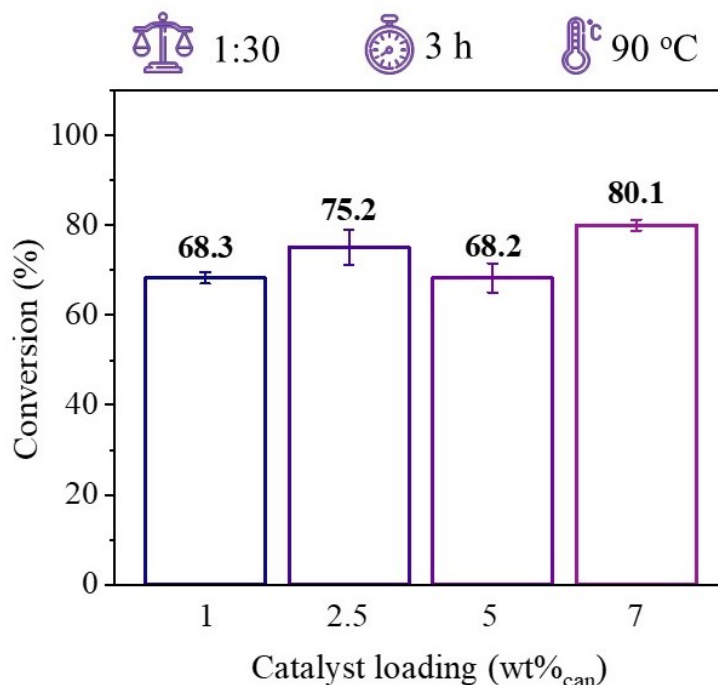


**Figure 4.7** Biodiesel conversions of 0.5-NSL catalysts purified by dialysis, when varying catalyst loading at 1, 2.5, 5, 7 wt%, using a 1:30 oil to methanol molar ratio, reacted at 90 °C for 3 hours, showing unacceptable results due to batch-to-batch variation

In order to understand the difference in products resulting from the hydrothermal treatment with NaOH, the ether linkages and subsequent mechanisms of depolymerisation were reviewed. Consolidating articles and reviews published on the depolymerisation of lignin, the following hypotheses were made on why the depolymerisation process was not reproducible. First, previous work emphasised the importance of suppressing addition and condensation reactions throughout the depolymerisation process<sup>140,141</sup>. This inhibits the concurrent oligomerisation and repolymerisation, enhancing the overall yield in the work presented by Roberts et al. by up to 85% when boric acid was used as a capping agent/protection group. Additionally, the temperature may have been too low, as publications typically report the highest yield at 300 °C reaction temperature<sup>141,143</sup>. Other researchers have investigated the effect of using an organic solvent in the depolymerisation process, with acetone being the preferred solvent for obtaining value-added phenolic monomers<sup>144</sup>. Lastly, Widyaya et al. (2016) investigated and emphasised the effects of employing a catalyst to promote oxidation reactions, in turn generating abundant hydroxyl (aromatic and alkyl) and carboxyl groups, useful as catalytic sites or for further modification<sup>145</sup>. In the absence of a protection group preventing repolymerisation, higher reaction temperatures and catalysts (e.g. metal oxides), the depolymerisation of lignin in this work was most likely uncontrolled, with side addition, condensation and oxidation reactions taking place. In order to optimise the depolymerisation process, assessment of the effect of different solvents with varying polarity at different temperatures and reaction times is necessary. Importantly, structural elucidation, namely through NMR spectroscopy, proves crucial in analysis of the depolymerisation process and the products generated. Overall, the hydrothermal depolymerisation conducted in this work required further investigation, control of reaction and potential additional functionalisation to promote the basicity of the lignin-derived product to qualify as a basic catalyst.

## Chapter 5- Conclusion and future works

### 5.1 Conclusion

In this work, solid acid catalysts from lignin precursors were successfully synthesised and their physico-chemical properties were analysed for their development as heterogeneous catalysts for the esterification of oleic acid. The corn stover catalyst was able to achieve 97.1% conversion of methyl oleate, only requiring 1:3 oleic acid to methanol molar ratio. In contrast, the SSL catalyst reached a conversion of 97.5% using a 1:9 oleic acid to methanol molar ratio. Both catalysts reached their optimal conversions within impressive reaction times of 30 minutes. Upon characterisation of the heterogeneous acid catalysts, the role of  $\text{SO}_3\text{H}$  density was revealed, proving to be pivotal for the esterification reaction. The abundant sulphonic acid groups pre-existing within the corn stover lignin demonstrate the catalytic potential of lignosulphonates mass produced as waste by the agricultural industry. On the other hand, the softwood lignin employed as a precursor for the SSL catalyst had significantly less sulphonic acid groups leftover from the extraction process, owing to the difference in monolignol ratios between softwood and grass lignins. Nonetheless, softwood lignin was successfully sulphonated using a greener source of sulphonic acid (TsOH) at a milder reaction temperature of 180 °C, compared to the typical concentrated sulphuric acid or high temperature pyrolytic methods. Whilst both the corn stover and SSL were capable of catalysing the esterification reaction at 90 °C, this temperature presented issues with kinetic model fitting, requiring a lower temperature of 70 °C to obtain a suitable regression analysis for the fitting into the pseudo-first order kinetic model. Additionally, neither catalyst was able to maintain conversion upon reuse due to the leaching of sulphonic acid catalytic sites throughout the esterification reaction. Although reusability is regarded as the main advantage of heterogeneous catalysts in biodiesel production, the utilisation of biomass waste from the

forestry and agricultural industries offers contribution to a circular economy, adding sustainability to the biodiesel process. The sufficient catalysis of oleic acid into methyl oleate by the solid acid catalysts allows them to be employed in the initial esterification of FFA's in non-edible and waste-cooking oils, as opposed to the non-environmentally friendly concentrated homogeneous sulphuric acid used in current biodiesel production from non-edible oils.

Investigation of synthesis of a basic lignin-derived catalyst was also conducted in this work, using molten salt carbonisation and base-catalysed activation methods. The molten salts proved unsuccessful, due to the lower temperatures used not meeting the criteria for conversion of inorganic salts to their molten form. The subsequent base-catalysed depolymerisation of lignin was carried out using NaOH. Whilst the material generated from this method (0.5-NSL) was capable of catalysing the transesterification of canola oil, the synthesis method was not reproducible, demonstrated by the major discrepancies between batches of catalyst, even after revision of purification methods.

## **5.2 Future works**

In aim to synthesise a basic catalyst from lignin precursors, further investigation into alternative procedures for the depolymerisation and activation of lignin should be carried out. Specifically, the inclusion of a protection group to prevent repolymerisation and comparison of different solvents and temperatures used in the depolymerisation reaction would offer insight and guidance towards optimal synthesis methods. Importantly, structural elucidation by NMR spectroscopy would offer critical insight to the products generated by activation methods, aiding in assessment of the validity and consequential reproducibility of the synthesis method. Furthermore, including a second step to endow basic sites from a strong base with a high pKa (e.g. potassium carbonate) would further evolve the basicity of the lignin catalyst, promoting its application in the

transesterification reaction. Preliminary experiments involving impregnation and pyrolysis of lignin using potassium carbonate show promise in the catalysis of canola oil into biodiesel.

## References

1. IEA - International Energy Agency. *CO2 Emissions in 2022*. (2022).
2. IEA - International Energy Agency. *World Energy Outlook 2019*. (2019)
3. Shafiee, S. & Topal, E. When will fossil fuel reserves be diminished? *Energy Policy* **37**, 181–189 (2009).
4. Ziolkowska, J. R. Biofuels technologies: An overview of feedstocks, processes, and technologies. *Biofuels a More Sustain. Futur. Life Cycle Sustain. Assess. Multi-Criteria Decis. Mak.* 1–19 (2020)
5. IEA - International Energy Agency. *Renewables 2022*, IEA, Paris. Analysis forecast to 2027. 158 (2022).
6. Santos, S. M., Nascimento, D. C., Costa, M. C., Neto, A. M. B. & Fregolente, L. V. Flash point prediction: Reviewing empirical models for hydrocarbons, petroleum fraction, biodiesel, and blends. *Fuel* **263**, 116375 (2020).
7. Nogueira, T. R. *et al.* Evaluation of oxidative stability of soybean biodiesel using ethanolic and chloroform extracts of *Platymiscium floribundum* as antioxidant. *Renew. Energy* **159**, 767–774 (2020).
8. De Oliveira, F. C. & Coelho, S. T. History, evolution, and environmental impact of biodiesel in Brazil: A review. *Renew. Sustain. Energy Rev.* **75**, 168–179 (2017).
9. Elkelawy, M., El Shenawy, E. A., Bastawissi, H. A. E. & El Shennawy, I. A. The effect of using the WCO biodiesel as an alternative fuel in compression ignition diesel engine on performance and emissions characteristics. *J. Phys. Conf. Ser.* **2299**, 0–14 (2022).
10. Okoye, P. U. *et al.* A review on recent trends in reactor systems and azeotrope separation strategies for catalytic conversion of biodiesel-derived glycerol. *Sci. Total Environ.* **719**, 134595 (2020).
11. Verma, P. & Sharma, M. P. Performance and emission characteristics of biodiesel fuelled diesel engines. *Int. J. Renew. Energy Res.* **5**, 245–250 (2015).
12. Abed, K. A., Gad, M. S., El Morsi, A. K., Sayed, M. M. & Elyazeed, S. A. Effect of biodiesel fuels on diesel engine emissions. *Egypt. J. Pet.* **28**, 183–188 (2019).
13. Ozgur, T., Tuccar, G., Ozcanli, M. & Aydin, K. Prediction of emissions of a diesel engine fueled with soybean biodiesel using artificial neural networks. *Energy Educ. Sci. Technol. Part A Energy Sci. Res.* **27**, 301–312 (2011).
14. Sorate, K. A. & Bhale, P. V. Biodiesel properties and automotive system compatibility issues. *Renew. Sustain. Energy Rev.* **41**, 777–798 (2015).
15. Ogunkunle, O. & Ahmed, N. A. A review of global current scenario of biodiesel adoption and combustion in vehicular diesel engines. *Energy Reports* **5**, 1560–1579 (2019).
16. Ganesan, R. *et al.* A detailed scrutinize on panorama of catalysts in biodiesel synthesis. *Sci. Total Environ.* **777**, 145683 (2021).

17. Rezania, S. *et al.* Review on transesterification of non-edible sources for biodiesel production with a focus on economic aspects, fuel properties and by-product applications. *Energy Convers. Manag.* **201**, 112155 (2019).
18. Atabani, A. E. *et al.* Non-edible vegetable oils: A critical evaluation of oil extraction, fatty acid compositions, biodiesel production, characteristics, engine performance and emissions production. *Renew. Sustain. Energy Rev.* **18**, 211–245 (2013).
19. Mathew, G. M. *et al.* Recent advances in biodiesel production: Challenges and solutions. *Sci. Total Environ.* **794**, 148751 (2021).
20. Yusoff, M. F. M., Xu, X. & Guo, Z. Comparison of Fatty Acid Methyl and Ethyl Esters as Biodiesel Base Stock: a Review on Processing and Production Requirements. *J. Am. Oil Chem. Soc.* **91**, 525–531 (2014).
21. Yadav, P., Athanassiadis, D., Yacout, D. M. M., Tysklind, M. & Upadhyayula, V. K. K. Environmental Impact and Environmental Cost Assessment of Methanol Production from wood biomass. *Environ. Pollut.* **265**, 114990 (2020).
22. Pullen, J. & Saeed, K. Investigation of the factors affecting the progress of base-catalyzed transesterification of rapeseed oil to biodiesel FAME. *Fuel Process. Technol.* **130**, 127–135 (2015).
23. Meher, L. C., Vidya Sagar, D. & Naik, S. N. Technical aspects of biodiesel production by transesterification - A review. *Renew. Sustain. Energy Rev.* **10**, 248–268 (2006).
24. Chanakaewsomboon, I., Tongurai, C., Photaworn, S., Kungsanant, S. & Nikhom, R. Investigation of saponification mechanisms in biodiesel production: Microscopic visualization of the effects of FFA, water and the amount of alkaline catalyst. *J. Environ. Chem. Eng.* **8**, 103538 (2020).
25. Trejo-Zárraga, F. *et al.* Kinetics of Transesterification Processes for Biodiesel Production. *Biofuels - State Dev.* (2018)
26. Changmai, B., Vanlalveni, C., Ingle, A. P. & Bhagat, R. Widely used catalysts in biodiesel production: a review. *RSC Adv.* **10**, 41625–41679 (2020).
27. Ruhul, A. M. *et al.* State of the art of biodiesel production processes: A review of the heterogeneous catalyst. *RSC Adv.* **5**, 101023–101044 (2015).
28. Refaat, A. A. Biodiesel production using solid metal oxide catalysts. *Int. J. Environ. Sci. Technol.* **2011 81** **8**, 203–221 (2010).
29. Maroa, S. & Inambao, F. A review of sustainable biodiesel production using biomass derived heterogeneous catalysts. *Eng. Life Sci.* **21**, 790–824 (2021).
30. Shan, R., Lu, L., Shi, Y., Yuan, H. & Shi, J. Catalysts from renewable resources for biodiesel production. *Energy Convers. Manag.* **178**, 277–289 (2018).
31. Alsultan, A. G. *et al.* Current State and Challenges on Biodiesel Production. 1–36 (2021).
32. Rizwanul Fattah, I. M. *et al.* State of the Art of Catalysts for Biodiesel Production. *Front. Energy Res.* **8**, 1–17 (2020).

33. Okechukwu, O. D., Joseph, E., Nonso, U. C. & Kenechi, N.-O. Improving heterogeneous catalysis for biodiesel production process. *Clean. Chem. Eng.* **3**, 100038 (2022).
34. EN 14214:2012+A1:2014 - Liquid petroleum products - Fatty acid methyl esters (FAME) for use in. <https://standards.iteh.ai/catalog/standards/cen/2d10b379-1d6d-4dc9-8f54-fe0e0dfbdb97/en-14214-2012a1-2014>.
35. D6751 Standard Specification for Biodiesel Fuel Blendstock (B100) for Middle Distillate Fuels. <https://www.astm.org/d6751-23a.html>.
36. Abdul Hakim Shaah, M. *et al.* A review on non-edible oil as a potential feedstock for biodiesel: physicochemical properties and production technologies. *RSC Adv.* **11**, 25018–25037 (2021).
37. Mahajan, S., Konar, S. K. & Boocock, D. G. B. Determining the acid number of biodiesel. *J. Am. Oil Chem. Soc.* **83**, 567–570 (2006).
38. Ambat, I., Srivastava, V. & Sillanpää, M. Recent advancement in biodiesel production methodologies using various feedstock: A review. *Renew. Sustain. Energy Rev.* **90**, 356–369 (2018).
39. Canakci, M. & Sanli, H. Biodiesel production from various feedstocks and their effects on the fuel properties. *J. Ind. Microbiol. Biotechnol.* **35**, 431–441 (2008).
40. IEA - International Energy Agency. Renewables 2020. *Paris* (2020)
41. Baroutian, S., Aroua, M. K., Raman, A. A. A. & Sulaiman, N. M. N. Potassium hydroxide catalyst supported on palm shell activated carbon for transesterification of palm oil. *Fuel Process. Technol.* **91**, 1378–1385 (2010).
42. Dias, J. M., Alvim-Ferraz, M. C. M. & Almeida, M. F. Comparison of the performance of different homogeneous alkali catalysts during transesterification of waste and virgin oils and evaluation of biodiesel quality. (2008)
43. Haas, M. J., Mcaloon, A. J., Yee, W. C. & Foglia, T. A. A process model to estimate biodiesel production costs. (2005)
44. Tesfaw, A., Senbeta, F., Alemu, D. & Teferi, E. Estimating the Economic Values of Restricted Monoculture Eucalyptus Plantations : A Choice Modeling Approach. *Int. J. Environ. Res. Public Heal.* **19**, (2022).
45. Velenturf, A. P. M. & Purnell, P. Principles for a sustainable circular economy. *Sustain. Prod. Consum.* **27**, 1437–1457 (2021).
46. Barona, E., Ramankutty, N., Hyman, G. & Coomes, O. T. The role of pasture and soybean in deforestation of the Brazilian Amazon. *Environ. Res. Lett.* **5**, 024002 (2010).
47. Kumar Mishra, V. & Goswami, R. A review of production, properties and advantages of biodiesel. *Biofuels* **9**, 273–289 (2018).
48. Blanco, M. I. & Azqueta, D. Can the environmental benefits of biomass support agriculture?-The case of cereals for electricity and bioethanol production in Northern Spain. *Energy Policy* **36**, 357–366 (2008).

49. Suren Rangaraju. 10 years of EU fuels policy increased EU's reliance on unsustainable biofuels. *Transport & Environment* (2021).
50. Guo, F., Fang, Z., Tian, X.-F., Long, Y.-D. & Jiang, L.-Q. One-step production of biodiesel from *Jatropha* oil with high-acid value in ionic liquids. *Bioresour. Technol.* **102**, 6469–6472 (2011).
51. Ragit, S. S., Mohapatra, S. K., Kundu, K. & Gill, P. Optimization of neem methyl ester from transesterification process and fuel characterization as a diesel substitute. *Biomass and Bioenergy* **35**, 1138–1144 (2011).
52. Ikwuagwu, O. E., Ononogbu, I. C. & Njoku, O. U. Production of biodiesel using rubber [*Hevea brasiliensis* (Kunth. Muell.)] seed oil. *Ind. Crops Prod.* **12**, 57–62 (2000).
53. Azad, A. K., Rasul, M. G., Khan, M. M. K., Sharma, S. C. & Islam, R. Prospect of Moringa seed oil as a sustainable biodiesel fuel in Australia: A review. *Procedia Eng.* **105**, 601–606 (2015).
54. Kumar, A., Sharma, S., An evaluation of multipurpose oil seed crop for industrial uses (*Jatropha curcas* L.): A review. *Ind. Crops Prod.* **28**, 1–10. (2008)
55. Gui, M. M., Lee, K. T. & Bhatia, S. Feasibility of edible oil vs. non-edible oil vs. waste edible oil as biodiesel feedstock. *Energy* **33**, 1646–1653 (2008).
56. Parawira, W. Biodiesel production from *Jatropha curcas*: A review. *Sci. Res. Essays* **5**, 1796–1808 (2010).
57. Srinivasan, S. The food v. fuel debate: A nuanced view of incentive structures. *Renew. Energy* **34**, 950–954 (2009).
58. Silitonga, A. S. *et al.* Overview properties of biodiesel diesel blends from edible and non-edible feedstock. *Renew. Sustain. Energy Rev.* **22**, 346–360 (2013).
59. Yunus khan, T. *et al.* Recent scenario and technologies to utilize non-edible oils for biodiesel production. *Renew. Sustain. Energy Rev.* **37**, 840-851 (2014)
60. Ho, K. C. *et al.* Biodiesel production from waste cooking oil by two-step catalytic conversion. *Energy Procedia* **61**, 1302–1305 (2014).
61. Grosmann, M. T. *et al.* Hydrated metal salt pretreatment and alkali catalyzed reactive distillation: A two-step production of waste cooking oil biodiesel. *Chem. Eng. Process. - Process Intensif.* **176**, 108980 (2022).
62. Mannan, M. & Al-Ghamdi, S. G. Complementing circular economy with life cycle assessment: Deeper understanding of economic, social, and environmental sustainability. *Circular Economy and Sustainability* **9**, 145-160 (2021).
63. Chung, Z. L. *et al.* Life cycle assessment of waste cooking oil for biodiesel production using waste chicken eggshell derived CaO as catalyst via transesterification. *Biocatal. Agric. Biotechnol.* **21**, 101317 (2019).
64. Talens Peiró, L., Lombardi, L., Villalba Méndez, G. & Gabarrell i Durany, X. Life cycle

- assessment (LCA) and exergetic life cycle assessment (ELCA) of the production of biodiesel from used cooking oil (UCO). *Energy* **35**, 889–893 (2010).
65. Anastas, P. & Eghbali, N. Green Chemistry: Principles and Practice. *Chem. Soc. Rev.* **39**, 301–312 (2009).
  66. Saini, J. K., Saini, R. & Tewari, L. Lignocellulosic agriculture wastes as biomass feedstocks for second-generation bioethanol production: concepts and recent developments. *3 Biotech* **5**, 337–353 (2015).
  67. Azadi, P., Inderwildi, O. R., Farnood, R. & King, D. A. Liquid fuels, hydrogen and chemicals from lignin: A critical review. *Renew. Sustain. Energy Rev.* **21**, 506–523 (2013).
  68. Zakzeski, J., Bruijninx, P. C. A., Jongerius, A. L. & Weckhuysen, B. M. The catalytic valorization of lignin for the production of renewable chemicals. *Chem. Rev.* **110**, 3552–3599 (2010).
  69. Amthor, J. S. Efficiency of lignin biosynthesis: A quantitative analysis. *Ann. Bot.* **91**, 673–695 (2003).
  70. Bajwa, D. S., Pourhashem, G., Ullah, A. H. & Bajwa, S. G. A concise review of current lignin production, applications, products and their environmental impact. *Ind. Crops Prod.* **139**, 111526 (2019).
  71. Hasan, M. S. *et al.* A Brief Review on Applications of Lignin. *J. Chem. Rev.* **5**, 56–82 (2023).
  72. Boarino, A. & Klok, H. A. Opportunities and Challenges for Lignin Valorization in Food Packaging, Antimicrobial, and Agricultural Applications. *Biomacromolecules* (2022)
  73. Zhu, Y., Li, Z. & Chen, J. Applications of lignin-derived catalysts for green synthesis. *Green Energy Environ.* **4**, 210–244 (2019).
  74. Costa, C. A. E., Vega-Aguilar, C. A. & Rodrigues, A. E. Added-Value Chemicals from Lignin Oxidation. *Molecules* **26**, (2021).
  75. Deshpande, R., Sundvall, L., Grundberg, H., Henriksson, G. & Lawoko, M. Structural basis for lignin recalcitrance during sulfite pulping for production of dissolving pulp from pine heartwood. *Ind. Crops Prod.* **177**, 114391 (2022).
  76. Venkata Mohan, S. *et al.* Waste biorefinery models towards sustainable circular bioeconomy: Critical review and future perspectives. *Bioresour. Technol.* **215**, 2–12 (2016).
  77. Sheldon, R. A. Biocatalysis and biomass conversion: Enabling a circular economy: Biocatalysis and Biomass Conversion. *Philos. Trans. R. Soc. A Math. Phys. Eng. Sci.* **378**, (2020).
  78. Kocaturk, E., Salan, T., Ozcelik, O., Alma, M. H. & Candan, Z. Recent Advances in Lignin-Based Biofuel Production. *Energies 2023, Vol. 16, Page 3382* **16**, 3382 (2023).
  79. Paysepar, H., Venkateswara Rao, K. T., Yuan, Z., Shui, H. & Xu, C. Production of

- phenolic chemicals from hydrolysis lignin via catalytic fast pyrolysis. *J. Anal. Appl. Pyrolysis* **149**, 104842 (2020).
80. Lu, X. & Gu, X. A review on lignin pyrolysis: pyrolytic behavior, mechanism, and relevant upgrading for improving process efficiency. *Biotechnol Biofuels*. **15**, 106 (2022).
  81. Nazir, M. H. *et al.* Development of lignin based heterogeneous solid acid catalyst derived from sugarcane bagasse for microwave assisted-transesterification of waste cooking oil. *Biomass and Bioenergy* **146**, 105978 (2021).
  82. Huang, M., Luo, J., Fang, Z. & Li, H. Biodiesel production catalyzed by highly acidic carbonaceous catalysts synthesized via carbonizing lignin in sub- and super-critical ethanol. *Appl. Catal. B Environ.* **190**, 103–114 (2016).
  83. Aro, T. & Fatehi, P. Production and Application of Lignosulfonates and Sulfonated Lignin. *Chem Sus Chem* **10**, 1861–1877 (2017).
  84. El Mansouri, N. E. & Salvadó, J. Analytical methods for determining functional groups in various technical lignins. *Ind. Crops Prod.* **26**, 116–124 (2007).
  85. Zhu, Y., Li, Z. & Chen, J. Applications of lignin-derived catalysts for green synthesis. *Green Energy Environ.* **4**, 210–244 (2019).
  86. Degen, I. A. Detection of the Methoxyl Group by Infrared Spectroscopy. *Applied Spectroscopy*. **22**, 164–166 (1968).
  87. Rashid, T., Kait, C. F. & Murugesan, T. A ‘fourier Transformed Infrared’ Compound Study of Lignin Recovered from a Formic Acid Process. *Procedia Eng.* **148**, 1312–1319 (2016).
  88. Zhang, L., Larsson, A., Moldin, A. & Edlund, U. Comparison of lignin distribution, structure, and morphology in wheat straw and wood. *Ind. Crops Prod.* **187**, 115432 (2022).
  89. Tejado, A., Peña, C., Labidi, J., Echeverria, J. M. & Mondragon, I. Physico-chemical characterization of lignins from different sources for use in phenol-formaldehyde resin synthesis. *Bioresour. Technol.* **98**, 1655–1663 (2007).
  90. Mandlekar, N. *et al.* An Overview on the Use of Lignin and Its Derivatives in Fire Retardant Polymer Systems. *Lignin - Trends Appl.* (2018)
  91. Contescu, A., Contescu, C., Putyera, K. & Schwarz, J. A. Surface acidity of carbons characterized by their continuous pK distribution and Boehm titration. *Carbon N. Y.* **35**, 83–94 (1997).
  92. Zhang, W. *et al.* One-pot synthesis of carbonaceous monolith with surface sulfonic groups and its carbonization/activation. *Carbon N. Y.* **49**, 1811–1820 (2011).
  93. Pi, Y. *et al.* Preparation of Activated Carbon-Based Solid Sulfonic Acid and Its Catalytic Performance in Biodiesel Preparation. *Front. Chem.* **10**, 1–10 (2022).
  94. da Luz Corrêa, A. P., Bastos, R. R. C., Rocha Filho, G. N. da, Zamian, J. R. & Conceição, L. R. V. da. Preparation of sulfonated carbon-based catalysts from murumuru kernel shell

- and their performance in the esterification reaction. *RSC Adv.* **10**, 20245–20256 (2020).
95. Yusuff, A. S. Kinetic and thermodynamic study on the esterification of oleic acid over SO<sub>3</sub>H-functionalized eucalyptus tree bark biochar catalyst. *Sci. Reports 2022 121* **12**, 1–14 (2022).
  96. Kumawat, M. K. & Rokhum, S. L. Biodiesel Production From Oleic Acid Using Biomass-Derived Sulfonated Orange Peel Catalyst. *Front. Catal.* **2**, 1–12 (2022).
  97. Mostafa Marzouk, N. *et al.* Process optimization of biodiesel production via esterification of oleic acid using sulfonated hierarchical mesoporous ZSM-5 as an efficient heterogeneous catalyst. *J. Environ. Chem. Eng.* **9**, 105035 (2021).
  98. Nainggolan, M. & Sinaga, A. Characteristics of fatty acid composition and minor constituents of red palm olein and palm kernel oil combination. *J. Adv. Pharm. Technol. Res.* **12**, 22–26 (2021).
  99. Wenchao, W., Fashe, L. & Ying, L. Effect of biodiesel ester structure optimization on low temperature performance and oxidation stability. *J. Mater. Res. Technol.* **9**, 2727–2736 (2020).
  100. Aparamarta, H. W., Gunawan, S., Husin, H., Azhar, B. & Tri Aditya, H. The effect of high oleic and linoleic fatty acid composition for quality and economical of biodiesel from crude *Calophyllum inophyllum* oil (CCIO) with microwave-assisted extraction (MAE), batchwise solvent extraction (BSE), and combination of MAE–BSE meth. *Energy Reports* **6**, 3240–3248 (2020).
  101. Murugesan, A. *et al.* Production and analysis of bio-diesel from non-edible oils-A review. *Renew. Sustain. Energy Rev.* **13**, 825–834 (2009).
  102. Diehl, B. & Randel, G. Analysis of biodiesel, diesel and gasoline by NMR spectroscopy – A quick and robust alternative to NIR and GC. *Lipid Technol.* **19**, 258–260 (2007).
  103. Demirbas, A., Bafail, A., Ahmad, W. & Sheikh, M. Biodiesel production from non-edible plant oils. *Energy Explor. Exploit.* **34**, 290–318 (2016).
  104. Gelbard, G., Brès, O., Vargas, R. M., Vielfaure, F. & Schuchardt, U. F. <sup>1</sup>H nuclear magnetic resonance determination of the yield of the transesterification of rapeseed oil with methanol. *J. Am. Oil Chem. Soc.* **72**, 1239–1241 (1995).
  105. Lee, S. Y. & Harris, M. T. Surface modification of magnetic nanoparticles capped by oleic acids: Characterization and colloidal stability in polar solvents. *J. Colloid Interface Sci.* **293**, 401–408 (2006).
  106. Degirmenbasi, N., Boz, N. & Kalyon, D. M. Biofuel production via transesterification using sepiolite-supported alkaline catalysts. *Appl. Catal. B Environ.* **150–151**, 147–156 (2014).
  107. Maleki, H., Kazemeini, M. & Bastan, F. Transesterification of Canola Oil to Biodiesel Using CaO/Talc Nanopowder as a Mixed Oxide Catalyst. *Chem. Eng. Technol.* **40**, 1923–1930 (2017).

108. Zhang, L., He, R. & Gu, H. C. Oleic acid coating on the monodisperse magnetite nanoparticles. *Appl. Surf. Sci.* **253**, 2611–2617 (2006).
109. Lotero, E. *et al.* Synthesis of Biodiesel via Acid Catalysis. *Ind. Eng. Chem. Res.* **44**, 5353–5363 (2005).
110. Sendzikiene, E., Makareviciene, V., Janulis, P. & Kitrys, S. Kinetics of free fatty acids esterification with methanol in the production of biodiesel fuel. *Eur. J. Lipid Sci. Technol.* **106**, 831–836 (2004).
111. Matsushita, Y. Conversion of technical lignins to functional materials with retained polymeric properties. *J. Wood Sci.* **61**, 230–250 (2015)
112. Horn, A. B. & Sully, K. J. ATR-IR spectroscopic studies of the formation of sulfuric acid and sulfuric acid monohydrate films. *Phys. Chem. Chem. Phys.* **1**, 3801–3806 (1999).
113. Bernard, P., Stelmachowski, P., Broś, P., Makowski, W. & Kotarba, A. Demonstration of the Influence of Specific Surface Area on Reaction Rate in Heterogeneous Catalysis. *J. Chem. Educ.* **98**, 935–940 (2021).
114. Mendaros, C. M., Go, A. W., Nietes, W. J. T., Gollem, B. E. J. O. & Cabatingan, L. K. Direct sulfonation of cacao shell to synthesize a solid acid catalyst for the esterification of oleic acid with methanol. *Renew. Energy* **152**, 320–330 (2020).
115. dos Santos, T. C. *et al.* Reduced graphene oxide as an excellent platform to produce a stable Brønsted acid catalyst for biodiesel production. *Fuel* **256**, 115793 (2019).
116. Śliwińska, A., Burchart-Korol, D. & Smoliński, A. Environmental life cycle assessment of methanol and electricity co-production system based on coal gasification technology. *Sci. Total Environ.* **574**, 1571–1579 (2017).
117. Kajaste, R., Hurme, M. & Oinas, P. Methanol-Managing greenhouse gas emissions in the production chain by optimizing the resource base. *AIMS Energy* **6**, 1074–1102 (2018).
118. Li, M. *et al.* Reusable and efficient heterogeneous catalysts for biodiesel production from free fatty acids and oils: Self-solidifying hybrid ionic liquids. *Energy* **211**, 118631 (2020).
119. Nie, Z. *et al.* Zirconia-coated magnetic Fe<sub>2</sub>O<sub>3</sub> nanoparticles supported 12-tungstophosphoric acid: A novel environmentally friendly catalyst for biodiesel production. *J. Chinese Chem. Soc.* **68**, 837–848 (2021).
120. Mandari, V. & Devarai, S. K. Biodiesel Production Using Homogeneous, Heterogeneous, and Enzyme Catalysts via Transesterification and Esterification Reactions: a Critical Review. *BioEnergy Res.* **2021 152 15**, 935–961 (2021).
121. AlSharifi, M. & Znad, H. Development of a lithium based chicken bone (Li-Cb) composite as an efficient catalyst for biodiesel production. *Renew. Energy* **136**, 856–864 (2019).
122. Zhang, H. *et al.* Nanocarbon-based catalysts for esterification: Effect of carbon dimensionality and synergistic effect of the surface functional groups. *Carbon N. Y.* **147**, 134–145 (2019).

123. Wang, L. H., Liu, H. & Li, L. Carbon-based acid catalyst from waste seed shells: Preparation and characterization. *Polish J. Chem. Technol.* **17**, 37–41 (2015).
124. Zhang, H. *et al.* Esterification of fatty acids from waste cooking oil to biodiesel over a sulfonated resin/PVA composite. *Catal. Sci. Technol.* **6**, 5590–5598 (2016).
125. Andrikopoulos, N. K. Triglyceride species compositions of common edible vegetable oils and methods used for their identification and quantification. *Food Rev. Intl.* **18**, 71–102 (2007).
126. Brahma, S. *et al.* Biodiesel production from mixed oils: A sustainable approach towards industrial biofuel production. *Chem. Eng. J. Adv.* **10**, 100284 (2022).
127. Alegría, A. & Cuellar, J. Esterification of oleic acid for biodiesel production catalyzed by 4-dodecylbenzenesulfonic acid. *Appl. Catal. B Environ.* **179**, 530–541 (2015).
128. Gokulakrishnan, N., Pandurangan, A. & Sinha, P. K. Esterification of acetic acid with propanol isomers under autogeneous pressure: A catalytic activity study of Al-MCM-41 molecular sieves. *J. Mol. Catal. A Chem.* **263**, 55–61 (2007).
129. Akubude, V. C. *et al.* Overview on Different Reactors for Biodiesel Production. *Biodiesel Technol. Appl.* 341–359 (2023)
130. Tabatabaei, M. *et al.* Reactor technologies for biodiesel production and processing: A review. *Prog. Energy Combust. Sci.* **74**, 239–303 (2019).
131. Testa, M. L., La Parola, V. & Venezia, A. M. Esterification of acetic acid with butanol over sulfonic acid-functionalized hybrid silicas. *Catal. Today* **158**, 109–113 (2010).
132. Zhang, B. *et al.* Reduced surface sulphonic acid concentration Alleviates carbon-based solid acid catalysts deactivation in biodiesel production. *Energy* **271**, 127079 (2023).
133. Lowe, B., Gardy, J., Wu, K. & Hassanpour, A. Mixed Metal Oxide Catalysts in Biodiesel Production. *Biodiesel Prod. Feed. Catal. Technol.* 143–166 (2022).
134. Lee, D. Preparation of a Sulfonated Carbonaceous Material from Lignosulfonate and Its Usefulness as an Esterification Catalyst. *Molecules* **18**, 8168 (2013).
135. Mo, X. *et al.* Activation and deactivation characteristics of sulfonated carbon catalysts. *J. Catal.* **254**, 332–338 (2008).
136. Dessbesell, L., Paleologou, M., Leitch, M., Pulkki, R. & Xu, C. (Charles). Global lignin supply overview and kraft lignin potential as an alternative for petroleum-based polymers. *Renew. Sustain. Energy Rev.* **123**, 109768 (2020).
137. Egun, I. L., He, H., Hu, D. & Chen, G. Z. Molten Salt Carbonization and Activation of Biomass to Functional Biocarbon. *Adv. Sustain. Syst.* **6**, (2022).
138. Wang, Q., Wei, W., Kingori, G. P. & Sun, J. Cell wall disruption in low temperature NaOH/urea solution and its potential application in lignocellulose pretreatment. *Cellulose* **22**, 3559–3568 (2015).
139. Shi, Z., Yang, Q., Kuga, S. & Matsumoto, Y. Dissolution of Wood Pulp in Aqueous

- NaOH/Urea Solution via Dilute Acid Pretreatment. *J. Agric. Food Chem.* **63**, 6113–6119 (2015).
140. Mohsenzadeh, A., Jeyhanipour, A., Karimi, K. & Taherzadeh, M. J. Alkali pretreatment of softwood spruce and hardwood birch by NaOH/thiourea, NaOH/urea, NaOH/urea/thiourea, and NaOH/PEG to improve ethanol and biogas production. *J. Chem. Technol. Biotechnol.* **87**, 1209–1214 (2012).
  141. Roberts, V. M. *et al.* Towards Quantitative Catalytic Lignin Depolymerization. *Chem. – A Eur. J.* **17**, 5939–5948 (2011).
  142. Li, J. *et al.* Alkali lignin depolymerization under eco-friendly and cost-effective NaOH/urea aqueous solution for fast curing bio-based phenolic resin. *Ind. Crops Prod.* **120**, 25–33 (2018).
  143. Toledano, A., Serrano, L. & Labidi, J. Organosolv lignin depolymerization with different base catalysts. *J. Chem. Technol. Biotechnol.* **87**, 1593–1599 (2012).
  144. Erdocia, X., Prado, R., Fernández-Rodríguez, J. & Labidi, J. Depolymerization of Different Organosolv Lignins in Supercritical Methanol, Ethanol, and Acetone to Produce Phenolic Monomers. *ACS Sustain. Chem. Eng.* **4**, 1373–1380 (2016).
  145. Widyaya, V. T., Vo, H. T., Dahnum, D. & Lee, H. Magnesium Oxide-catalyzed Oxidative Depolymerization of EFB Lignin. *Bull. Korean Chem. Soc.* **37**, 515–521 (2016).